Copyright Warning & Restrictions

The copyright law of the United States (Title 17, United States Code) governs the making of photocopies or other reproductions of copyrighted material.

Under certain conditions specified in the law, libraries and archives are authorized to furnish a photocopy or other reproduction. One of these specified conditions is that the photocopy or reproduction is not to be "used for any purpose other than private study, scholarship, or research." If a, user makes a request for, or later uses, a photocopy or reproduction for purposes in excess of "fair use" that user may be liable for copyright infringement,

This institution reserves the right to refuse to accept a copying order if, in its judgment, fulfillment of the order would involve violation of copyright law.

Please Note: The author retains the copyright while the New Jersey Institute of Technology reserves the right to distribute this thesis or dissertation

Printing note: If you do not wish to print this page, then select "Pages from: first page # to: last page #" on the print dialog screen

ABSTRACT

HEAT TRANSFER ENHANCEMENT FROM A HEAT PIPE IMMERSED HORIZONTALLY IN WATER, UNDER NATURAL CONVECTION CONDITIONS, WITH THE AID OF GAS INJECTION

by
Evangelos J. Minakas

An experimental study has been performed to estimate the degree of heat transfer enhancement from a horizontal heat pipe, immersed in water with the aid of air injection. This thesis investigates the effects of different shroud shapes, shroud distances from the heat pipe, air injection rates, air injection configurations and air injection distances on the augmentation of heat transfer. Water was the experimental fluid and its temperature ranged from 17-60 °C, the surface temperature of the heat pipes varied from 18-75 °C.

It was discovered that the shape of the shrouds is a contributing factor on the heat transfer enhancement. There was heat transfer enhancement of 350 % for straight shrouds and 400 % for curved shrouds when all others parameters remained the same. The heat transfer enhancement due to water circulation only was 100 % for the 7/16 heat pipe, and 30 % for both the 0.5 inch and 0.75 inch HP-1 heat pipes at high power input rates. Water circulation within the tank improved as the number of openings increased on the injection pipe and this resulted in higher heat transfer rates. The shroud distance and air injection distance greatly influence the augmentation of heat transfer.

HEAT TRANSFER ENHANCEMENT FROM A HEAT PIPE IMMERSED HORIZONTALLY IN WATER, UNDER NATURAL CONVECTION CONDITIONS, WITH THE AID OF GAS INJECTION

by
Evangelos J. Minakas

A Thesis
Submitted to the Faculty of
New Jersey Institute of Technology
in Partial Fulfillment of the Requirements for the Degree of
Masters of Science in Mechanical Engineering

Department of Mechanical Engineering

May 1997

APPROVAL PAGE

HEAT TRANSFER ENHANCEMENT FROM A HEAT PIPE IMMERSED HORIZONTALLY IN WATER, UNDER NATURAL CONVECTION CONDITIONS, WITH THE AID OF GAS INJECTION

Evangelos J. Minakas

Dr. Robert Kirchner, Thesis Advisor — Date
Professor of Mechanical Engineering, NJIT

Dr. John V. Droughton, Committee Member — Date
Associate Chairperson of Mechanical Engineering
Professor of Mechanical Engineering, NJIT

Dr. Earnest S. Geskin, Committee Member — Date
Professor of Mechanical Engineering, NJIT

BIOGRAPHICAL SKETCH

Author: Evangelos J. Minakas

Degree: Master of Science

Date: May 1997

Undergraduate and Graduate Education:

- Master of Science in Mechanical Engineering
  New Jersey Institute of Technology, Newark, NJ, 1997

- Bachelors of Science in Mechanical Engineering Technology
  New Jersey Institute of Technology, Newark, NJ, 1994

Major: Mechanical Engineering

To my beloved family

ACKNOWLEDGMENT

The author wishes to express his sincere gratitude to Dr. Robert Kirchner for his guidance, support and encouragement during the course of this research. Special thanks to Don Rosander for his technical support and advice. Many thanks to Joe Glaz and David Singh for their help in manufacturing the different components of the experimental apparatus. Additionally the help of Dr. Droughton and Dr. Geskin are gratefully acknowledged.

The author is grateful to Sheridan Quarless and Heather Rochester for their support and advice throughout the author's graduate education. Finally, the author wishes to thank the New Jersey Institute of Technology Graduate Studies Program for the graduate assistantship support provided throughout this work.

TABLE OF CONTENTS

TABLE OF CONTENTS
(Continued)

TABLE OF CONTENTS
(Continued)

Chapter **Page**

LIST OF TABLES

LIST OF TABLES
(Continued)

LIST OF TABLES
(Continued)

LIST OF FIGURES

LIST OF FIGURES
(Continued)

LIST OF FIGURES
(Continued)

Figure **Page**

LIST OF FIGURES
(Continued)

Figure **Page**

LIST OF FIGURES
(Continued)

Figure **Page**

LIST OF FIGURES
(Continued)

Figure **Page**

CHAPTER 1

INTRODUCTION

1.1 Statement of the Problem

A body immersed in a fluid experiences a buoyancy force equal to the weight of the displaced fluid. This force is caused by the temperature, pressure and composition distributions in the region near the immersed body and provides the mechanism of natural convection (Thomas, p. 459). If the surface temperature of the immersed body is different than the temperature of the surrounding fluid, a density gradient within the fluid will be created. For example, if a cold vertical plate is placed in a warm stationary fluid, the temperature of the fluid near the wall will decrease by conduction heat transfer. This will cause the density of the fluid to decrease and will result in a downward flow of the more dense fluid. An upward fluid flow can be created if a hot plate is placed in a cooled fluid. The flow created by the density gradient will result in the development of a hydrodynamic boundary layer of thickness (δ) and a thermal boundary layer of thickness (Δ). The thickness at any location of these layers mainly depends on the smoothness of the surface, the temperature difference between the surface and the fluid, and the physical properties of the fluid. The temperature and velocity distributions within the boundary layers are shown for a cooled and heated plate in figure 1-1. Figure 1-1 also shows the two-dimensional forces acting on a finite small element inside the boundary layers.

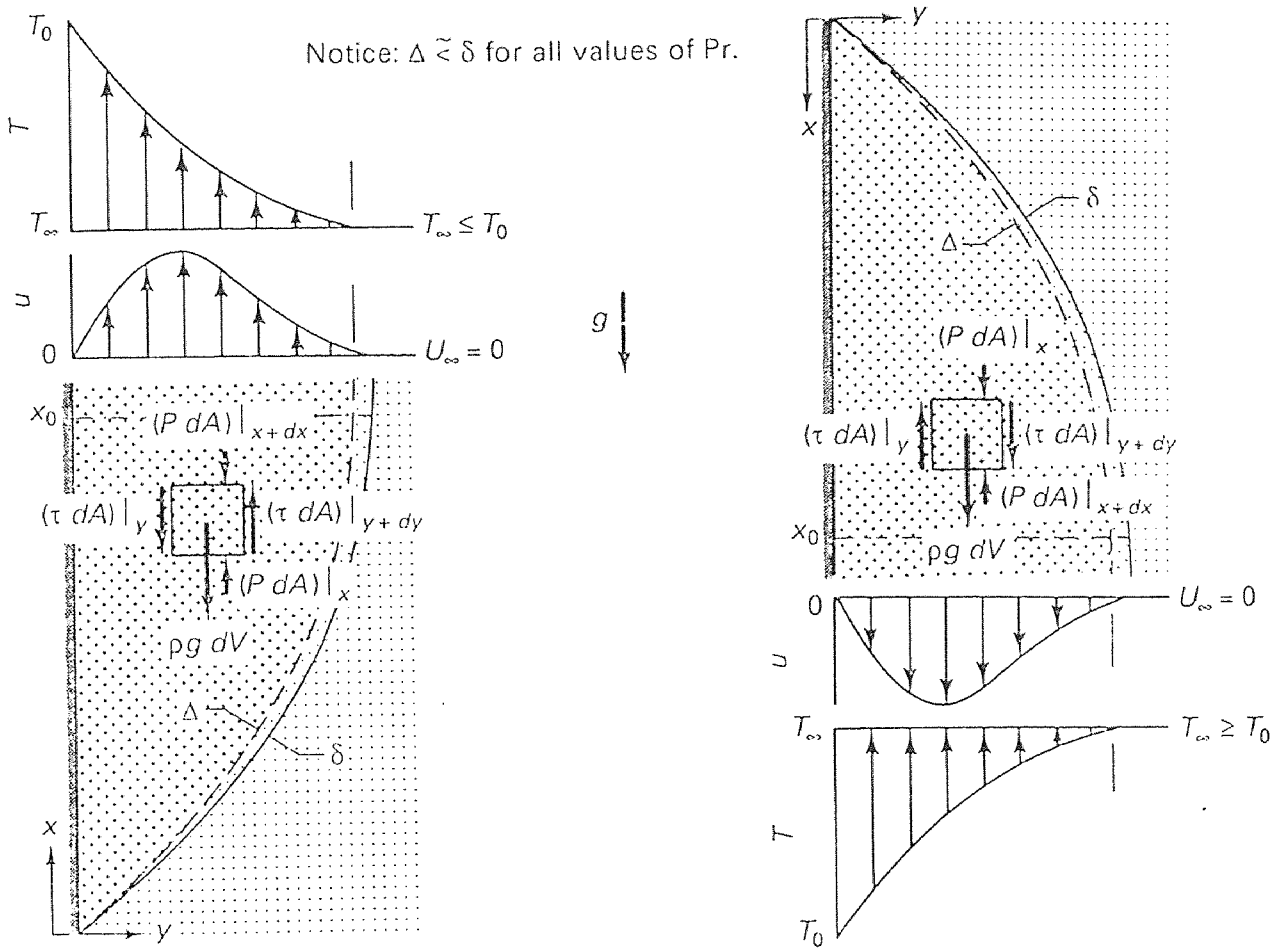

(a) Heated Plate (b) Cooled Plate

Figure 1-1 Examples of free convection from (a) Heated plate and (b) Cooled plate Temperature and velocity profiles are shown

Figure 1-2 shows the thermal boundary layer of a heated cylinder under natural convection conditions in air. If the diameter of the cylinder is small the hydrodynamic boundary layer looks similar to the thermal boundary layer. When the thermal boundary layer is somehow agitated by an external force, in order to increase the local velocities, the heat transfer from the immersed surface to the surrounding liquid will increase.

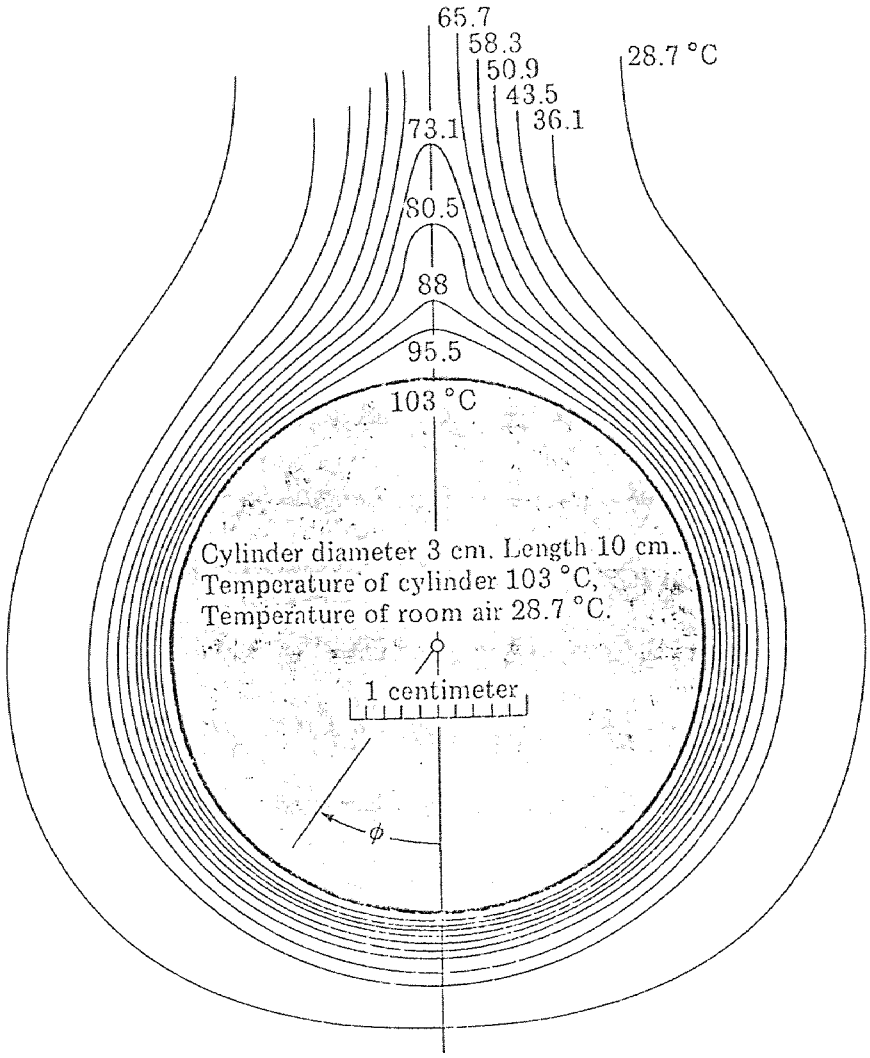

Figure 1-2 Isotherms of a heated horizontal cylinder at $Gr_D=1.5 \times 10^5$

For the last half of the twentieth century considerable research is done in the area of enhancing heat transfer from heated surfaces immersed in liquids. The techniques for enhancing heat transfer are separated into two categories: (a) passive and, (b) active techniques. "Passive techniques employ the use of special surface configurations and fluid additives to enhance the heat transfer whereas active techniques use external power (such as electric or magnetic) and surface vibrations" (White, p. 532).

A very efficient and economic active technique of enhancing convective heat transfer is injecting gas bubbles near the region of the heated surface. The main contributors of enhancing the heat transfer with gas injection are: the turbulence created as the bubbles rise through the fluid and, conduction between the bubbles and heated surface. The motion of a single gas bubble in a stagnant fluid is very complicated. If the temperature of the injected gas is different than the temperature of the fluid the bubble will expand or contract as it rises through the fluid creating a three dimensional flow of the fluid directly adjacent to the bubble. Turbulence is also created in the wakes of the bubbles and due to their rise through the fluid. Depending on the injection technique, surface contamination and surface tension of the fluid, the gas bubbles can create a secondary motion by spinning, rotating or having a zigzag pattern as they rise through the fluid. If the bubble makes contact with the heated surface, heat will be conducted away from the passing bubble. The combination of all these effects make gas injection a very efficient technique of enhancing heat transfer from a heated body immersed in a liquid.

1.2 Background Information

A summary of several articles and authors that affected this research is presented below.

Tamari and Nishikawa, [30], analyzed the effects of bubbles injected in water and ethyl alcohol to a vertical heated immersed plate. They varied the normal distance of the nozzles from the heated surface, the dimensions of the heated plate, and the number of nozzles. They discovered that the closer the normal distance

between the nozzles and the heated surface, the higher the heat transfer enhancement. Also the distance between two adjacent nozzles is critical for the heat transfer enhancement. The heat transfer increased as the distance between two adjacent nozzles decreased, up to a critical distance. If the distance of the nozzles was less than this critical distance then the heat transfer enhancement decreased. The enhancement of heat transfer was not affected by the number of nozzles if the quantity of the injected air was held constant. The dimensions of the plate did not have any effect on the enhancement of heat transfer. The heat transfer was greater in water than in ethyl alcohol because of difference in the physical properties of the fluids. The reason for the different heat transfer rates under the same loads is that the air bubbles in ethyl alcohol meet and unite more quickly than those in pure water because the surface tension of the bubbles' membranes are smaller in ethyl alcohol than in water. The coalesced bubbles dissolute and disperse into tiny bubbles less than 1 mm in diameter. This makes the stirring effect of the bubbles in ethyl alcohol less than that in water which results in lower heat transfer coefficients for ethyl alcohol.

Akira and Lykoudis, [1], enhanced the heat transfer coefficients in liquid metals from a vertically heated surface with the aid of nitrogen gas injection. They discovered that the heat transfer was enhanced two to three fold with gas injection when the heat fluxes of the vertical plate were small, whereas the heat transfer enhancement was less than 50% at high heat flux rates. The reason for the high heat transfer rates in low heat flux rates was that the thermal boundary layer is in the order of 20-25 mm and the magnitude of the boundary layer in high heat fluxes was

between 5-10 mm. In the low heat transfer cases, the bubbles were able to penetrate the thick thermal boundary layer and enhance the heat transfer rate, whereas in the high heat flux rates the bubbles appeared outside the thin boundary layer and were not able to augment the heat transfer from the heated surface to the liquid metal. The overall heat transfer enhancement due to bubble-induced turbulence was a collective action of both the induced liquid motion by the bubbles and the turbulence created in their trails. The researchers of this experiment were not able to establish the individual contribution of each of these factors.

Iguchi and Morita, [22], experimented with the heat transfer between bubbles and liquid water during cold gas injection. The injected gas was air, and it was cooled to a temperature of -110 °C (using a liquid nitrogen heat exchanger) and then injected into a tank of water. The bubbles expanded due to heat transfer from the warmer liquid as they moved upwards through the fluid. Bubbles injected at ambient temperature had a rugged surface in contrast to the bubbles injected at low temperatures which had a smooth surface. The smooth surface indicated that those bubbles were expanded equally in all directions which means that the liquid velocity around the bubbles is the same in all directions. The turbulence created by the bubbles injected at ambient temperature was greater than the turbulence created by the bubbles at low temperatures.

Hahne and Windisch, [17], investigated the effects of vapor bubbles upon the heat transfer coefficient in a twin finned-tube arrangement. They compared the results to the heat transfer for a single finned tube. The experiments were conducted in an insulated vessel with R-11 as the working fluid. For the twin-finned

arrangement the tubes were placed one on top of the other such that the turbulent motion of the bubbles and surrounding fluid from the lower tube, when boiling took place, would affect the heat transfer of the upper tube. In the nucleate boiling regime the bubbles rising from the lower tube increased the heat transfer of the upper tube by as much as 200%. The heat transfer of the lower tube was not influenced by the upper tube. At fully developed nucleate boiling there was no enhancement in heat transfer for the twin tube arrangement. Fin spacing played a major role in the heat transfer enhancement. The tube with the more widely spaced fins gave a higher heat transfer augmentation. The pitch between the tubes also was a contributing factor on the magnitude of the heat transfer enhancement. The closest arranged tubes give the smallest enhancement. For the upper tube the heat transfer was observed to be two terms. One is the heat flux from the bubble influence area due to nucleate boiling and the other is the heat transfer from the remaining surface due to convection. When a bubble departs from a heated surface, due to unsteady heat conduction, it causes an unsteady flow of liquid to the wall and creates a so-called bubble influence area on the heated surface. The influence area of a bubble on plain tubes is assumed to be a band with a width of twice the departing bubble diameter. The heat transfer from the remaining surface is due to convection. The convection term can be broken down into three independent terms. There is heat convection from the bottom surface, from the top surface and, from the sides of the tube. The top term is usually very small because the boundary layer is not affected by the onflow of bubbles created by the lower tube. The bottom and sides terms are affected by the onflow of bubbles. To calculate the contribution of

each of the terms separately, the volume flow density of the bubbles on the bottom and sides had to be measured. This volume flow density is assumed to be constant at the bottom surface of the tube but it is variable along the sides.

Gusev and Shklover, [15], measured the enhancement of heat transfer from a horizontal cylinder immersed in water. The cylinder was heated by having hot water pass through it. The temperature of the water was known before it entered the cylinder and after it left. The heat removed was calculated using the equation $\dot{Q} = \dot{m}c_p\left(T_i - T_o\right)$. Eight air injection nozzles were placed directly under the cylinder. The distance of the injection nozzles from the bottom surface of the cylinder, and the size of the nozzles were varied. The temperature range of the fluid was between 8.2-30.1 °C and the surface temperature of the cylinder varied between 15.7-63.1 °C. They concluded that the heat transfer was enhanced by 500% at the low heat transfer rates and as much as 300% at the higher heat transfer rates when using the highest air injection rate. When the nozzle was placed along the side of the cylinder the heat transfer was enhanced by as much as 20% and that was due to pure circulation of the water in the tank. The distance of the nozzle from the lower surface of the cylinder played a major role in the degree of enhancement. When the distance of the injection nozzles from the bottom surface of the cylinder was 18 times the diameter of the heated cylinder the enhancement was 400% whereas the enhancement was 300% when the distance was 1.8 times the diameter of the cylinder.

Pfeil and Sparrow, [33], experimented with the enhancement of natural convection from a heated cylinder when it was placed inside an insulated channel

that acted as a shroud. The experiments were conducted using air as the surrounding fluid. The cylinder was heated electrically and it was placed at the midway point of the channel's height. The vertical distance between the walls of the channel were varied as well as the height of the channel and the kind of insulation used around the walls of the channel. The cylinder was placed inside the rectangular channel and heated for 8 hours before any measurements were taken. Since the contributing factors of heat transfer from the cylinder to the surrounding surfaces will be convection and radiation, he set out to calculate the contribution of each term. He concluded that the radiation term is very small compared to the convection and it accounts for only 5.5-7.5 % of the total heat transfer for the temperature ranges of his experiments. A heated cylinder creates a density deficit between the fluid adjacent to its surface and the ambient fluid. The less dense fluid rises and is replaced by the more dense air that resides in the ambient. When the shroud placed around a heated cylinder is not very wide, the fluid that rises during the period the cylinder is heated, is being replaced by fluid entering from the bottom of the shrouded cylinder. This creates a flow rate of air around the cylinder and the direction is from the bottom of the channel to the top. If the shroud is too wide, the replaced fluid will come from the fluid that resides around the cylinder, and there will be a very small air velocity created by the difference of densities which will corresponds to very small heat transfer enhancement. When the shroud is slender the fluid that rises will be replaced by fluid entering from the bottom opening of the channel. He found that the heat transfer was increased when the height of the wall was very large compared to the diameter of the cylinder and the distance between

the walls that run along the length of the cylinder was the smallest. The increase of heat transfer was 40% for the most extreme channel shape. When the wall spacing was 10 times the cylinder diameter there was no significant increase in heat transfer from the cylinder's surface. The reason was that the air velocity, due to density differences, was very small when the channel's width was ten times the cylinder's diameter. The different insulation placed on the walls did not have any effect on the heat transfer enhancement even though the temperature distribution along the wall was different for the three types of insulation used. It was concluded that the temperature distribution along the height of the shrouds was due to natural convection from the moving fluid rather than radiation from the cylinder to the surrounding walls.

1.3 Objective

The aim of this thesis is to experimentally investigate the enhancement of heat transfer in relation to the following parameters

- Air injection rate
- Air injection configuration
- Shroud shape
- Shroud distance
- Air injection distance
- Water circulation only

Three different size heat pipes were immersed in a water tank and electrically heated by two 750 watts cartridge heaters, the temperature of the heat pipes and

water was measured at different power inputs and the heat transfer coefficient was calculated. The same procedure was followed when air was injected into the tank at different rates and distances. Shrouds were also placed around the heat pipe to direct the flow pattern of the rising air bubbles. The enhancement of heat transfer coefficient was as much as 500% in low power inputs and 300% at higher power inputs at the most extreme configuration which give a good agreement with the existing results by Gusev and Shklover, [15].

1.4 Need for this Research

Even though there is a lot of existing research in this topic, there are several differences on the techniques and experimental procedure used in these experiments from the ones published in the papers. Significant differences are: the use of a heat pipe as the means of heat transfer from an outside power source to inside the water tank; the use of shrouds in directing the flow of bubbles around the heat pipes and; the single injection pipe used to inject air at different rates and distances.

In the available literature the cylinder immersed in liquid was heated in two ways. Either it was electrically heated through conduction by a low resistance wire coiled in the inside surface of the hollow cylinder or through convection by hot water flowing through the cylinder at different rates. In this thesis a very efficient heat transfer device, the heat pipe, was used. In the literature air was injected using single air injection nozzles or a series of nozzles connected to an air supply compressor, in this thesis the air is injected from a pipe with series of openings, that can be adjusted to form different injection configurations. To the knowledge of this

author, the use of different shroud shapes to direct the flow of air bubbles around the heat pipe has not been investigated by other researchers.

1.5 Industrial Applications

There have been a lot of industrial applications for heat pipes this century. Space vehicles use them to dissipate the heat obtained from the sun keeping the vehicle at relatively safe temperatures, computers, solar collectors and heat exchangers are some other ways where heat pipes are utilized. Using the techniques described in this thesis the efficiency for these applications could be improved. The industry that can benefit most from this research is the nuclear power industry and in more detail the power generator on the nuclear power plants. In most plants the generator is cooled by a stream of water injected on the bottom surface of the generator. When power failure occurs the constant supply of this stream of water is cut-off and the temperature rises to levels that are fatal to the equipment within the generator. An alternative is to immerse the lower half of the generator in a tank of water and use the techniques described here to remove excess heat from the generator during power down situations.

CHAPTER 2

THEORETICAL BACKGROUND OF TWO-PHASE FLOW

2.1 Theoretical Background

The basic equations for conservation of mass, momentum and, energy are developed by applying the fundamental principles pertaining to mass, momentum and, energy to a control volume of fluid around the heat pipe (Thomas, p. 391). Since the fluid surrounding the heat pipe has two components (water and air) the fundamental principles should be applied for each component separately. "Moreover the balance equation for the single component will have to account for the mass, momentum and, energy exchange between the two components" (Kakac, p. 1230) . The equations that result from applying the fundamental principles are very complicated and computer software packages are needed to solve them. Sabre 1 and Sabre 3 are computer programs developed specifically for solving two phase flow problems using finite difference approximations.

The aim of this thesis is not to find an exact solution to these partial differential equations but rather to start with the basic equations that describes the mass, momentum and, energy exchange of a control volume simplified them, and non-dimensionalize them. Once the non-dimensional analysis is applied a set of dimensionless parameters will arise. The objective of this thesis is to determine how these parameters correlate in terms of heat transfer enhancement. Traditionally the dimensionless analysis should be done for each component (air and water) within the

control volume separately but since an exact solution for these equations is beyond the scope of this thesis, the fundamental principles will be applied to the mixture of fluid surrounding the heat pipe which will arise to one equation for mass, momentum and, energy.

2.1.1 Conservation of Mass Equation

The coordinate system used for the equations bellow are cylindrical because the diameter of the cylinder is small compared to the width of the water tank. According to Pfeil, [32], if the width of the water tank is more than ten times the diameter of the cylinder then it is assumed that the cylinder is in an infinite tank.

The conservation of mass equation (equation 2-1) is applied to the control volume shown in figure 2-1

$$\sum \dot{m}_{in} = \sum \dot{m}_{out} + \frac{\Delta m}{\Delta t} \qquad \text{Equation (2.1)}$$

for steady state conditions the last term in equation (2.1) becomes zero. Using the definition of partial derivative equation (2.1) becomes

$$\frac{1}{r}\frac{\partial}{\partial r}(r\rho u_r) + \frac{1}{r}\frac{\partial}{\partial \theta}(\rho u_\theta) + \frac{\partial}{\partial z}(\rho u_z) = 0 \qquad \text{Equation (2.2)}$$

Equation (2.2) written in tensor notation takes the form

$$\nabla \cdot (\rho u) = 0 \qquad \text{Equation (2.3)}$$

where u = the velocity vector

∇ = the divergence

ρ = the density of the mixture.

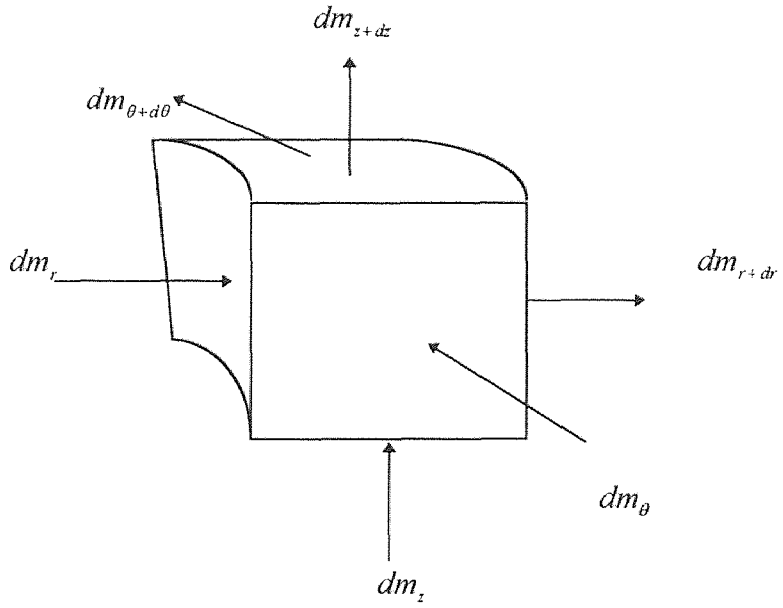

Figure 2-1 Control volume of fluid adjacent to heat pipe

2.1.2 Conservation of Momentum Equation

To develop the conservation of momentum equation Newton's second law of motion (summation of forces in each direction is equal to the rate of change of momentum in that direction) is applied to the control volume shown in figure 2-1

$$\sum F_i = \frac{\partial}{\partial x_i}(mu_i) \qquad \text{Equation (2.4)}$$

For fluids Newton's second law leads to the famous Navier-Stokes equation

$$\rho\frac{DV}{Dt} = -\nabla P + F + \mu\nabla^2 V \qquad \text{Equation (2.5)}$$

where P = pressure

F = gravitational (buoyancy) force

V = velocity vector

ρ = density of fluid inside control volume

$$\frac{D}{Dt} = \frac{\partial}{\partial t} + V \cdot \nabla$$

$$\nabla^2 = \frac{\partial^2}{\partial r^2} + \frac{1}{r}\frac{\partial}{\partial r} + \frac{1}{r^2}\frac{\partial^2}{\partial \theta^2} + \frac{\partial^2}{\partial z^2}$$

The term on the left hand side of equation (2.5) is called the substantial or material derivative and represents the acceleration. To simplify the equation steady state is assumed, and pressure gradient exists in the Z direction only. Equation (2.5) written out in full (for Z direction only) becomes:

$$\rho\left[\frac{\partial u_z}{\partial t} + u_r\frac{\partial u_z}{\partial r} + \frac{u_\theta}{r}\frac{\partial u_z}{\partial \theta} + u_z\frac{\partial u_z}{\partial z}\right] =$$

$$F_z - \frac{\partial P}{\partial z} + \mu\left[\frac{\partial^2 u_z}{\partial r^2} + \frac{1}{r}\frac{\partial u_z}{\partial r} + \frac{1}{r^2}\frac{\partial^2 u_z}{\partial \theta^2} + \frac{\partial^2 u_z}{\partial z^2}\right] \qquad \text{Equation (2.6)}$$

Similar expressions are written for the radial and circumferential directions.

2.1.3 Conservation of Energy

The conservation of energy equation is derived by applying the first law of thermodynamics (rate of creation of energy equals zero) to the control volume. The general heat transfer equation is as follows:

$$\sum \dot{E}_{IN} = \sum \dot{E}_{OUT} + \frac{\Delta E}{\Delta t} \qquad \text{Equation (2.7)}$$

and in differential form it becomes

$$\frac{\partial Q}{\partial t} + \Phi + \nabla \cdot (k \nabla T) - \nabla \cdot q_r = \rho \left(\frac{De}{Dt} + P \frac{D}{Dt} \left(\frac{1}{\rho} \right) \right) \qquad \text{Equation (2.8)}$$

where e = internal energy

k = thermal conductivity

T = temperature

P = Pressure

Q = internal heat generation

q_r = radiation heat flux vector

ρ = density

Φ = Mechanical or viscous dissipation.

The mixture inside the control volume is assume to be in steady state, there is no mechanical or viscous dissipation, no radiation and has constant thermal conductivity and density. After all these assumptions take place equation (2.8) reduces to

$$k \nabla^2 T = \rho \frac{De}{Dt} \qquad \text{Equation (2.9)}$$

where $e = cT$ and c is the specific gas coefficient. Substitution yields

$$k \nabla^2 T = c \rho \frac{DT}{Dt} \qquad \text{Equation (2.10)}$$

or written out in full it becomes

$$k \left(\frac{\partial^2 T}{\partial r^2} + \frac{1}{r} \frac{\partial T}{\partial r} + \frac{1}{r^2} \frac{\partial^2 T}{\partial \theta^2} + \frac{\partial^2 T}{\partial z^2} \right) = c \rho \left(\frac{\partial T}{\partial t} + u_r \frac{\partial T}{\partial r} + \frac{u_\theta}{r} \frac{\partial T}{\partial \theta} + u_z \frac{\partial T}{\partial z} \right)$$

Equation (2.11)

2.2 Dimensionless Analysis

2.2.1 Background

Dimensionless analysis is very important in the fluid mechanics and heat transfer area. "It is the only way to correlate data taken from a model to a prototype. If there is geometric similarity, flow pattern, and dimensionless parameters between the model and the prototype the size of the model it is not important" (Brighton, p. 85). The most popular technique for dimensionless analysis is the Buckingham Pi Theorem. This theorem requires that all the relevant variables to a given problem are known. Then these variables are combined together to form dimensionless groups. "According to Buckingham's theorem, the maximum number of dimensionless groups equals the number of physical variables minus the number of fundamental dimensions required to define the dimensions of those variables" (Brighton, p. 85). The advantage of this technique is that one does not have to know the differential equations that describe the flow or energy exchange of the model with its surroundings to find the dimensionless numbers. This is extremely helpful when complex geometry or phase changes are involved. There is a restriction to this technique. If any extraneous variables are introduced or a relevant one is missing it will lead to an erroneous analysis. Another technique that is widely used for dimensionless analysis is the differential equation technique. This technique requires the analyst to know the differential equations that describe the flow or energy exchange of the model with its surroundings. Once these equations are found or derived they are put into dimensionless form by non-dimensioning each term or variable in the equation. When this takes place a set of non-dimensional parameters

arise. These parameters can be grouped together to form dimensionless numbers. The data taken in the experiments will be presented in terms of these dimensionless numbers. The differential equation technique is safer than Buckingham's Pi Theorem and will be used to determine the dimensionless parameters that affect this problem.

2.2.2 Non-Dimensional Form of the Continuity Equation

Because of the complexity of the equation that describe this problem a set of simplified assumptions, called Boussinesq assumptions, will be used. This analysis assumes that (Ronald p. 321):

- density is constant in the continuity and momentum equation except in the body force term;
- density gradients are caused only by composition and temperature gradients;
- time-steady convection exists;
- all other properties are constant.

After all these assumptions take place the non-dimensional form of the continuity equation simply becomes

$$\nabla' \cdot u' = 0 \qquad \text{Equation (2.12)}$$

where

$$\nabla' = \frac{D}{r}\frac{\partial}{\partial\left(\frac{r}{D}\right)} + \frac{D}{r}\frac{\partial}{\partial\theta} + \frac{\partial}{\partial\left(\frac{z}{D}\right)}$$

and

$$u' = \left(\frac{ru_r}{DU_\infty}\right) + \left(\frac{Du_\theta}{U_\infty}\right) + \left(\frac{u_z}{U_\infty}\right)$$

D is a characteristic dimension of the model such as the heat pipe's diameter and U_∞ is the velocity of the mixture outside the hydrodynamic boundary layer.

2.2.3 Non-Dimensional Form of Momentum Equation

The conservation of momentum equation is

$$\rho\frac{Du}{Dt} = -\frac{\partial P}{\partial z} + \rho g + \mu\nabla^2 u \qquad \text{Equation (2.13)}$$

where

$$\frac{Du}{Dt} = \frac{\partial u}{\partial t} + u\cdot\nabla u \qquad \text{Equation (2.14)}$$

The first term of equation (2.14) represents the change at a fixed point in the fluid and the second term, the convective term, accounts for changes following the motion of the fluid. Since the assumption of steady state is made the first term becomes zero and the density takes the value of the mixture residing outside the boundary layers and it becomes ρ_∞. Making the mentioned simplification and substitution, equation (2.14) becomes

$$\rho_\infty(u\cdot\nabla u) = \rho g - \frac{\partial P}{\partial z} + \mu\nabla^2 u \qquad \text{Equation (2.15)}$$

The variable density is expanded in a Taylor series in terms of temperature and, composition gradients.

$$\rho = \rho_\infty + (T - T_\infty)\left(\frac{\partial \rho}{\partial T}\right)_{P_\infty, w_\infty} + (w - w_\infty)\left(\frac{\partial \rho}{\partial w}\right)_{P_\infty, T_\infty} +$$

$$(T - T_\infty)^2\left(\frac{\partial \rho}{\partial T}\right)^2_{P_\infty, w_\infty} + (w - w_\infty)^2\left(\frac{\partial \rho}{\partial w}\right)^2_{P_\infty, T_\infty} +$$

$$\left(\frac{\partial \rho}{\partial w}\right)_{P_\infty, T_\infty}\left(\frac{\partial \rho}{\partial T}\right)_{P_\infty, w_\infty}(w - w_\infty)(T - T_\infty) + \ldots\ldots\ldots \quad \text{Equation (2.16)}$$

The second and third terms of the Taylor series can be omitted because they represent a very small change in density. The term w in equation (2.16) stands for the mass fraction of the liquid (mass of gas phase divided by the total mass of the mixture). Making the mentioned simplifications equation (2.16) becomes

$$\rho = \rho_\infty + (w - w_\infty)\left(\frac{\partial \rho}{\partial w}\right)_{P_\infty, T_\infty} + (T - T_\infty)\left(\frac{\partial \rho}{\partial T}\right)_{P_\infty, w_\infty} \quad \text{Equation (2.17)}$$

Where ρ represents the density of the mixture and is defined as

$$\rho = \rho^1 + \rho^2 \quad \text{Equation (2.18)}$$

where ρ^1 = partial density of liquid phase

ρ^2 = partial density of gas phase

Partial density of a component is defined as

$$\rho_i = \frac{m_i}{V} \quad \text{Equation (2.19)}$$

where V = the total volume the different components in the mixture occupy

m_i = mass of ith component

ρ_i = density of ith component

Substitution of equation (2.16) into equation (2.15) yields

$$u \cdot \nabla u = -\frac{1}{\rho_\infty}\frac{\partial P}{\partial z} + \nu \nabla^2 u + \frac{1}{\rho_\infty}\frac{\partial \rho}{\partial T}(T - T_\infty)g + \frac{1}{\rho_\infty}\frac{\partial \rho}{\partial w}(w - w_\infty)g \quad \text{Equation (2.20)}$$

It is convenient to introduce the compressibility coefficients

$$\beta_t = -\frac{1}{\rho_\infty}\left(\frac{\partial \rho}{\partial T}\right)_{p_\infty, W_\infty} \quad \text{Equation (2.21)}$$

and

$$\beta_w = -\frac{1}{\rho_\infty}\left(\frac{\partial \rho}{\partial w}\right)_{P_\infty, T_\infty} \quad \text{Equation (2.22)}$$

Substituting these equations into equation (2.20)

$$u \cdot \nabla u = -\frac{1}{\rho_\infty}\frac{\partial P}{\partial z} + \nu \nabla^2 u - \beta_t(T - T_\infty)g - \beta_w(w - w_\infty)g \quad \text{Equation (2.23)}$$

Making equation (2.19) non-dimensional

$$u' \cdot \nabla' u' = -\frac{\partial P'}{\partial z'} + \frac{1}{\mathrm{Re}}(\nabla')^2 u' - \frac{Gr_t}{\mathrm{Re}^2}T' - \frac{Gr_w}{\mathrm{Re}^2}w' \quad \text{Equation (2.24)}$$

where $P' = \left(\frac{P - P_\infty}{\rho_\infty g D}\right)$

$$z' = \frac{z}{D}$$

$$T' = \left(\frac{T - T_\infty}{T_s - T_\infty}\right)$$

$$w' = \left(\frac{w - w_\infty}{w_s - w_\infty}\right)$$

with u' and ∇' same as before

Three important dimensionless groups arise from this non-dimensional analysis of the conservation of momentum equation and those are the Reynolds Number

(Re), the thermal Grashof Number (Gr_t) and, the composition Grashof Number (Gr_w), where

$$\mathrm{Re} = \frac{U_\infty D}{\nu}$$

$$Gr_t = \left(\frac{D^3 \beta_t (T_s - T_\infty) g}{\nu^2} \right)$$

$$Gr_w = \left(\frac{D^3 \beta_w (w_s - w_\infty) g}{\nu^2} \right)$$

In natural convection we assume either isothermal mass transfer (Gr_t=0) or uniform composition heat transfer (Gr_w=0)

2.2.4 Non-Dimensional Form of the Energy Equation

The non-dimensional form of the energy equation simply becomes

$$\frac{D\phi}{Dt} = \frac{1}{Pe} (\nabla')^2 \phi \qquad \text{Equation (2.25)}$$

or written out in full it becomes

$$\frac{\partial^2 \phi}{\partial \left(\frac{r}{D} \right)^2} + \frac{D}{r} \frac{\partial \phi}{\partial \left(\frac{r}{D} \right)} + \left(\frac{D}{r} \right)^2 \frac{\partial^2 \phi}{\partial \theta^2} + \frac{\partial^2 \phi}{\partial \left(\frac{z}{D} \right)^2} =$$

$$\frac{1}{Pe} \left(\frac{\partial \phi}{\partial \left(\frac{tU_\infty}{D} \right)} + \frac{u_r}{U_\infty} \frac{\partial \phi}{\partial \left(\frac{r}{D} \right)} + \frac{u_\theta D^2}{r U_\infty} \frac{\partial \phi}{\partial \theta} + \frac{u_z}{U_\infty} \frac{\partial \phi}{\partial \left(\frac{z}{D} \right)} \right) \qquad \text{Equation (2.26)}$$

where

$$Pe = \frac{D U_\infty \rho c}{k}$$

and

$$\phi = \left(\frac{T - T_{\infty}}{T_s - T_{\infty}} \right)$$

An important dimensionless group arising from this equation is the Peclet number and it can be written in term of the Prandtl number and Reynolds number

$$Pe = \mathrm{Pr}\,\mathrm{Re} \qquad \text{Equation (2.27)}$$

"When simplifying the energy equation it was assumed that the mixture inside the control volume was in thermodynamic equilibrium at every moment. This assumption is not ideally valid but it presents a sensible approximation as far as the complex system of fluid mixture is concerned" (Kakac p. 1231).

2.3 Dimensionless Parameters

There are eleven dimensionless parameters that arise from non-dimensionalyzing the three partial differential equations among which are dimensionless time, pressure, distance, diameter, and length. The four distinct dimensionless numbers discovered are: the Reynolds Number (Re), Prantdl number (Pr), Grashof composition number (Gr_w) and, Grashof thermal number (Gr_t). For the problem under consideration we will assume that a particle has constant surface temperature which makes Gr_w become zero (Gr_w=0).

These numbers have physical meaning. The Reynolds number is a measure of the ratio of the inertia to viscous forces. When the Reynolds number is small the viscous forces dominate and when the Reynolds number is large inertia forces dominate. The Prandtl number is a ratio of hydrodynamic diffusion to thermal

diffusion. The Grashof number is a ratio of the buoyancy force to the viscous force. In natural convection data is usually presented in terms of Nusselt and Rayleigh numbers. The Rayleigh number is the product of the Grashof and Prandlt numbers and it represents the ratio of buoyancy forces to change in viscous forces in the boundary layer. Traditionally, the dimensionless form of the coefficient of heat transfer is the Nusselt number, which may be defined as the ratio of the convective heat transfer to fluid conduction heat transfer under the same conditions. From the conservation equation, a dimensionless grouping of Gr/Re^2 is observed. This is the ratio of the buoyancy force to the inertia force.

As mentioned in chapter one, when a heated surface is immersed in a cold fluid heat is being convected away and this convection is called natural convection because it occurs without the help of any mechanical devices. When mechanical devices are used, like a blower or a pump, to direct a fluid over a heated surface this process is called forced convection. When both the effects of natural and forced convection are significant in a heat transfer process then it said to have mixed convection. Mixed convection is divided into three sections

- Free convection is dominant when the $Gr \gg Re^2$. Forced convection can be omitted.
- Forced convection is dominant when $Re^2 \gg Gr$. Free convection can be omitted.
- Both free and forced convection have to be accounted for when $Re^2 \cong Gr$.

2.4 Uncertainty Analysis

The equipment used to get the data when the experimental data (thermocouple meter, volt meter and, amp meter) was taken have a degree of uncertainty associated with them. The uncertainty for the thermocouple reading is ± 5%, for the volt meter ± 2% and, for the amp meter ± 2% of the full scale reading. The error created by these uncertainties could be considerable when low power inputs are used or the temperature difference between the thermocouples on the heat pipe and the fluid is very small. The equation for the heat transfer coefficient is

$$h = \frac{P \cdot I}{A_s\left(T_w - T_\infty\right)} \qquad \text{Equation (2.28)}$$

where P = voltage reading

I = current reading

A_s = surface are of heat pipe immersed in water

T_w = average surface temperature of heat pipe

T_∞ = average temperature of water

To find the uncertainty of equation (2.28) its partial derivative has to be taken with respect to the measured quantities. Taking the partial derivative of equation (2.28) we get

$$w_R = \left[\sum_{i=1}^{\infty}\left(\frac{\partial h}{\partial x_i} w_i\right)^2\right]^{1/2} \qquad \text{Equation (2.29)}$$

where w_R = uncertainty of heat transfer coefficient

$\frac{\partial h}{\partial x_i}$ = partial derivative of equation (2.28) with respect to ith quantity

w_i = uncertainty of ith component

written out in full equation (2.29) becomes

$$w_R = \left[\left(\frac{\partial h}{\partial P} w_p \right)^2 + \left(\frac{\partial h}{\partial I} w_i \right)^2 + \left(\frac{\partial h}{\partial (T_w - T_\infty)} w_{(T_w - T_\infty)} \right)^2 \right]^{1/2} \qquad \text{Equation (2.30)}$$

where $\dfrac{\partial h}{\partial P} = \dfrac{I}{A_s (T_w - T_\infty)}$

$$\frac{\partial h}{\partial I} = \frac{P}{A_s (T_w - T_\infty)}$$

$$\frac{\partial h}{\partial (T_w - T_\infty)} = -\frac{P \cdot I}{A_s (T_w - T_\infty)^2}$$

w_p = 0.02 * volt reading

w_i = 0.02 * amp reading

$w_{(T_w - T_\infty)}$ = 0.05 * temperature difference

The equation to calculate the error is

$$Error = \left(1 - \frac{(h - w_R)}{h} \right) \cdot 100\% \qquad \text{Equation (2.31)}$$

The error for our experiments is on the average 6%. The uncertainty will be indicated in the Nusselt number versus Rayleigh number graphs (appendix A, B, C, D) by vertical bars on the different points of the curves.

CHAPTER 3

EXPERIMENTAL APPARATUS AND PROCEDURE

3.1 Experimental Apparatus

This chapter gives a detailed description of the equipment used to carry out the experiments and collect the data. A list of the equipment used is shown below.

- Staco variable transformer, range 0-120/140 volts
- 2704A Thermometer, maximum temperature 200 °C
- Cartridge heater, model CIR-30301, capacity 750 watts
- 20 gallon glass aquarium
- T-type thermocouples, range -200 °C to 1250 °C
- Air flow meters, models VFB and VFA, range 0.2-200 SCFH
- Speedaire pressure regulator, model 4Z028, range 0-150 psig
- Heat Pipe, HP-1, 0.75 inch diameter, range 40-180 °C, capacity 450 watts
- Half inch thick fiberglass plates, maximum temperature 200 °F
- Heat pipe 0.4375 inch diameter, range 70-220 °F, capacity 80 watts
- Copper curved shaped shrouds, maximum temperature 650 °F
- Heat pipe, HP-1, 0.5 inch diameter, range 70-220 °F, capacity 250 watts
- Aluminum cylindrical and rectangular stainless steel heaters, maximum temperature 800 °F

A flow chart of the experimental apparatus is given in figure 3-1

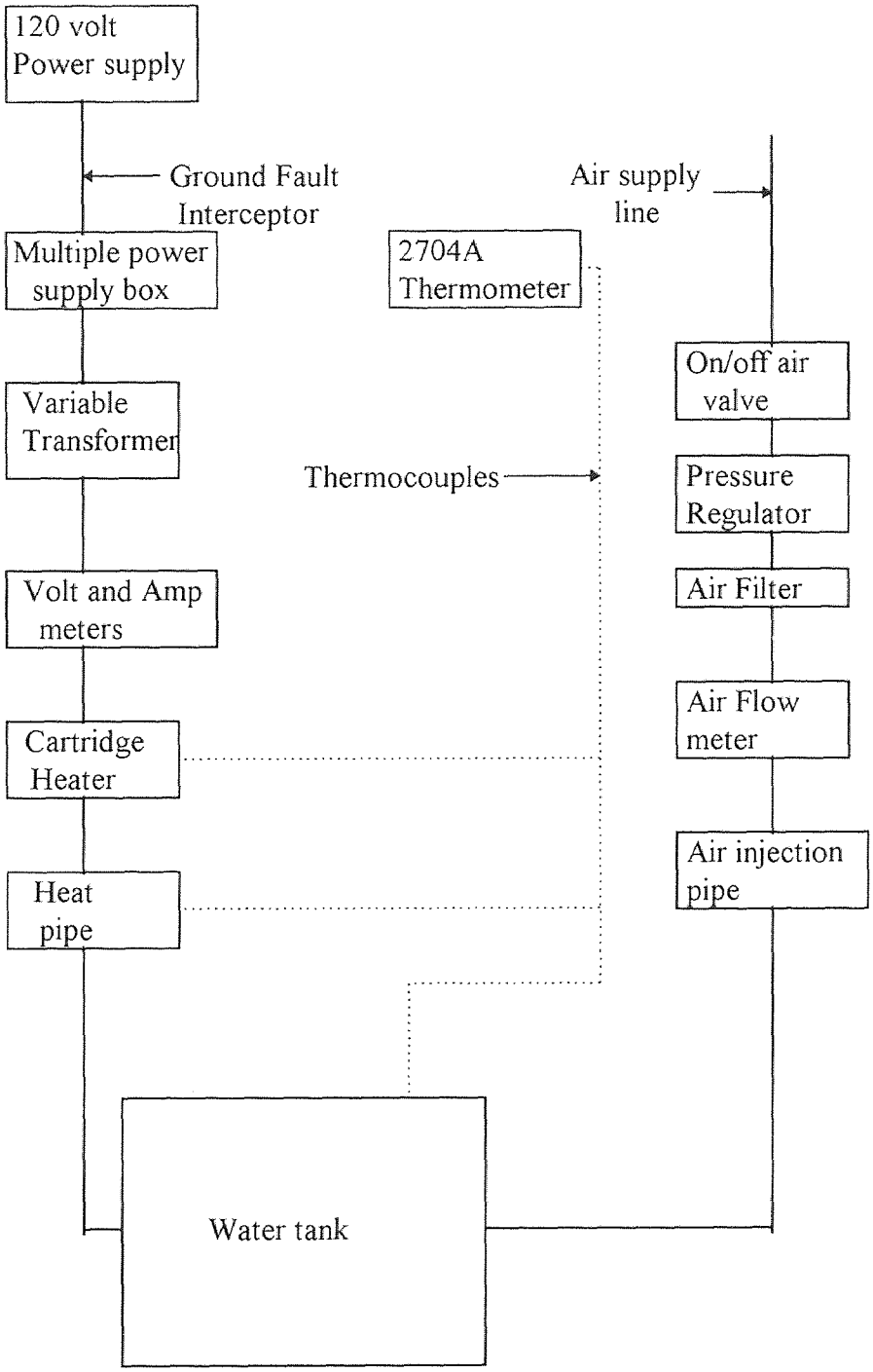

Figure 3-1 Flow chart of experimental apparatus

3.1.1 The Heat Pipes

Heat pipes were used to transfer heat from an outside source to inside the tank. There were three different size and capacity heat pipes used in these experiments.

The first heat pipe was made from stainless steel and it was 7/16 inches in diameter, 15 inches long with a heat capacity of about 80 watts. The second heat pipe (HP-1) was made from copper and it was 0.50 inches in diameter, 18 inches long with a heat capacity of 250 watts. The third heat pipe (also a HP-1) was 0.75 inches in diameter, 18 inches long with a heat capacity of 450 watts. The reasons for using heat pipes as means of transferring heat to the water inside the tank are:

- there are no moving parts making the heat pipe maintenance free
- high thermal conductance, as much as ten times the conductance of copper at the same size
- the surface temperature is virtually the same throughout the length and circumference of the pipe

"Heat pipes operate by continuous evaporation and condensation of a fluid in an enclosed pipe lined with a wicking material. Gas fills the hollow core whereas liquid saturates the wicking material" (Thomas, p. 621). When heat is supplied in one end of the pipe (evaporator section), the fluid evaporates and travels down the length of the pipe where the heat is rejected and the vapor condenses (condenser section). Condensation takes place because the temperature of the pipe at the other end is slightly less than the temperature at the heat addition end. The fluid circulating within a heat pipe is shown in figure 3-2.

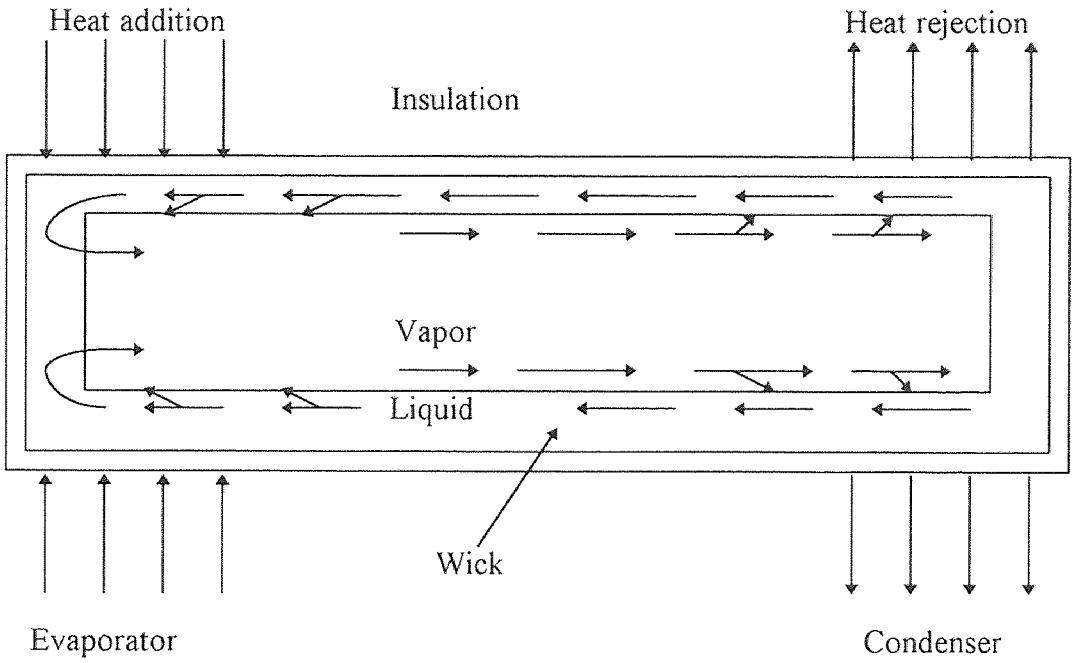

Figure 3-2 Flow of working fluid in a heat pipe

The circulation is caused by (Cole, p. 923):

- the evaporation of the fluid in the heated portion of the wick
- the condensation of fluid back into the cooled section of the wick
- capillary liquid flow within the wick

If the length of the pipe is small this cycle takes a very small amount of time to be completed thus creating nearly an isothermal surface throughout the heat pipe.

The heat pipe's working temperature and heat transfer capacity depends in the wicking material, the surface area of the heat pipe and, the working fluid. The stainless steel heat pipe used first in the experiments had ammonia as working fluid and a carbon sintered wick. The HP-1 heat pipes had water as working fluid and the wicking material was made from a carbon mesh screen.

3.2.2 The Air Flow Meters

The air flow meters purchased for these experiments were a VFB-55-SSV meter with flow range of 20-200 Standard Cubic Feet per Hour (SCFH), a VFA-4-BV with flow range of 0.2-2 SCFH and, a VFA-5-BV with flow range of 2-20 SCFH. These were obstruction meters with a ball indicating the flowrate of the air, inside a tapered tube mounted vertically to a calibrated scale. The diameter of the float is slightly less than the inside diameter of the tube creating an annular passage. The air flows from the bottom to the top of the meter, lifting the float to a point were the opening between the float and the tapered tube is large enough for the air to pass through the meter. The forces involved as the float comes to an equilibrium position are

1. The weight of the float, acting downwards
2. The velocity pressure of the air multiplied by the projected area of the float, acting upwards
3. The buoyancy of the float, acting upwards
4. Viscous aerodynamic drag of the air on the float, acting upwards

A calibrated scale is placed behind the tube and when these forces come into equilibrium a reading is recorded from the middle of the float. The VFB model has an accuracy of ± 3.0 % and the VFA models had and accuracy of ± 5.0 % full scale reading. The VFB model was ordered with a brass metering valve for precise adjustments and was connected in series with the two VFA models. A schematic of the VFB flow meter is shown in figure 3-3. A pointer flag was also purchased with the VFB flow meter for reproducible flow rates and more precise readings on the

scale. To get rid of the impurities in the air supply an air filter was connected in series with the flow meters. A pressure regulator was also connected in series to decrease the pressure of the air supply line (100 psig) to the air flow meter.

In all the experiments available through the literature the air was injected in the water tank by individual air nozzles. In these experiments the air was injected in the water tank from a ten inch long CPVC pipe, 3/4 inch in diameter with a series of holes drilled on the top. To allow for different air injection configurations these holes were taped shut with duct tape or with copper screws of the same diameter as the openings. The size of each individual opening was 3/36 inch in diameter which is small compared to the diameter of the air pipe. This resulted in a small pressure drop along the length of the pipe. Thus the amount of air released from each opening was the same, resulting in a uniform rate of bubble creation along the length of the pipe. There were fifteen holes drilled at intervals of 0.65 inches. The average bubble diameter departing from these holes was 10 mm. The diameter of the air bubbles became smaller as the air injection rate decreased which made it easier for the smaller bubbles to penetrate the thermal boundary layer. The pressure differential between the injected air and water (hydrodynamic pressure) resulted in a pressure impulse to be created every time a bubble is being release by the injection pipe. This impulse travels along the length of the supply line in the opposite direction of the flow and it creates an oscillation of the meters' float. This oscillation was not very vivid at the high air injection rates but it became a problem when the 0.5 SCFH injection rate was used.

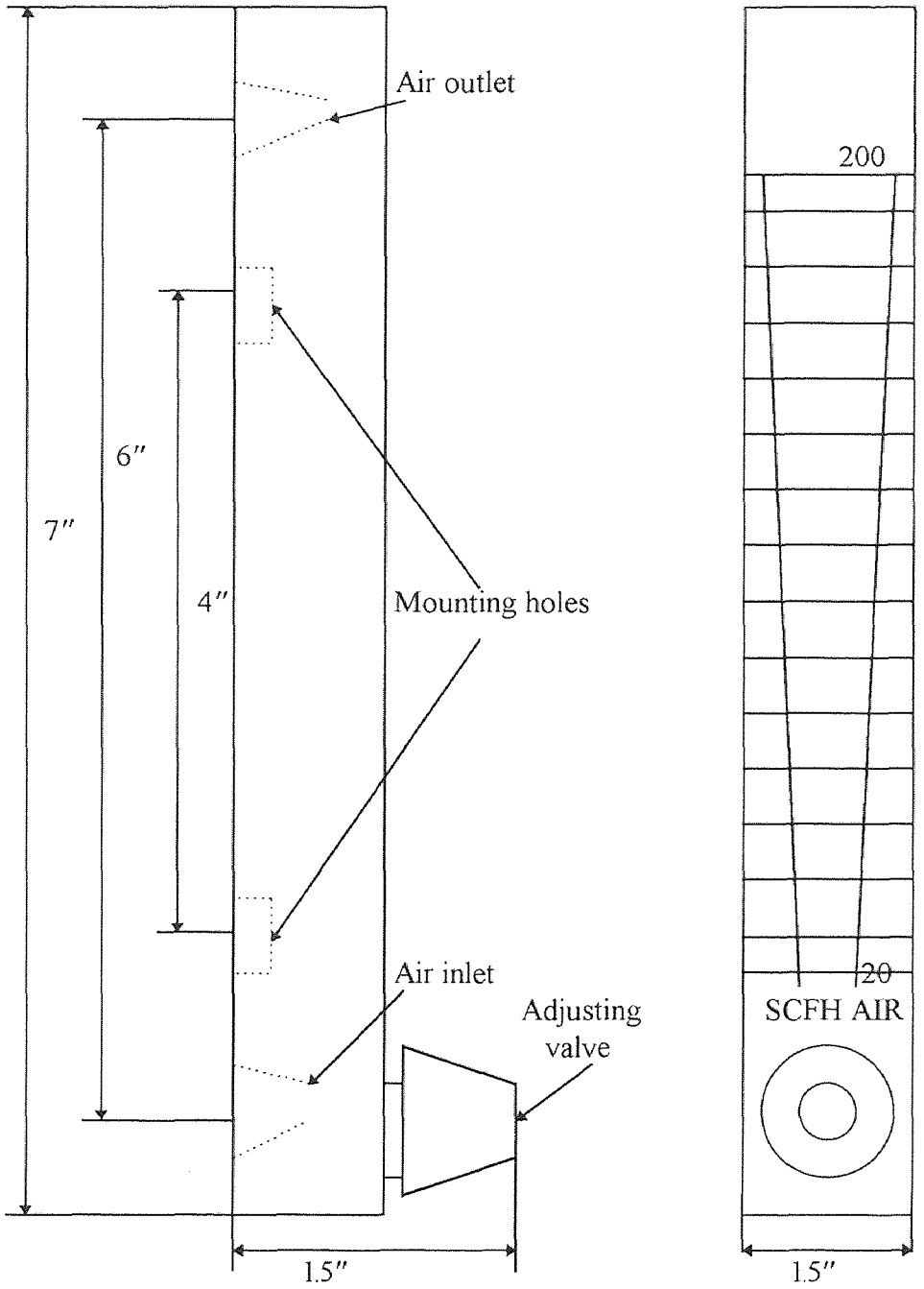

(a) Side view of air flow meter

(b) Front view of flow meter

Figure 3-3 Side and front view of air flow meter

To direct the flow pattern of the air bubbles around the heat pipe, either curved or straight shrouds were used. The curved shape shrouds were made from a two inch hollow copper pipe, ten inches long and 0.125 inches thick. The pipe was cut in half and the two halves were soldered together as to create a S shape shroud. Two thin strips of copper were silver soldered six inches apart on each shroud. Holes were drilled in these strips, 1/8 inches in diameter, and the shrouds were screwed onto a wooden base which was long enough to overlap with the plexiglas plates. The base rested on top of the plexiglas plates which allowed for variable distances of the shrouds from the heat pipes. The straight shrouds were made from half-inch thick plexiglas, and they were four inches tall by ten inches long. Figure 3-4 and 3-5 gives a pictorial representation of the straight and curved shrouds respectively. Figure 3-6 shows the front views of the shrouds as they were inserted in the water tank.

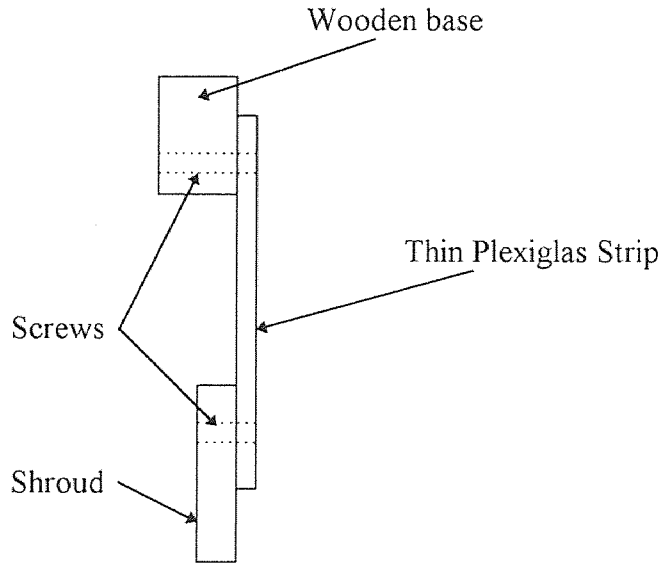

Figure 3-4 Pictorial representation of straight shroud

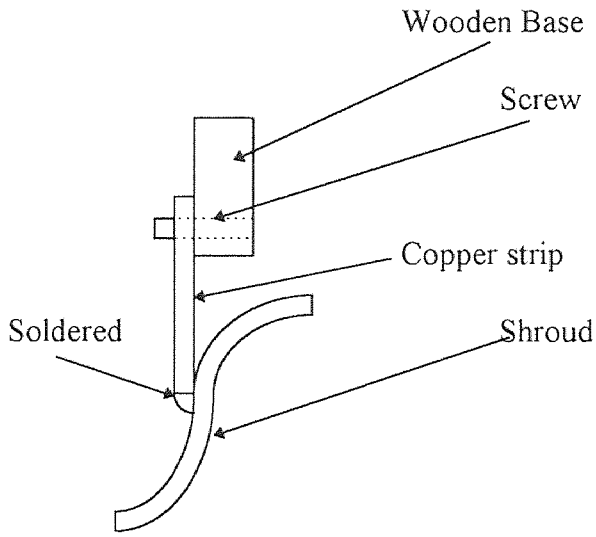

(a) Front view of curved shroud

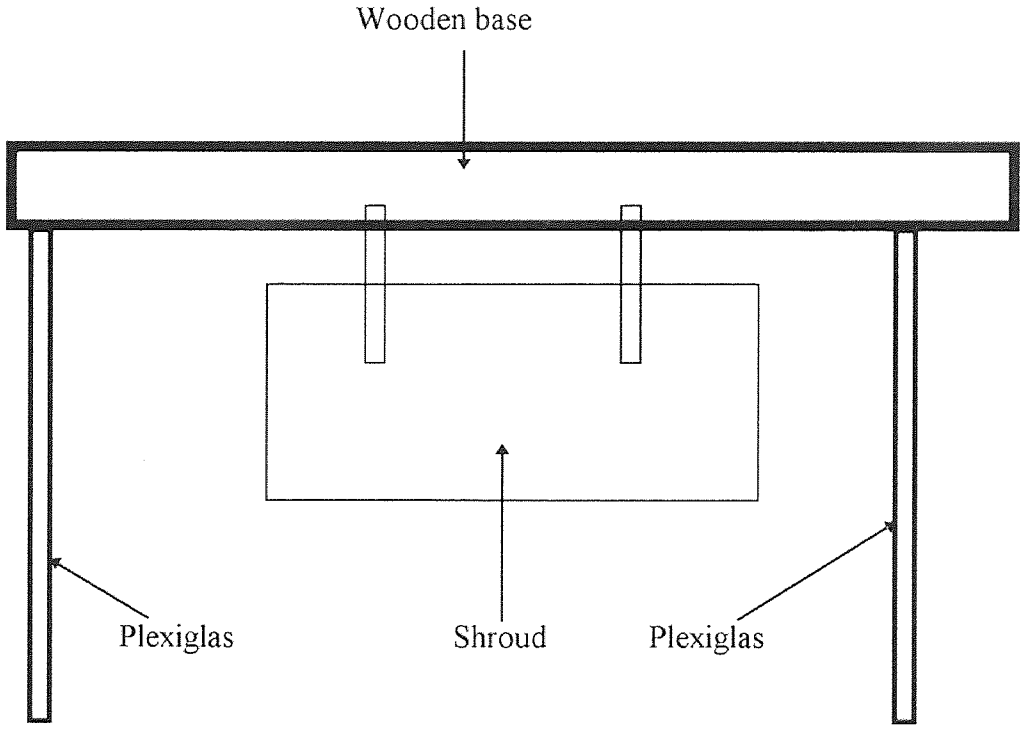

(b) Side view of shroud

Figure 3-5 Schematic of shroud with base

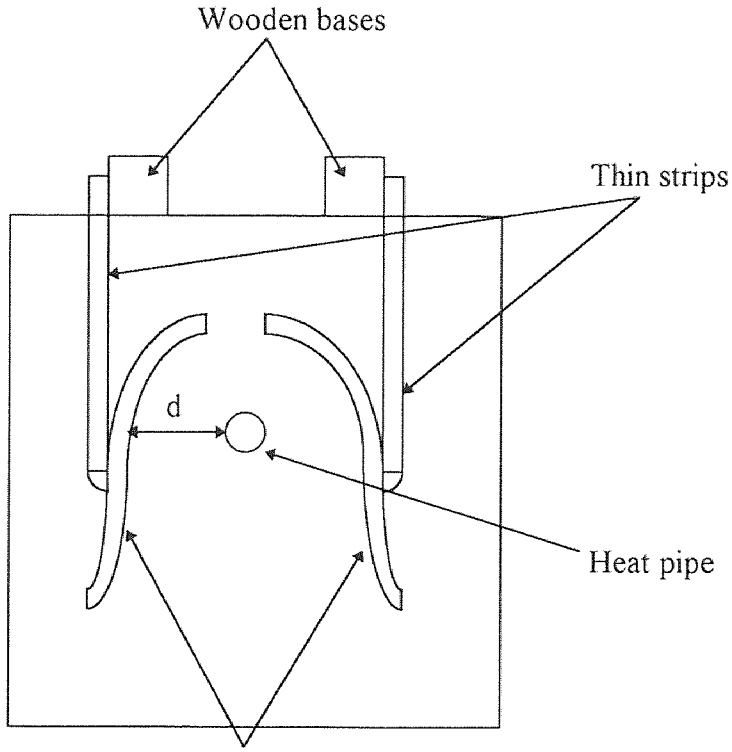

(a) End view of curved shrouds

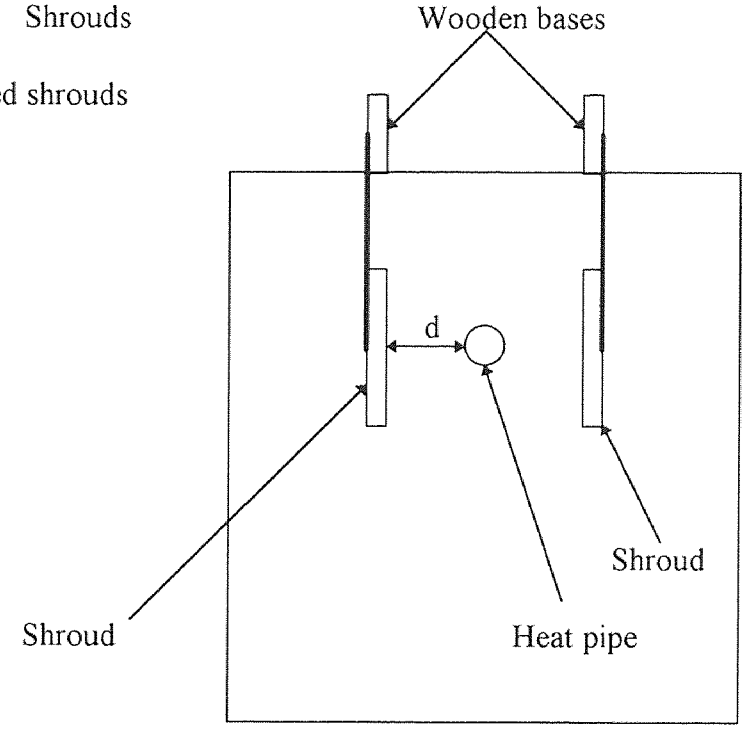

(b) End view of straight shroud

Figure 3-6 End views of curved and straight shrouds

3.1.3 The Water Tank

The tank used for these experiments was a 20 gallon glass aquarium. The lengths of the heat pipes were purposely selected to be less than length of the aquarium for the following reasons. First, the heat capacity of the pipes were too small to heat the water, inside the original size of the tank, to high temperatures. Second, for safety reasons it is easier to drill holes through plastic plates than through the aquarium's glass. Finally, if the heat pipe does not go all the way through the tank the pipe will act as a fin and the heat transfer from the end of the fin will be significant. The overall heat transfer coefficient will be a function of the heat transferred from the circumference of the pipe and from the end. To simplify the analysis, either insulation is placed at the end, or the heat pipe has to be long enough to assume it as an infinite length fin where the end effects do not account for a significant amount of heat transfer. To avoid this problem the overall length of the tank was reduced by inserting two plexiglas plates inside the water tank.

The length of the tank was decreased by twelve inches once these two Plexiglas plates (12 inches wide 16 inches tall and half inch thick, six inches form each end of the tank) were inserted. The corners of the Plexiglas were sanded so that the bottom sides of the plates made a tight contact with the bottom of the tank. Before the Plexiglas was placed in the tank two holes (one in each plate) were drilled. The size of the holes were half inch in diameter for the 7/16" heat pipe, 11/16" for the 0.5" heat pipe and 17/16" for the 0.75" heat pipe. These holes were drilled eleven inches from the bottom of the tank to allow for a wide range of air injection distances, and the heat pipes were far enough from the surface so that the

surface tension of the fluid will not to be factor on the heat transfer augmentation. A schematic of the water tank with the Plexiglas plates and the heat pipe is shown in figure 3-7.

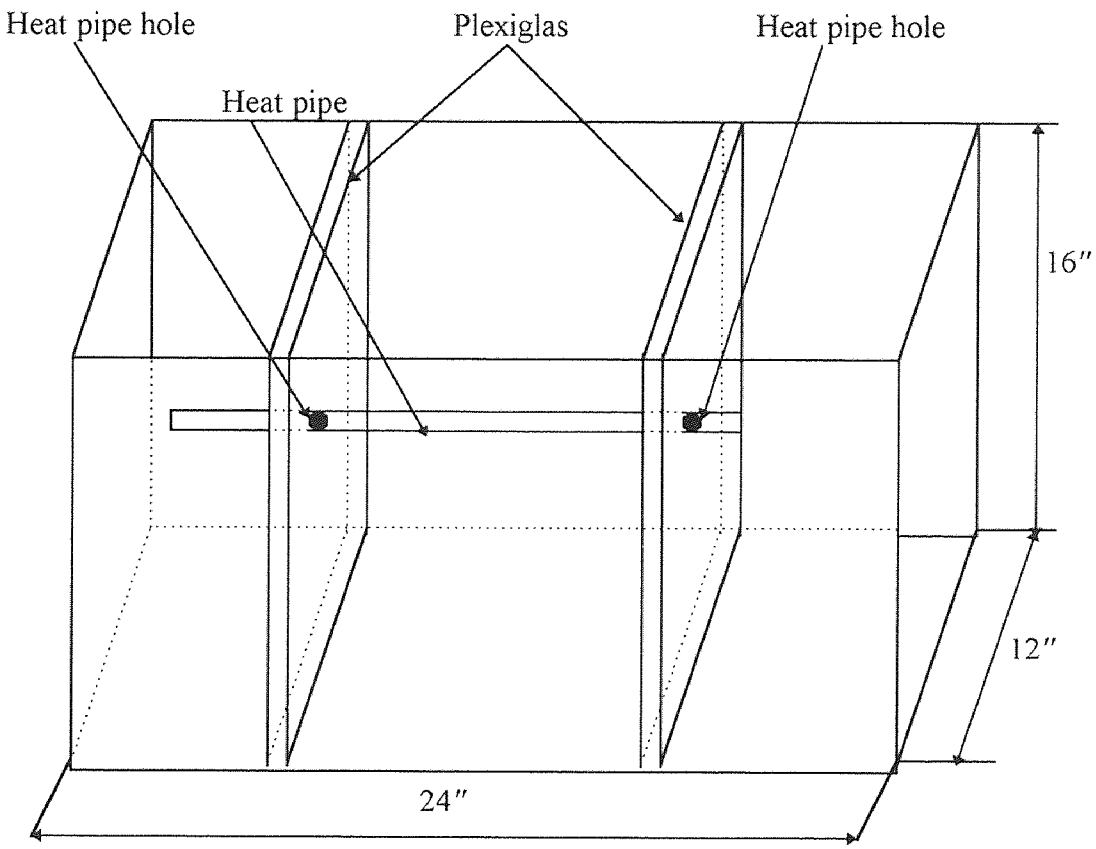

Figure 3-7 Isometric view of water tank with Plexiglas plates and heat pipe

The heat pipes with their o-rings were inserted through the holes and glued into place with silicon caulk. The o-rings were place around the heat pipes to prevent water from leaking, they were made from Teflon and were selected for their insulation properties and resistance to high temperature ranges. Silicon caulk was placed in the base of the Plexiglas as the plates were inserted into the tank. Silicon

was also placed on both sides of the Plexiglas plates (that made contact with the tank's glass) to prevent water from leaking and to stabilize the plates. To avoid any accidents while working with high temperatures, silicon caulk was also placed on top of the original epoxy of the tank.

Insulation was placed between the heater and the Plexiglas to protect the plastic plate from the high temperatures of the heater. Insulation was also placed on the opposite side of the tank to minimize the heat lost resulting from the overhang of the heat pipe. The insulation used was Fiberglas with a resistance value of R-11 and it was 3.5 inches thick. The water tank was not insulated because there was no other means of removing the heat given away by the heat pipe other than radiation or convection from the surface of the tank or the fluid.

3.1.4 The Heater and Cartridges

The heater block for the HP-1 heat pipes was made from a stainless steel rectangular block, three inches wide by three inches tall and four inches long. The heat pipe hole, drilled in the mid-plane of the block, was four inches deep. The cartridges holes were 3.25 inches deep and were offset by 1 inch (center-to-center distance) from the heat pipe hole. The heater block was screwed together by using two thin steel plates, each with four holes drilled into them. This heater block was first machined for the half-inch diameter heat pipe and then the hole was modified to accommodate the 0.75 inch heat pipe. A schematic of this heater block is shown in figure 3-8.

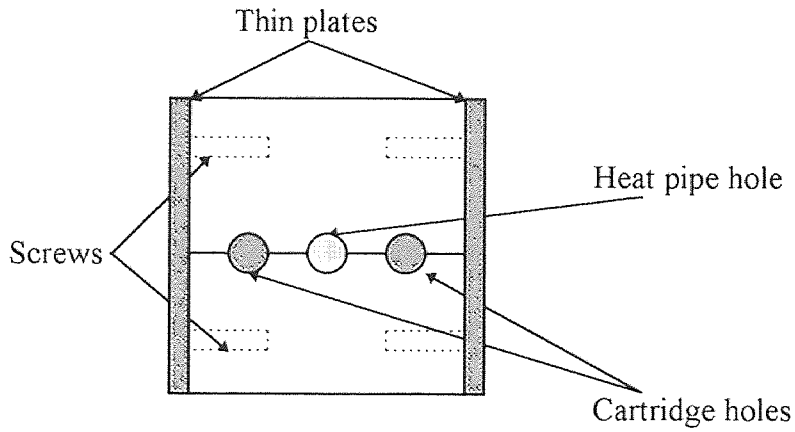

(a) Front view of rectangular heater block

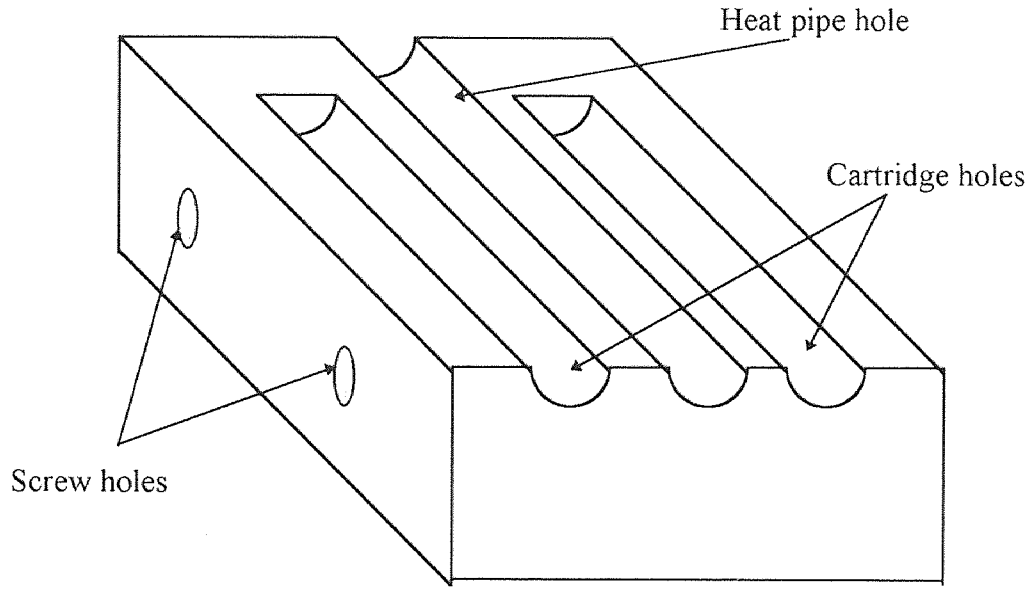

(b) Isometric view of half the rectangular heater block

Figure 3-8 Schematic of the rectangular heater block

The material used to make the cylindrical heater (for the 7/16 inch ammonia heat pipe) was an aluminum solid pipe two inches in diameter. The pipe was cut four inches long and three holes were drilled into it. The cartridge holes were offset from the centerline of the aluminum pipe by 5/8 inches and they were drilled on the back side of the heater. The heat pipe hole was coincided with the centerline and was drilled on the front side. The cartridge holes are half inch in diameter and 3.25 inches deep whereas the heat pipe hole was 7/16 inches in diameter and only 1.25 inches deep. Once the holes were drilled the pipe was cut in half through the centerline. The reason for choosing aluminum was its temperature range (up to 800 °F) and its machinability and relatively high thermal conductivity. The heat pipe, heater and cartridges were clamped together using two automotive type clamps. Figure 3-9 shows a schematic of the cylindrical heater. Figure 3-10 shows a schematic of the tank with the heater attached to it. The surfaces where cutting and drilling took place were rough and the contact between the different surfaces was not ideal. To improve the contact surface between the heater and the heat pipes and cartridge heater, the holes were sanded using aluminum oxide sanding paper. A heat sink compound (TYPE 44) was also used for good thermal contact. The compound had a continuous operating temperature of 100 °C and a range of -40 °C to 200 °C.

The cartridges used for these experiments were two 750 watt, 120 volt CIR-30301 cartridges with type "F" manganese nickel wires. The surface temperatures of the cartridge heaters can exceed 1500 °F. The leads were insulated with Fiberglass wire which had a maximum operating temperature of 392 °F.

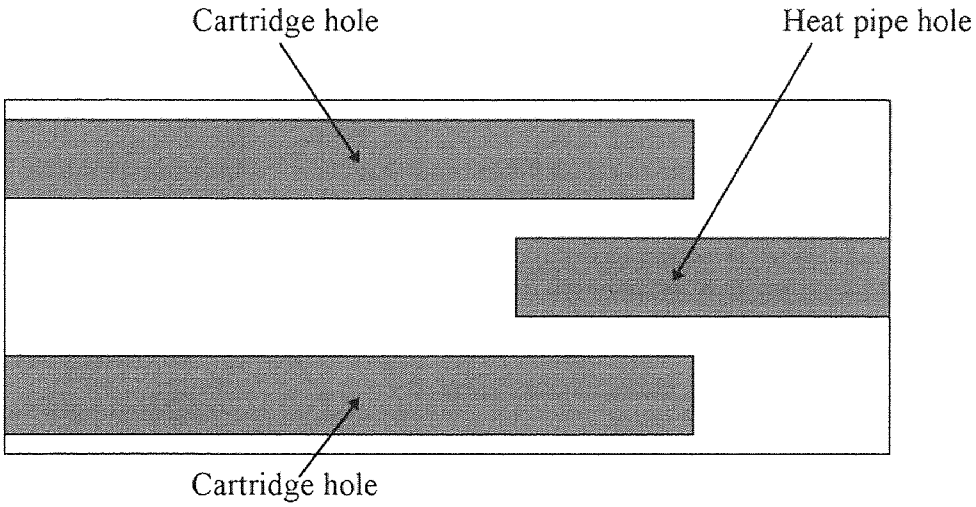

(a) top view of heater

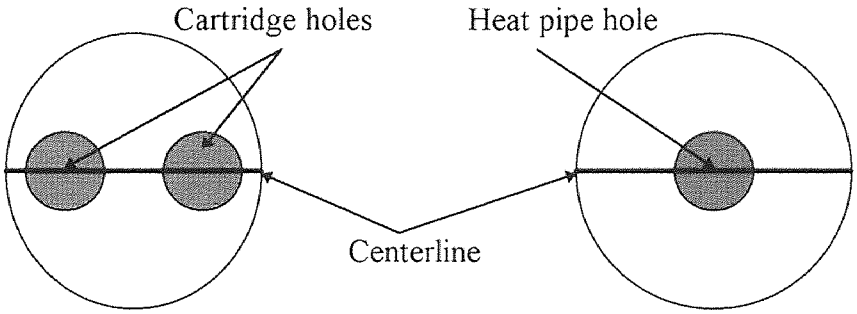

(b) back view of heater

(c) front view of heater

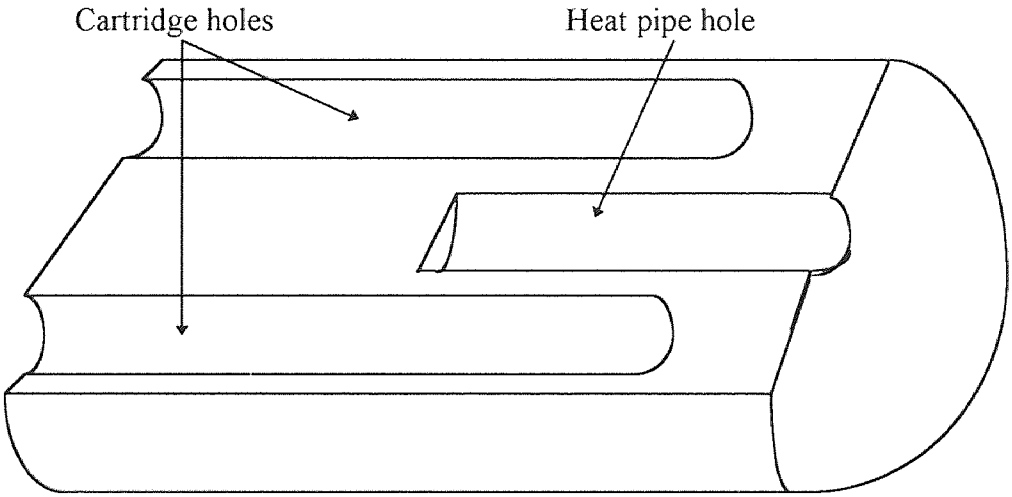

(d) Isometric view of heater

Figure 3-9 Four views of heater

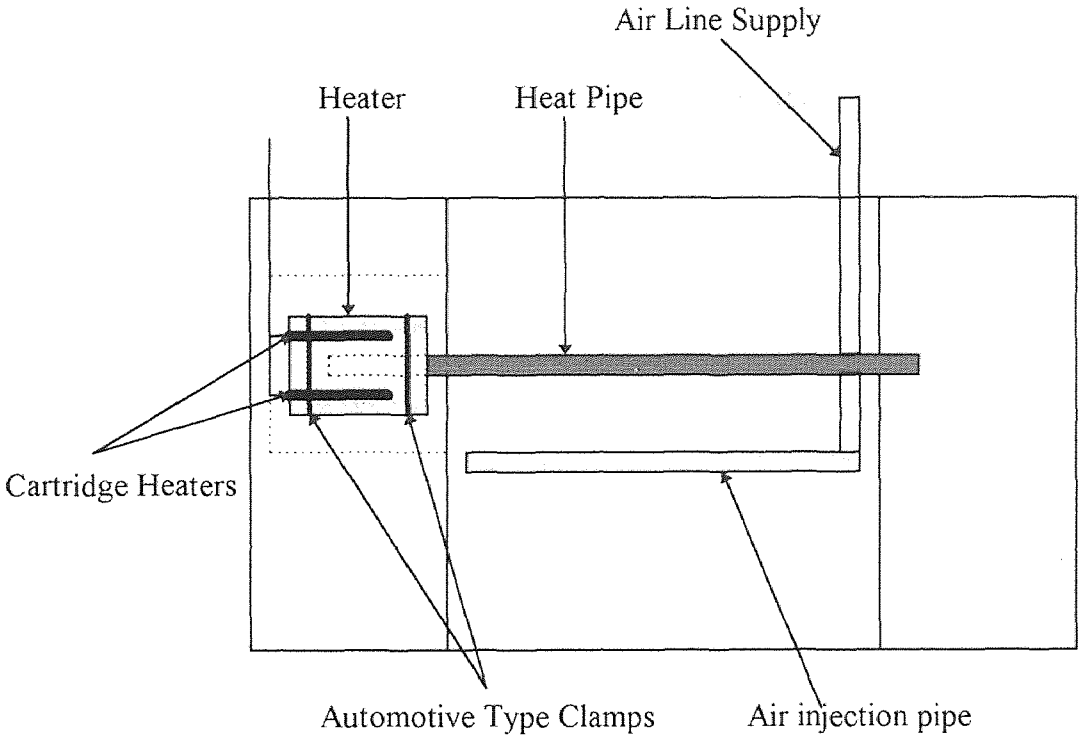

(a) Front View of water tank with heater, heat pipe and cartridges

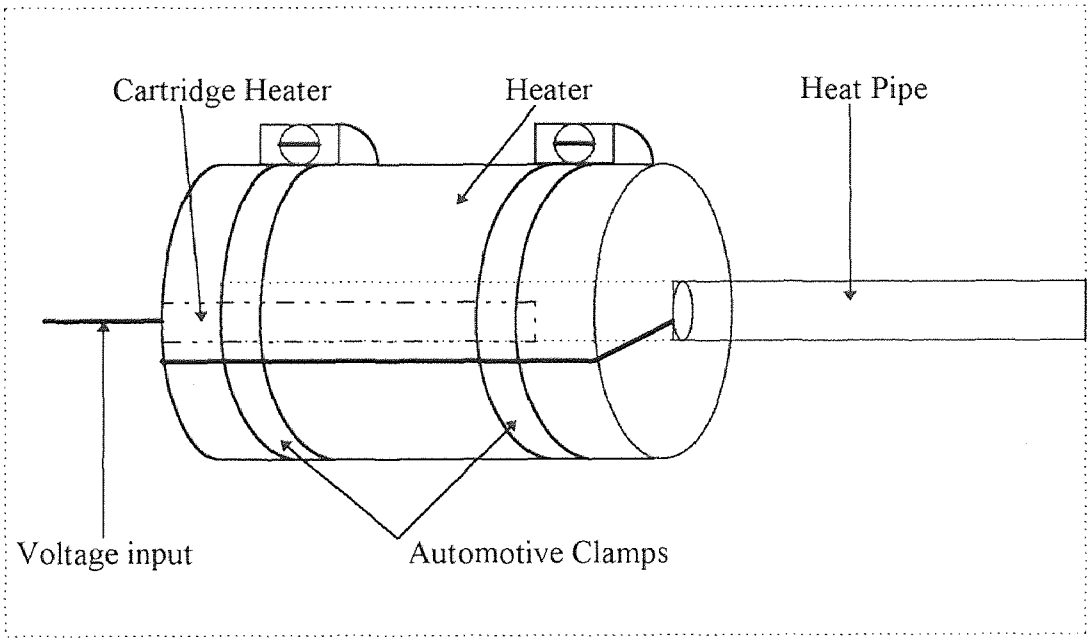

(b) Magnification of heater section

Figure 3-10 Side view of water tank with heater and heat pipe

3.1.5 The 2704A Thermometer

There were twelve K type thermocouples used to monitor the temperatures of the heat pipe, heater and, water. The readings of these thermocouples were taken using a twelve channel Thermo Electric switch box, a 80 TK Thermocouple module and a 2704A thermometer. The thermocouples were made in the lab using the same thermocouple wire. The thermocouples wire was cut at lengths of six feet and the leads were welded together using a thermocouple welder, model 116SRL. To improve the conductivity between the two leads of the thermocouple, the welder releases argon gas as the welding takes place. The thermocouples were capable of measuring temperatures in the range of 1250 °C but the meter could only read temperatures up to 200 °C. Calibration of the thermocouples took place in the beginning of the experiments. The thermocouples were taped together and they were dipped into an ice bath where their temperature was recorded. Their temperature was also recorded when they were dipped into a beaker with boiling water. The temperature in both cases was read from a mercury thermometer and was compared to the thermocouples' readings. All of the thermocouples gave a reading of 2.3 °C higher than the mercury thermometer and that number was subtracted from each reading when the data was taken.

3.2 Experimental Procedure

This section describes how each experiment ran and how was the data gathered, analyzed and presented in such a way as to be compared to existing literature. To determine a safe heat capacity for the heat pipes, they were heated in water for ten

hours carefully monitoring the surface temperature of the heater and heat pipe. Power was supplied to the heater at increments of 30 watts. When the surface temperature of the heater reached the 140 °C range the power was turned off and the amount of power previous to the cut off point was taken to be the allowable heat capacity of the heat pipe. To secure reproducible results the air injection position of the air pipe was controlled by two sets of concentric cylinders. One of the sets was glued to a wooden base and the other was clamped to the injection pipe. The wooden base was placed in the empty tank and the injection pipe cylinders were aligned with the base cylinders. The shroud's distance was duplicated by marking both edges of its base which made contact with the plexiglas plates.

Once the heater and cartridges were clamped or screwed into place with the heat pipe, fiberglass insulation was placed around and on both ends of the heater to minimize the loss of heat. Two small holes were cut through the insulation to allow for the cartridge's leads, the heater's thermocouple(s) and ground wire to be connected with the power supply or the switch box.

Three thermocouples were glued at intervals of three inches apart on the heat pipe. Five thermocouples were placed inside the water tank at intervals of two inches and various elevations and distances from the sides of the tank, two thermocouples were placed on the surface of the heater and two more at the outer surface of the insulation surrounding the heater. The power supplied to the cartridge heaters was controlled by an auto transformer which had a voltage range from 0 to 140 volts. To avoid any accidents (since the water was electrically

heated) a ground fault interceptor cable was used for power supply to the auto transformer. This cable will turn off the circuit if there is a detection of a hot to ground short. The output of the transformer was connected in series with a voltage and amp meter so the power supplied was calculated using the equation

$$Q = V \cdot I \cdot \cos\theta \qquad \text{Equation (3-1)}$$

where Q = Power

V = Voltage reading

I = Current reading

$\cos\theta$ = phase between current and voltage

the phase angle between the current and voltage was less than 1 degree which made the cartridge heaters almost 100% efficient.

Once the power had been recorded and steady state was reached a series of readings was recorded. Steady state is reached when the thermocouples on the heat pipe do not change their temperature readings more than ± 0.1 °C for two consecutive minutes or when the temperature difference between the heat pipe and water reached steady state.

Some of the power transferred to the cartridges is lost due to the internal resistance of the wires. This amount is very small and can be neglected. A small amount of the energy supplied by the heaters is lost due to the heat pipe's contact with the Plexiglas (conduction from the o-rings) and the insulation (1.50 inches of insulated heat pipe length at heater side, 0.25 inches of insulated heat pipe overhang at opposite side, insulation around and on both ends of the heater). The o-rings were made from Teflon which is a good heat insulator and the contact area between

the o-ring and the plexiglas was very small resulting in an insignificant amount of heat transfer. The heat lost through the insulation was calculated using either equation (3-2) for the cylindrical heater or equation (3-3) for the rectangular heater.

$$q_{radial} = -kA_s \frac{(T_s - T_o)}{\ln\left(\frac{r_o}{r_s}\right)} \qquad \text{Equation (3-2)}$$

$$q_{cylindrical} = -kA_s \frac{(T_s - T_o)}{L} \qquad \text{Equation (3-3)}$$

where k = thermal conductivity of insulation

T_s = surface temperature of heater (average of two thermocouple readings)

T_o = outside temperature of insulation (average of two insulation readings)

A_s = surface area of insulation

r_o = outside radius of insulation

r_i = inside radius of insulation

L = thickness of insulation

Even though the power lost through the insulation was insignificant compared to the amount supplied to the heat pipe, this amount was calculated and subtracted from the total amount supplied to the heater. The heat transfer coefficient is then calculated using the equation

$$h = \frac{P}{A(T_s - T_\infty)} \qquad \text{Equation (3.4)}$$

where h = heat transfer coefficient

P = Power supplied to the heat pipe

T_w , T_s = Surface temperature of heat pipe (average of three thermocouples)

T_∞ = Bulk fluid temperature (average of five thermocouples in water tank)

A = Surface area of heat pipe immersed in water (πDL)

D = Diameter of heat pipe

L = Length of heat pipe immersed in water

The heat transfer coefficient was calculated at different power inputs carefully monitoring the surface temperature of the heater. Once the heat transfer coefficient was found the Nusselt number was plotted versus the Rayleigh number

$$Nu = \frac{hD}{k} \qquad \text{Equation (3-5)}$$

and

$$Ra = \frac{\rho^2 c g \beta_l D^3 (T_w - T_\infty)}{k\mu} \qquad \text{Equation (3-6)}$$

where k = thermal conductivity of water

c = specific heat of water

g = gravity constant

β_l = coefficient of thermal expansion

ρ = density of water

μ = dynamic viscosity of water

The physical quantities of water were found using the thermodynamic tables at atmospheric pressure at an average bulk temperature of

$$T_{ave} = \frac{T_s + T_\infty}{2} \qquad \text{Equation (3.7)}$$

The same procedure was followed when the investigated parameters were varied. These parameters are:

1. Air injection rate
2. Shroud Shape
3. Air injection configuration
4. Shroud distance from heat pipe
5. Approach velocity of air bubbles
6. Water circulation

To evaluate the heat transfer enhancement due to different air injection rates the air pipe was placed underneath the heat pipe at a dimensioless distance of ten (Z/D =10) for the ammonia and 0.5 inch diameter heat pipes. The injection distance of Z/D=5 was used in the 0.75 inch heat pipe.

where Z = vertical distance between heat pipe and air injection pipe

D = diameter of heat pipe

The air valve was activated and air was supplied to the air pipe. The air injection rates varied (by adjusting the control valve located on bottom of the VFB flow meter) from 10 Standard Cubic Feet per Hour (SCFH) to 50 SCFH. No shrouds were placed in the tank, and the air injection configuration remained the same throughout the duration of these experiments.

The correlation between the enhancement in heat transfer and air injection configuration was investigated by injecting air at 10 SCFH from a dimensionless vertical distance of five (Z/D =5). First, five ports were left open on the air injection pipe and a set of data points were collected. Then the number of openings increased

to ten and finally fifteen. There were no shrouds in the tank during these experiments.

The effect of the approach velocity of the rising bubbles was explored by varying the vertical distance between the heat pipe and injection pipe. A vertical dimensionless distance of two, seven and ten units were investigated for the ammonia heat pipe, dimensionless distances of two, five and ten were experimented with for the 0.5 inch heat pipe and finally, distances of one, five and ten for the 0.75 inch heat pipe. The approach velocity of the bubbles increased as the distance between the heat pipe and air pipe increased. The approach velocity of the bubbles was not calculated due to precise equipment needed for the analysis. There were no shrouds in the tank and the air injection configuration and rate remained the same while these experiments took place.

The trend between shroud distance and heat transfer augmentation was investigated by lowering the S shape shrouds into the water at horizontal dimensionless distances (d/D) of one, two and four from the ammonia and 0.5 inch heat pipes and distances of one, and three for the 0.75 inch heat pipe.

where d = horizontal distance between shrouds and heat pipe

D = diameter of heat pipe

The air injection rate, Z/D distance and, air injection configuration stayed the same during these experiments.

The heat transfer enhancement due to different shroud shapes was investigated. First the curved shape shrouds were placed in the tank at a dimensionless distance of one (d/D=1) from the heat pipes. The Z/D distance was ten for the ammonia and

0.5 inch heat pipes. The Z/D distance was five for the 0.75 inch heat pipe. The straight shrouds were then placed in the water tank and the experiments were repeated. The injection rate was 50 SCFH for ammonia heat pipe and 10 SCFH for both HP-1 heat pipes.

The effects of heat transfer enhancement due to pure water circulation with and without shrouds in the tank was considered. The air injection pipe was placed at the same height as the heat pipe and air was injected at 10 SCFH.

Prior to each experiment the tank was emptied and cleaned to avoid any dust particles (from the air supply line or room) to reside in the surface of the liquid or heat pipe. Dust particles on the surface of the heat pipe will act as insulation whereas in they will alter the surface tension of the fluid if the reside in the surface. The water tank was carefully sealed with plastic film every time the experiments had to be completed the next day. For all the runs the water inside the tank was saturated with air before any heat was supplied to the heater. This was done by bubbling the water for twenty minutes before the experiments are ran which prevents any air from being absorbed by the water as the bubbles rise through the fluid.

CHAPTER 4

RESULTS AND DISCUSSION

After analyzing the data, a curve representing the natural convection conditions was graphed for each heat pipe. This curve was compared to the curves obtained from investigating the different heat transfer augmentation parameters mentioned in chapters one and three. The uncertainty of each point was not represented in these graphs to avoid confusion since several points of the curves lie close to each other. During the experiments of the last heat pipe (HP-1, 0.75" diameter) additional experiments were done for reasons given in the appropriate paragraph.

4.1 Air Injection Rate Effect

The air injection rates investigated in all three heat pipes were: 10 Standard Cubic Feet per Hour (SCFH), 30 SCFH and, 50 SCFH. Figure 4-1 represents the heat transfer enhancement due to these rates for the 7/16" ammonia heat pipe. The top curve represents the 50 SCFH air flow while the next two are for the 30 and 10 SCFH air flows respectively, the air injection distance was held constant at Z/D=10. The bottom curve represents the ammonia heat pipe under natural convection conditions. It is clearly seen that the heat transfer increases as the air injection rate increased. That does not mean that if the air injection rate increases indefinitely large the heat transfer coefficient will also keep increasing. There will be a maximum value the air flow can rise to before it will act as an insulation rather than an augmentation agent. This particular problem was not within the scope of this thesis and was not

investigated. Figure 4-2 represents the heat transfer enhancement for the 0.5" heat pipe at injection distance of ten (Z/D=10) and injection rates similar to the ammonia heat pipe. In this graph almost all of the curves are blend into each other with the 10 SCFH curve starting at the highest value. The 50 SCFH curve which starts at the same value as the 30 SCFH curve finishes at the lowest value which supports the point made earlier about an optimum air flow rate. It was discovered that at the higher air injection flow rates the heat pipe was more efficient and would carry more of heat supplied by the heater block. The temperature difference between the heat pipe and the water did not changed very much (this is very clear at the 0.75" heat pipe) for the different flow rates. This leads to the conclusion that the heat carried away by the increased amount of air bubbles due to conduction was lost in the environment when air bubbles disperse as they reached the surface of the water. The temperature difference between the water and heat pipe should have decreased at the higher injection rates since more heat is carried away (by conduction) from the increased amount of air bubbles. The air bubbles moved faster through the tank at the higher flow rates (due to improved water circulation and, larger size) and did not had the chance to loose the heat they gained by conduction with the heat pipe inside the tank. This conclusion is also supported by figure 4-3 where the two curves for the 30 and 50 SCFH are identical. The only difference between these experiments with the previous one is the injection distance is Z/D=5. I suspect that this optimum flow rate is a function of the fluids' height residing above the heat pipe and will increase as the depth of the heat pipe increases because this gives more time for the bubbles to get rid of the excess heat they picked up by conduction.

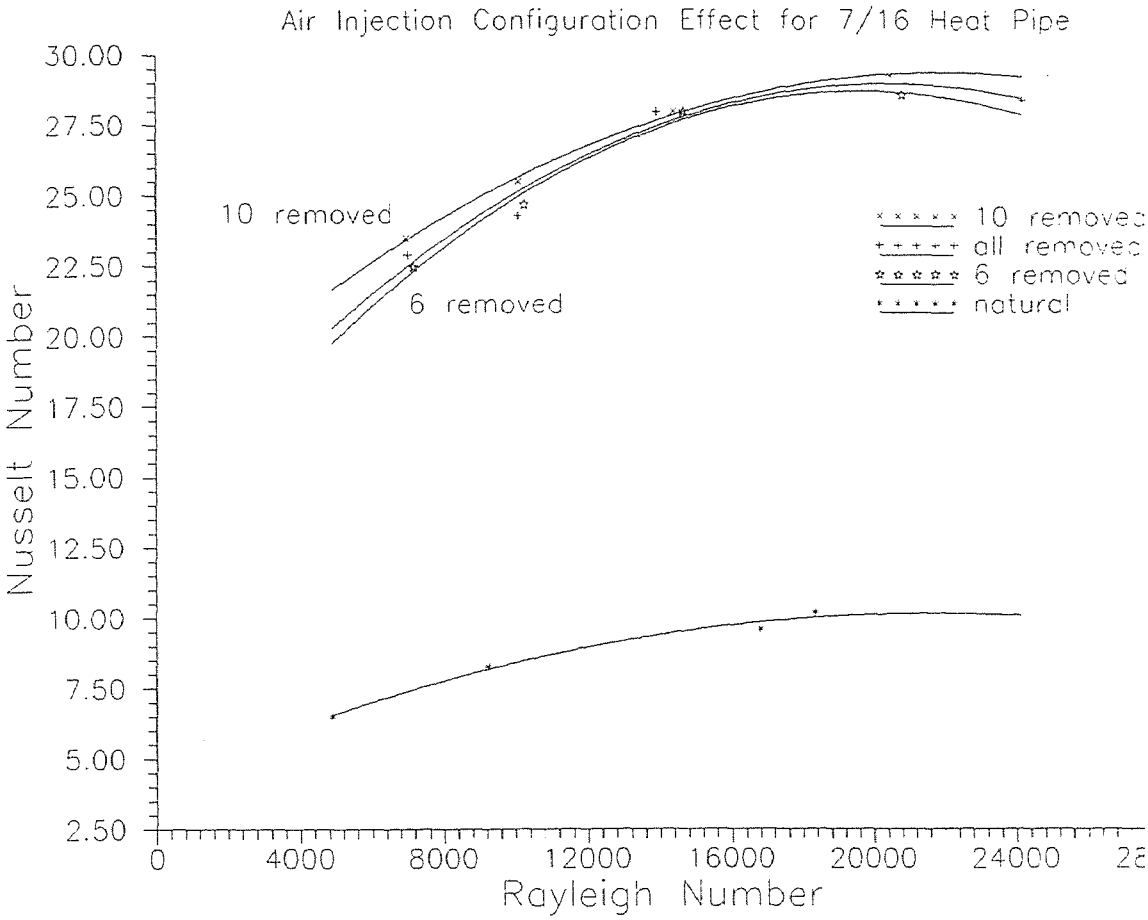

Figure 4-1: Air injection rates effect for 7/16" heat pipe.

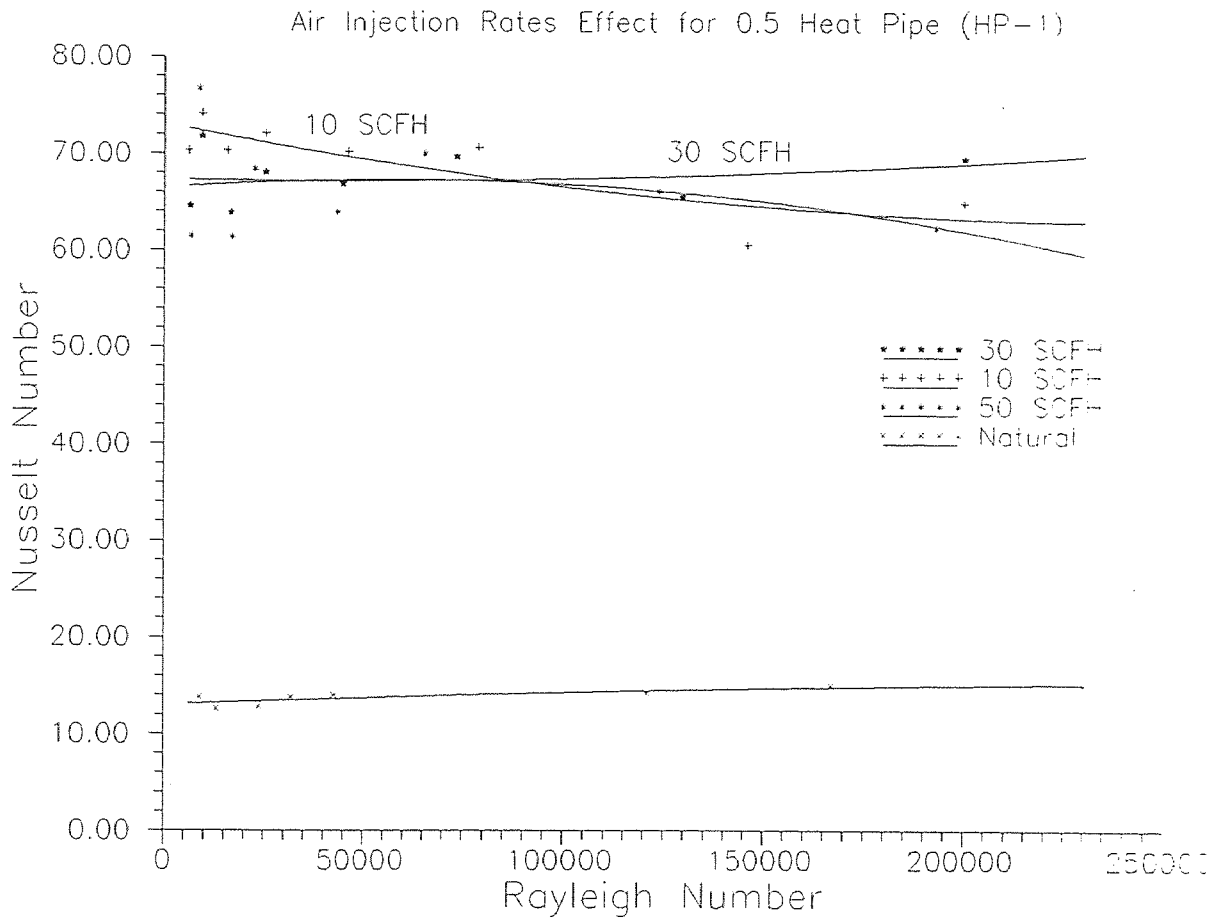

Figure 4-2: Air injection rates effect for 0.5" heat pipe.

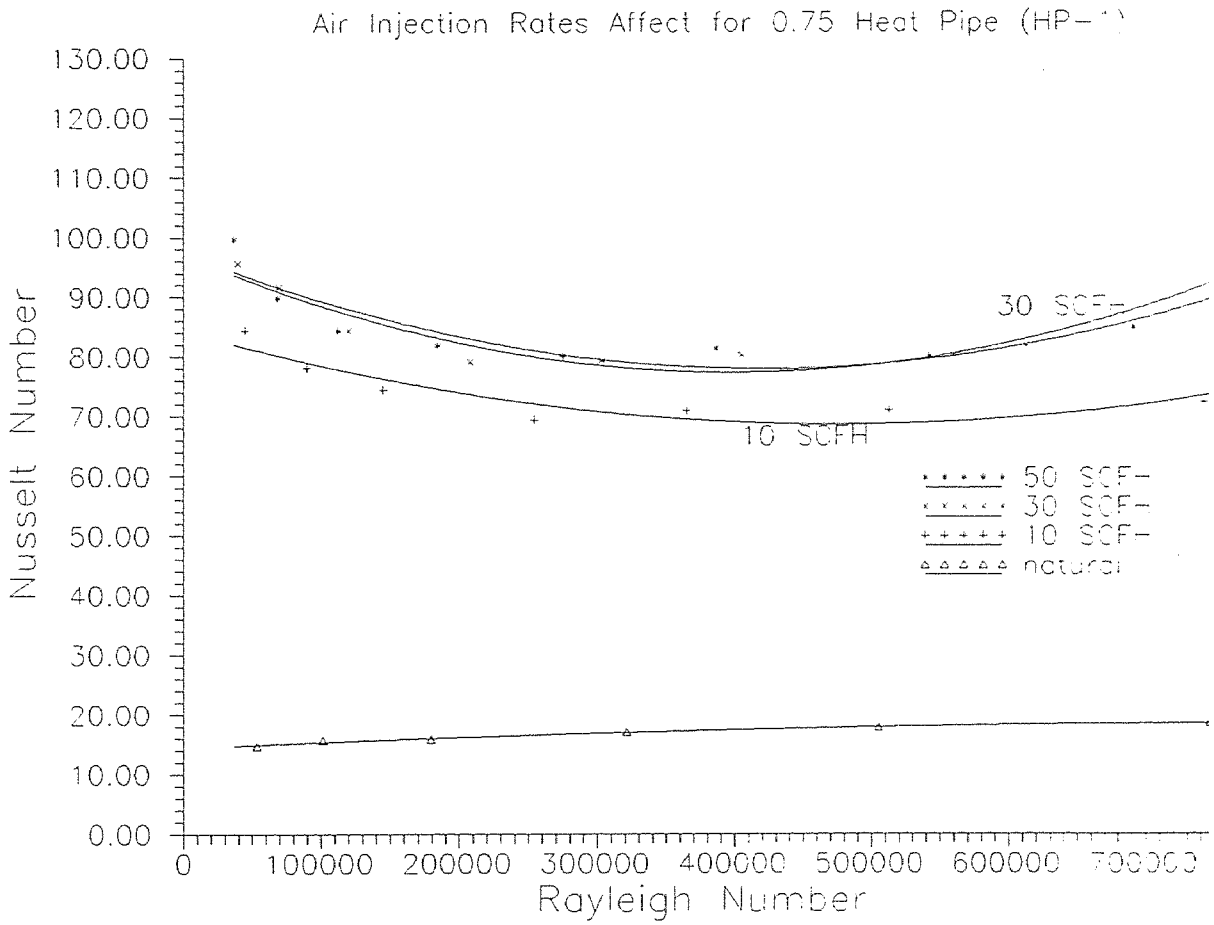

Figure 4-3: Air injection rates effect for 0.75" heat pipe

4.2 Air Injection Distance Effect

The next set of experiments investigated the effect of heat transfer augmentation on the injection distances between the heat pipes and air pipe. The first curve of figure 4-4 represents an air injection distance of Z/D=10 for the 7/16" heat pipe. The airflow was 50 SCFH for all three curves. The heat transfer enhancement was 500% at Z/D=10, 400% at Z/D=7 and, 300% at Z/D=2. It is clearly seen that the heat transfer strongly depends on the air injection distance and will increase as the distance between the heat pipe and air injection pipe increases. Here again there is an optimum point since the contributing factors of the heat transfer enhancement are both the turbulence created by the rising bubbles and, the conduction of the bubbles with the hot surface of the heat pipe. To find these two different terms one has to repeat the experiments using the same parameters but instead of aligning the air injection pipe with the heat pipe they should be purposely out of line so that the rising bubbles pass close but do not touch the heat pipe. This will give the heat transfer enhancement due to the bubble induced turbulence and if this term is subtracted from the original experiment the remaining term will represent the heat transfer by the bubbles due to conduction. Figure 4-5 shows the heat transfer enhancement for the 0.5" heat pipe at different injection distances. This enhancement was 250% for Z/D=2, 300% for Z/D=5 and, 400% when Z/D=10. Here it can be concluded that the heat transfer enhancement increases as the injection distance increases. The heat transfer is very large at low Rayleigh number but it decreases as the heat input increases. The reason for this observation is that the thermal boundary layer created around the heat pipe decreases in size as the heat input to the heat pipe increases.

This results in a smaller effect created by the turbulence of the rising bubbles thus decreasing the effect of this augmentation technique at the higher power inputs. Figure 4-6 shows the heat transfer enhancement due to air injection distances for the 0.75" heat pipe. The distances used were Z/D=1, Z/D=5 and, Z/D=10. The heat transfer enhancement was 350% for the Z/D=1 injection distance and about 400% for both the other two distances. This supports the point made earlier about an optimum injection distance since at Z/D=10 the air injection pipe was literally resting on the bottom of the tank (the tank is 10.5 inches deep from the lower surface of the heat pipe) which resulted in a smaller amount of bubbles touching the surface of the heat pipe as they rise through the fluid, virtually diminishing the heat conduction term of the bubbles and enhancing the heat transfer from the heat pipe by water turbulence only. The turbulence created by the rising bubbles can be divided into three separate terms as mentioned in chapter one. The zigzag pattern of the rising bubbles becomes more extreme when the air flow is high and the air injection distance is large. Even though the heat pipe and air injection pipes were aligned before each experiment took place it was observed that at times less than 50% of the air bubbles made contact with the 0.75" heat pipe when the air injection distance was in its most extreme case (Z/D=10). This explains why the surface temperature of the heat pipe was hotter when Z/D=10 than when Z/D=5 by more than 2 °C, at the higher power inputs.

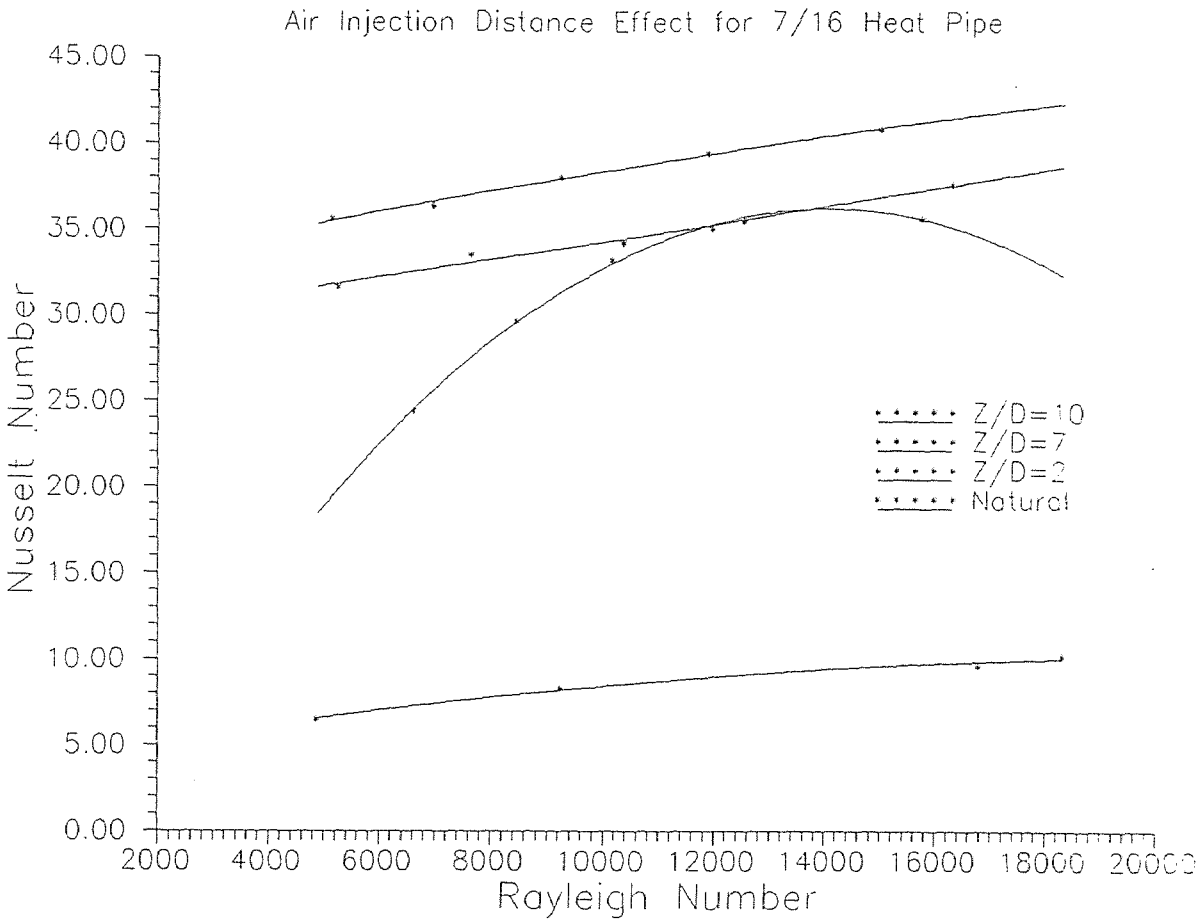

Figure 4-4: Air injection distance effect for 7/16" heat pipe.

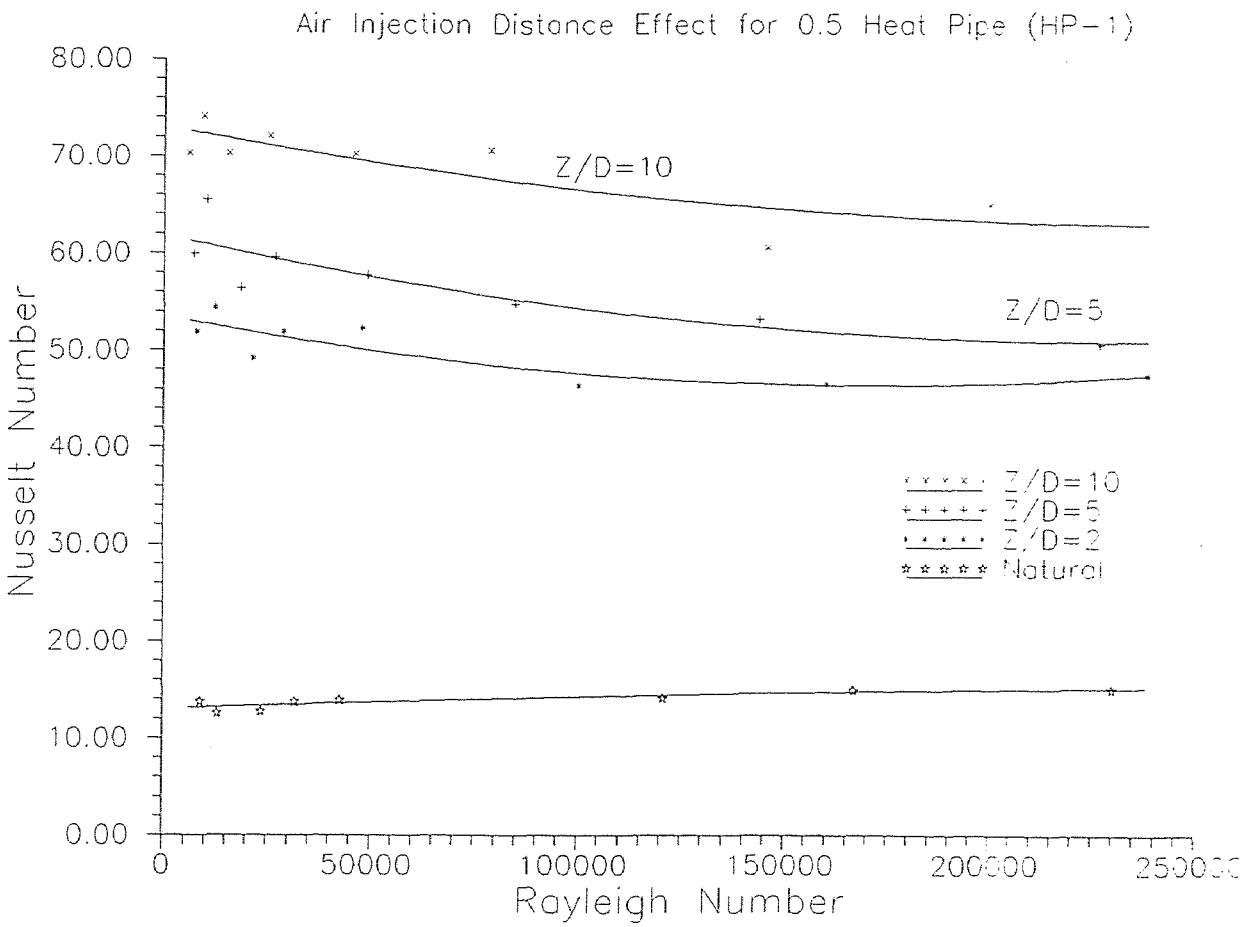

Figure 4-5: Air injection distance effect for 0.5" heat pipe.

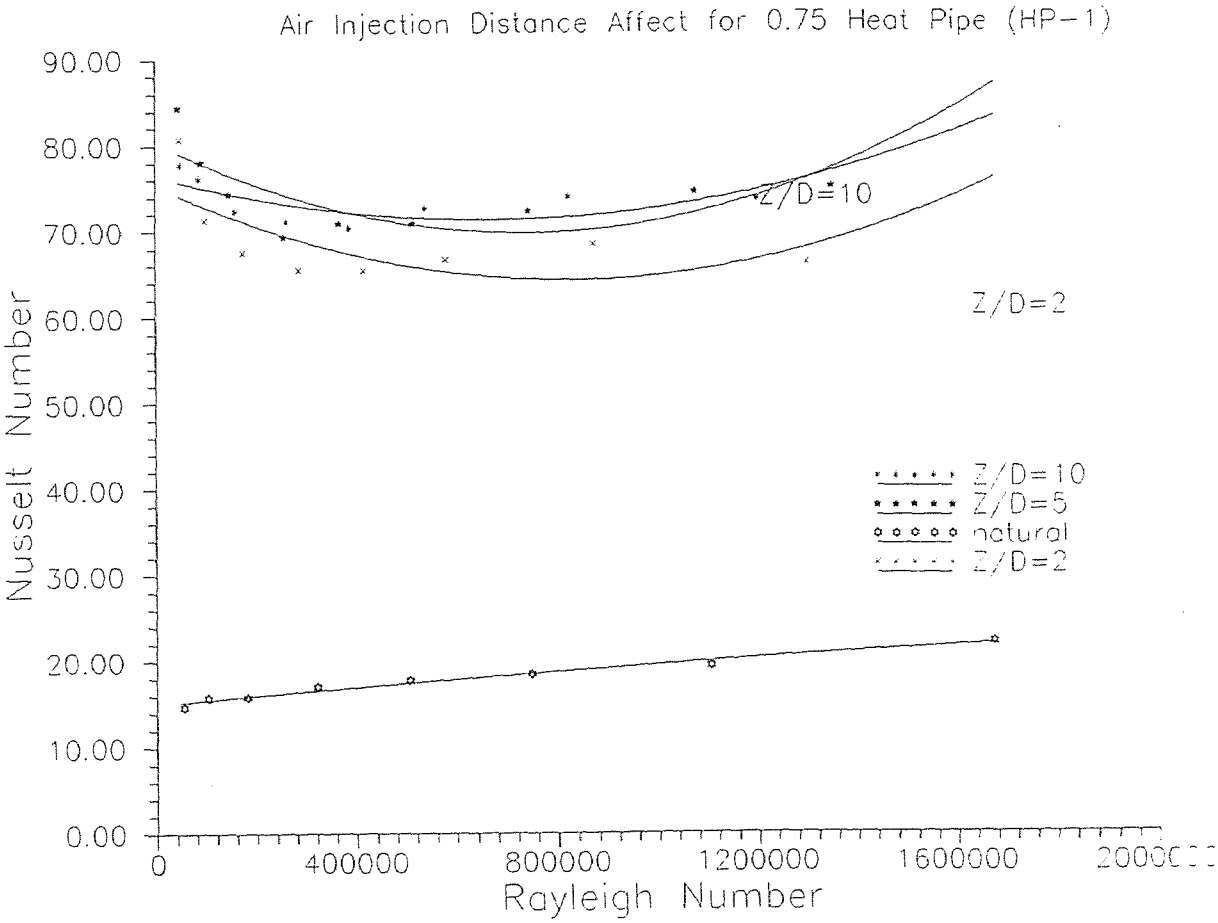

Figure 4-6: Air injection distance effect for 0.75" heat pipe.

4.3 Air Injection Configuration Effect

The idea behind experimenting with different air injection configurations is that the water circulation within the tank improves as there are more openings from the air pipe even if the amount of injected air remains the same. The heat transfer by conduction also improves when there are more openings in the injection pipe because the air bubbles' rise velocity decreases as there were more openings in the injection pipe, increasing contact time between the heat pipe and bubbles. Figure 4-7 shows the effect of air injection configuration for the ammonia heat pipe when the air injection rate was 10 SCFH the air injection distance was Z/D=5. First experiments were run with six openings on the air injection pipe, then ten and finally all fifteen ports were open. The heat transfer enhancement was about 300% for all three experiments which leads to the conclusion that for these experiments the air injection configuration does not have a significant effect as long as the amount of injected air stays the same for that particular heat pipe. This conclusion is not true for the next two graphs, figures 4-8 and 4-9, which display a small but distinct difference between the different air injection configurations. The heat transfer enhancement was 400% when all of the ports were open for the 0.5" heat pipe and about 380% when the number of openings decreased to five or nine. The air injection rate was 10 SCFH and the injection distance Z/D=5 for both HP-1 heat pipes. Figure 4-9 shows a significant difference between the enhancement due to five openings and when there are eight or all of the ports are open. The heat pipe's surface temperature was 3 °C cooler when there were fifteen openings as opposed to when there were eight or five openings.

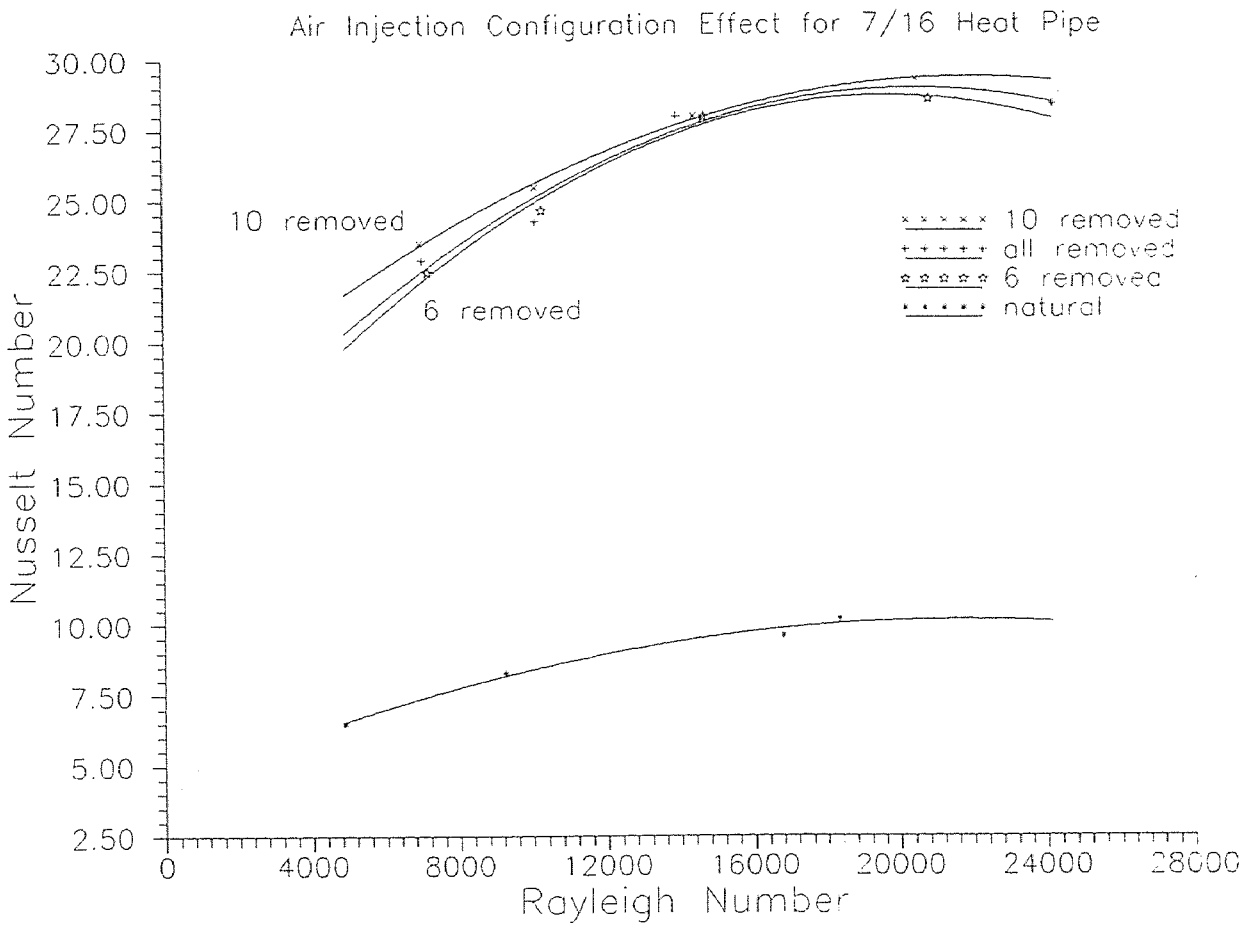

Figure 4-7: Air injection configuration effect for 7/16" heat pipe.

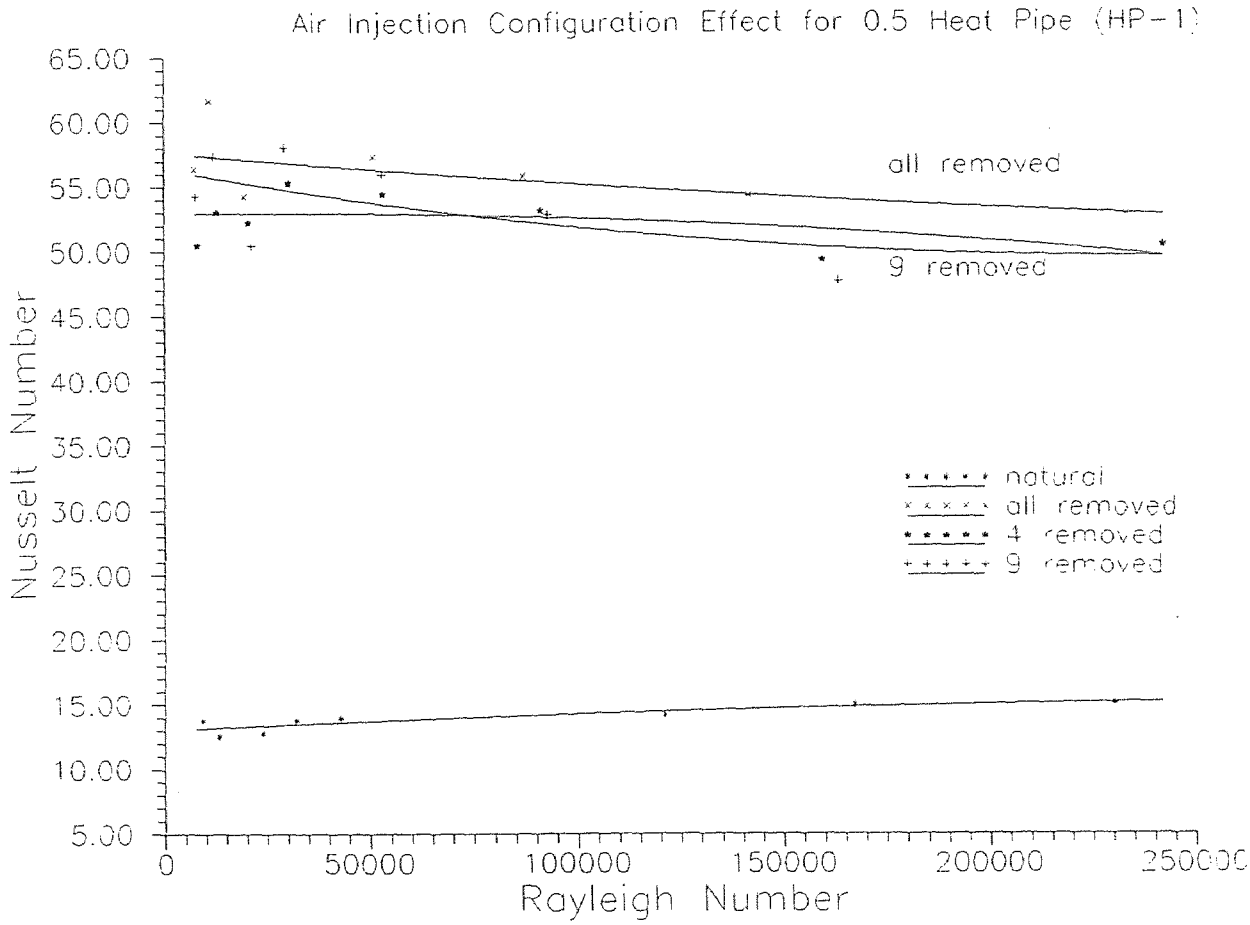

Figure 4-8: Air injection configuration effect for 0.5" heat pipe.

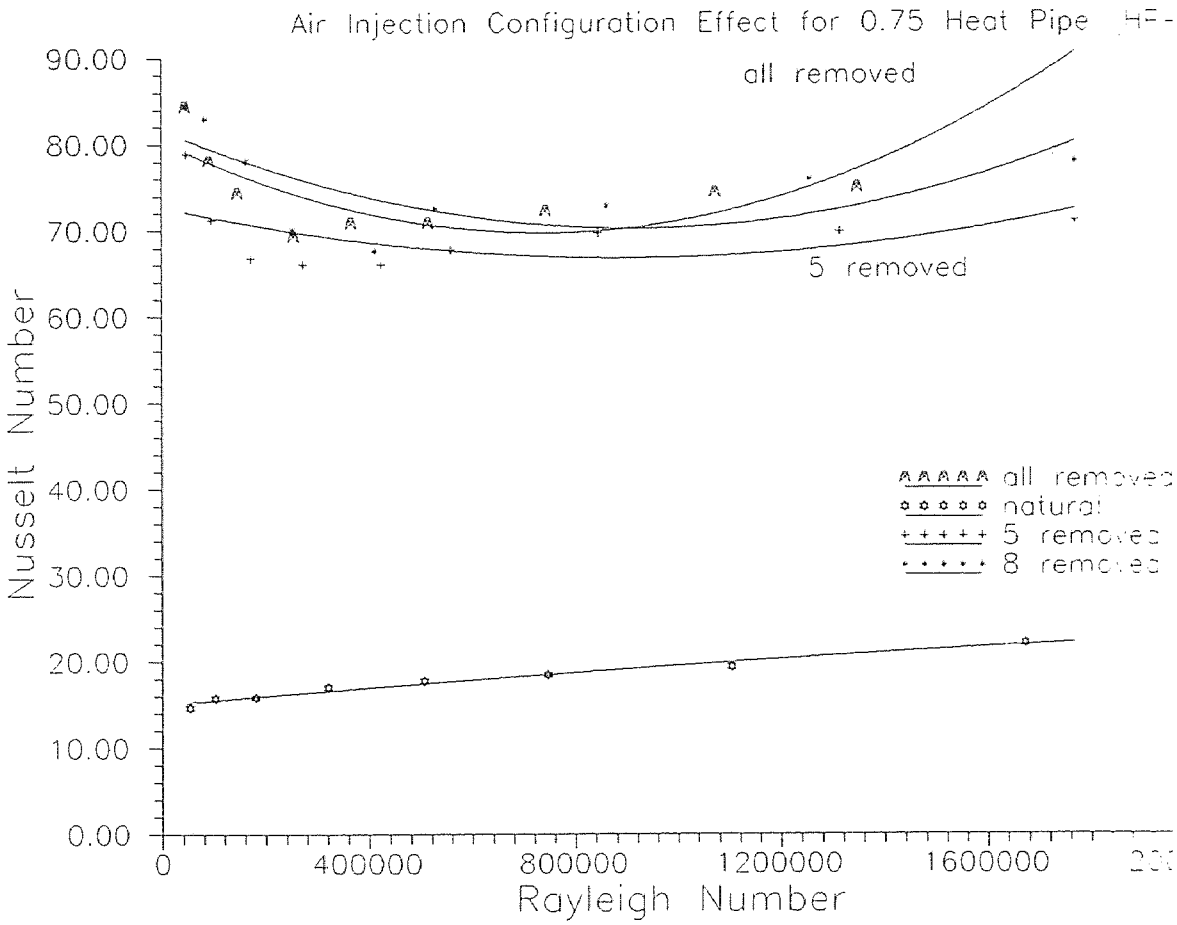

Figure 4-9: Air injection configuration effect for 0.75" heat pipe.

4.4 Curved Shroud Distance Effect

As mentioned in the previous section the heat transfer coefficient by conduction to the air bubbles will increase if the contact time between the air bubbles and the heat pipes is increased. This can be done in several ways. First by decreasing the air injection rate the water circulation within the tank will decrease and the bubbles will rise at a slower rate which will increase the time of contact between the heat pipe and air bubble. Also if the size of the heat pipe is increased drastically there will be an increase in the contact time between the bubbles and heat pipe surface. As a single elliptical bubble rises through the tank and makes contact with the lower surface of the heat pipe the air bubble deforms and rises along the sides of the heat pipe conducting heat along the way. When the bubble breaks away from the heat pipe it starts loosing its heat to the colder surrounding fluid as it rises through the tank. The air bubble never makes contact with the top portion of the heat pipe because at that point it breaks away. If a shroud is made such as to force the bubbles go all the way around the heat pipe, it will increase the amount of time the bubbles are in contact with the heat pipe conducting away more of the pipe's heat thus increasing the temperature of the vapor inside the bubble. The hotter bubble will deliver more heat energy to the surrounding fluid, decreasing the surface temperature of the heat pipe and increasing the temperature of the fluid. This will result in higher heat transfer coefficients making the shrouds a very good heat transfer enhancement technique. The shroud's distance from the heat pipe is very important since at long distances from the heat pipe the shroud will have no effect or will create a negative effect by decreasing the heat transfer enhancement due to bubble turbulence. Figure 4-10

shows the heat transfer enhancement for the ammonia heat pipe due to curved shrouds placed around the tank at dimensionless distances of d/D=1,2 and,4. The air injection rate was 50 SCFH and the injection distance was Z/D=8. The heat transfer increased by 300% but it is not clear from this graph what the significance of the shrouds are since the shrouds were made from a two inch hollow copper pipe and the heat pipe was 7/16" inches in diameter which do not force the bubbles to travel all the way around the heat pipe. The same is true for the 0.5" heat pipe which represented in the next graph (figure 4-11). For this heat pipe the air injection distance was Z/D=8 and the air injection distance was 10 SCFH. The top curve represents the heat enhancement when the shrouds are 0.5 inches from the side of the heat pipe and its points are very close to the other two curves which represent a distance of 2 inches (d/D=4) and when there were no shrouds in the tank. It was noticed that when the shrouds were 0.5 inches away from the heat pipe the two shrouds made contact with each other and the bubbles were unable to escape from the top. Since the length of the shrouds were smaller than the overall length of the tank the bubbles were able to escape from the sides. Figure 4-12 shows the heat transfer enhancement for the 0.75 inch heat pipe at an air injection distance of Z/D=5 and air injection rate of 10 SCFH. There is a distinctive difference between the different shroud distances from the heat pipe. The heat transfer enhancement was 400% at d/D=1, 350% when no shrouds were in the tank and, 300% when the curved shroud distance was d/D=3. This supports both assumptions of a critical shroud distance and increase due to bubble conduction but was only evident from the larger diameter heat pipe since the physical size of the shrouds made it impossible to conclude the same for the smaller heat pipes.

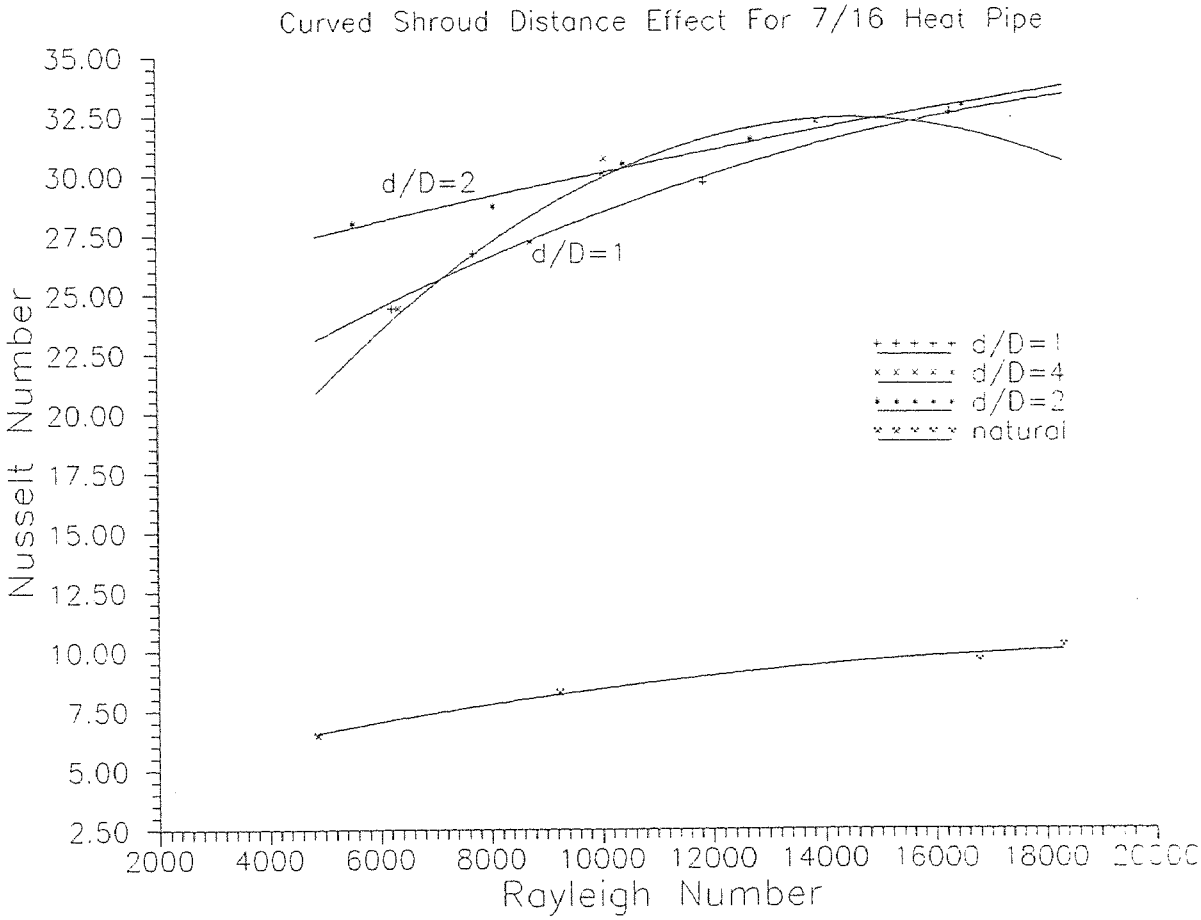

Figure 4-10: Curved shroud distance effect for 7/16" heat pipe.

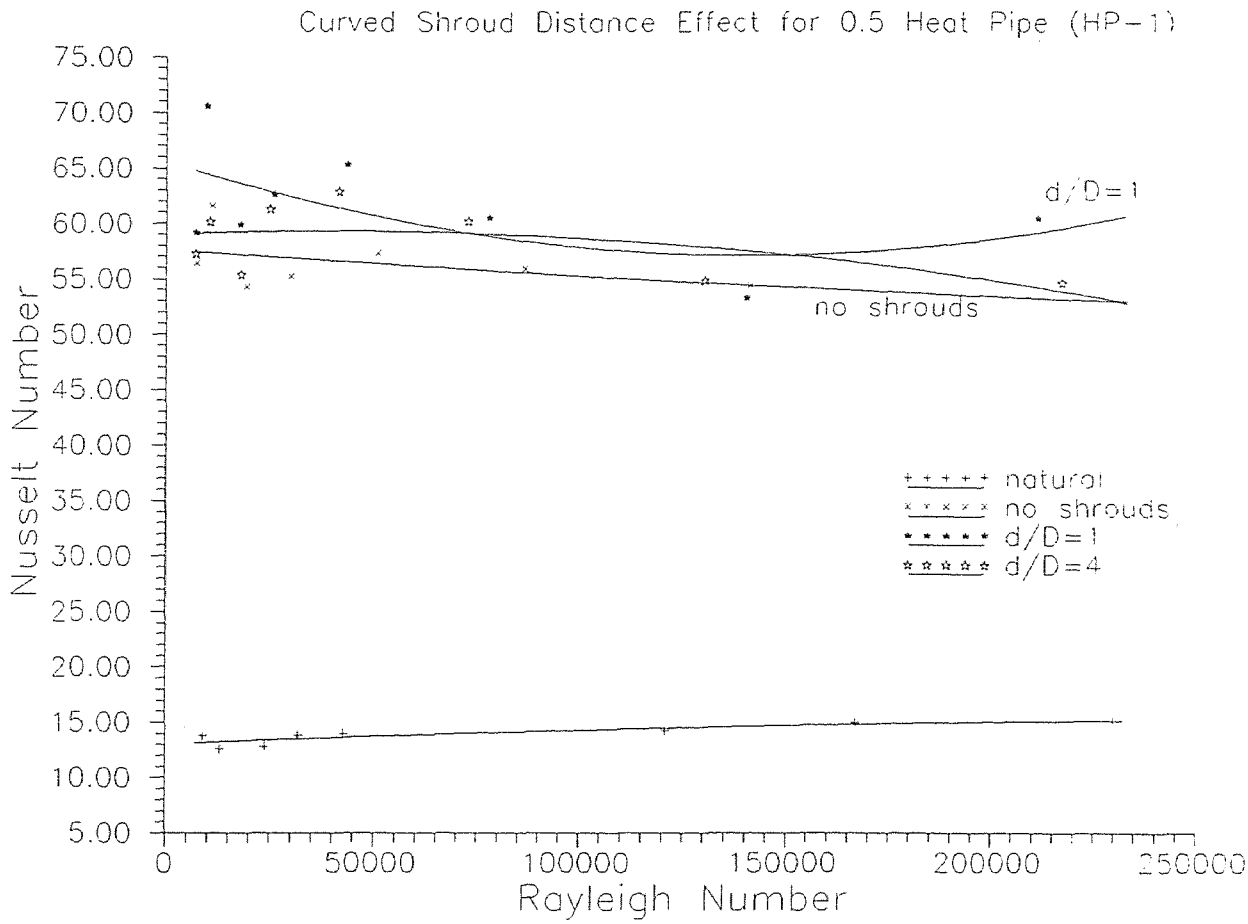

Figure 4-11: Curved shroud distance effect for 0.5" heat pipe.

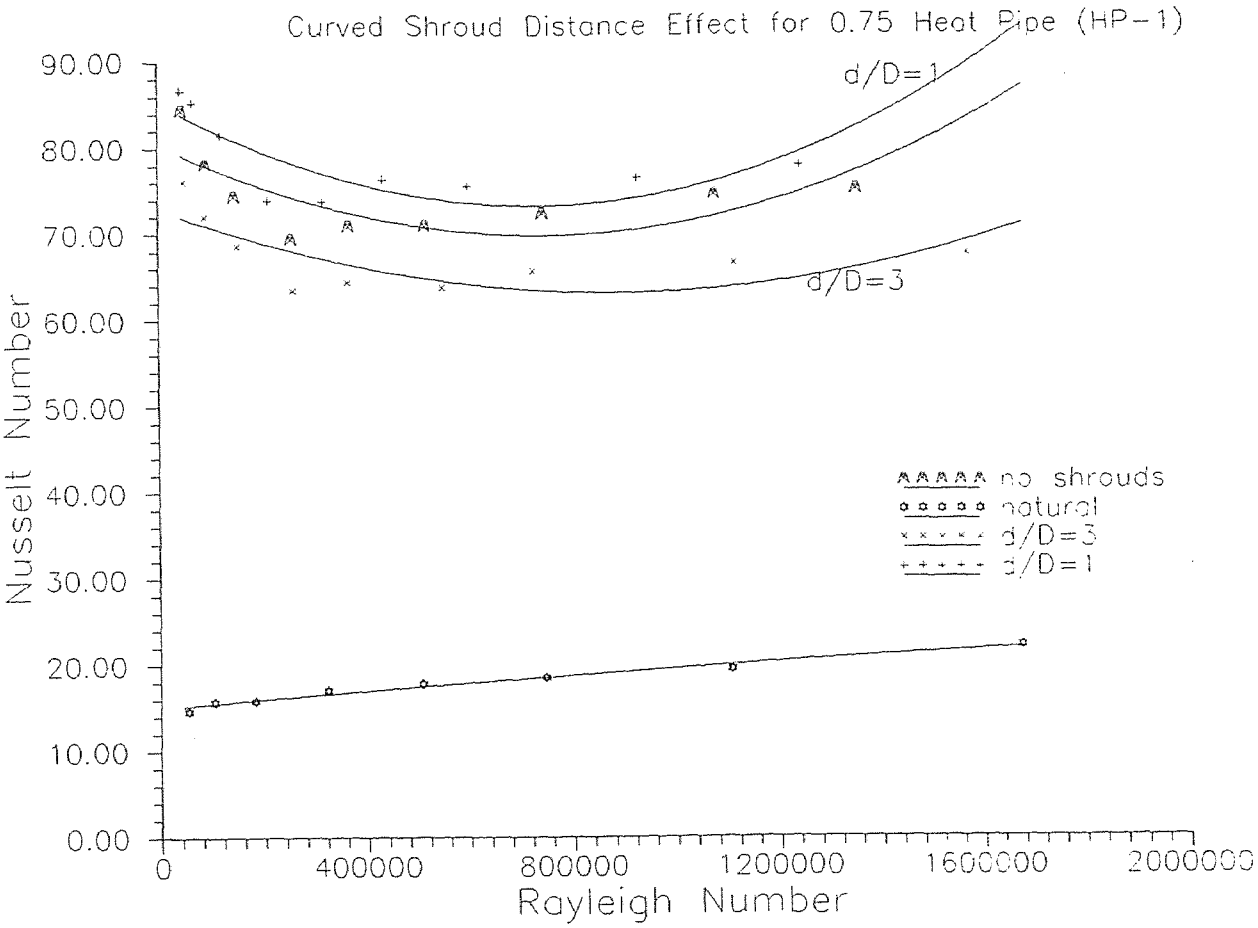

Figure 4-12: Curved shroud distance effect for 0.75" heat pipe.

4.5 Shroud Shape Effect

The shape of the shrouds placed around the heat pipes also has an effect in the heat transfer enhancement. Some shapes will be more efficient than others, while other shapes will have a counteracting effect and impede the heat transfer enhancement which will make these shrouds not useful for our purposes. Since the whole idea behind the use of shrouds is to make the air bubbles penetrate the thermal boundary layer increasing the heat transfer by turbulence and conduction, the most efficient shroud of the two selected (straight and curved shrouds) will be the curved one because it forces the bubbles to follow the round shape of the cylindrical heat pipe. The distances of the shrouds, air injection rates, air injection distances and configuration was were held constant while experimenting with the different shroud shapes. Figure 4-13 shows the heat transfer enhancement for the ammonia heat pipe at an injection distance of Z/D=8, injection rate of 50 SCFH and shroud distances of 7/16 inches; also the experiment was repeated with no shrouds in the tank to investigate the contributing factor of the different shape shrouds. It can be seen that even for this heat pipe the straight shroud gives the least amount of enhancement but it is not clear what the difference between the curved shroud experiment and no shroud experiment is. A small but more distinct difference between the curves is shown in the next figure which represents the three curves for the 0.5 inch heat pipe. The air injection distance was Z/D=5, the air injection rate was 10 SCFH and, the shrouds' distance was 0.5 inches. The heat transfer with the curved shrouds was 10% more than when no shrouds were in the tank and 30% more when the straight shrouds were placed at the same distance as the curved shrouds. The reason for this

significant difference is that the straight shrouds impede the heat transfer enhancement due to bubble turbulence by constraining the turbulence created by the zigzag motion and expansion of the bubbles. The air bubbles leave from the sides of the heat pipes as they do when there are no shrouds in the tank. Both of the two different shape shrouds take away from the turbulence action of the rising bubbles but the curved shroud more than makes up the difference by increasing the contact time of the bubbles with the heat pipe. Figure 4-15 represents the heat transfer augmentation of the 0.75" heat pipe and it also shows a clear distinction between the three curves especially when the heat pipe operates at high power rates. There is heat transfer enhancement of 400% for the curved shrouds, 380% for no shrouds and 350% for the straight shrouds. The surface temperature of the heat pipe is lower by 3 °C when the curved shrouds are used as compared to when no shrouds are in the tank and only 2 °C when the straight shrouds are in the tank. The following table shows the average heat pipe surface temperature at selected power inputs of the different shrouds used in these experiments. Also the case of no shrouds in the tank is shown in the last column of the table.

Table 4.1: Average heat pipe temperature at selected power inputs

Power Input	Curved Shroud	Straight Shroud	No Shrouds
240 watts	39.975	42.25	42.2
280 watts	44.45	46.7	47.175
324 watts	49.625	51.9	52.6
383 watts	55.15	57.55	58.425

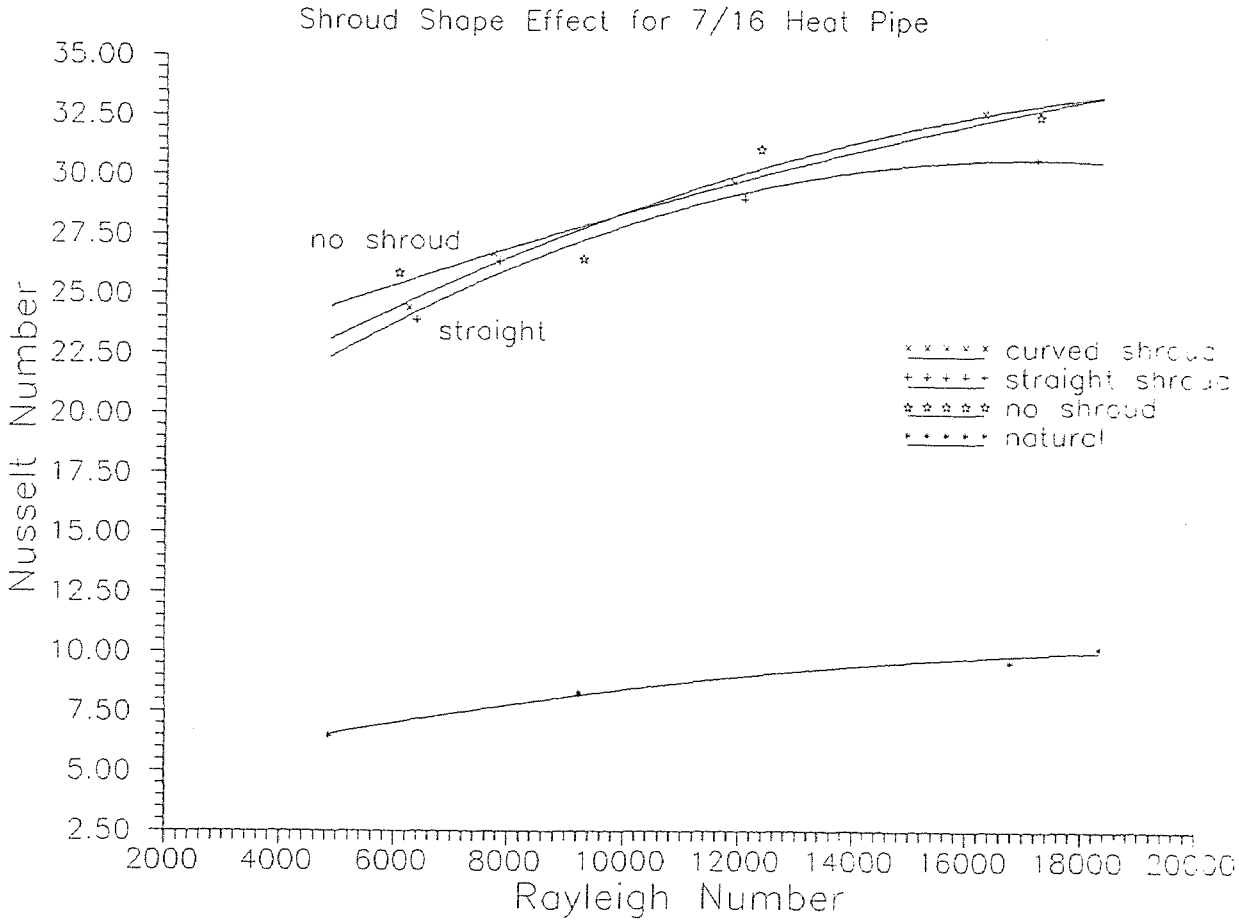

Figure 4-13: Shroud shape effect for 7/16" heat pipe.

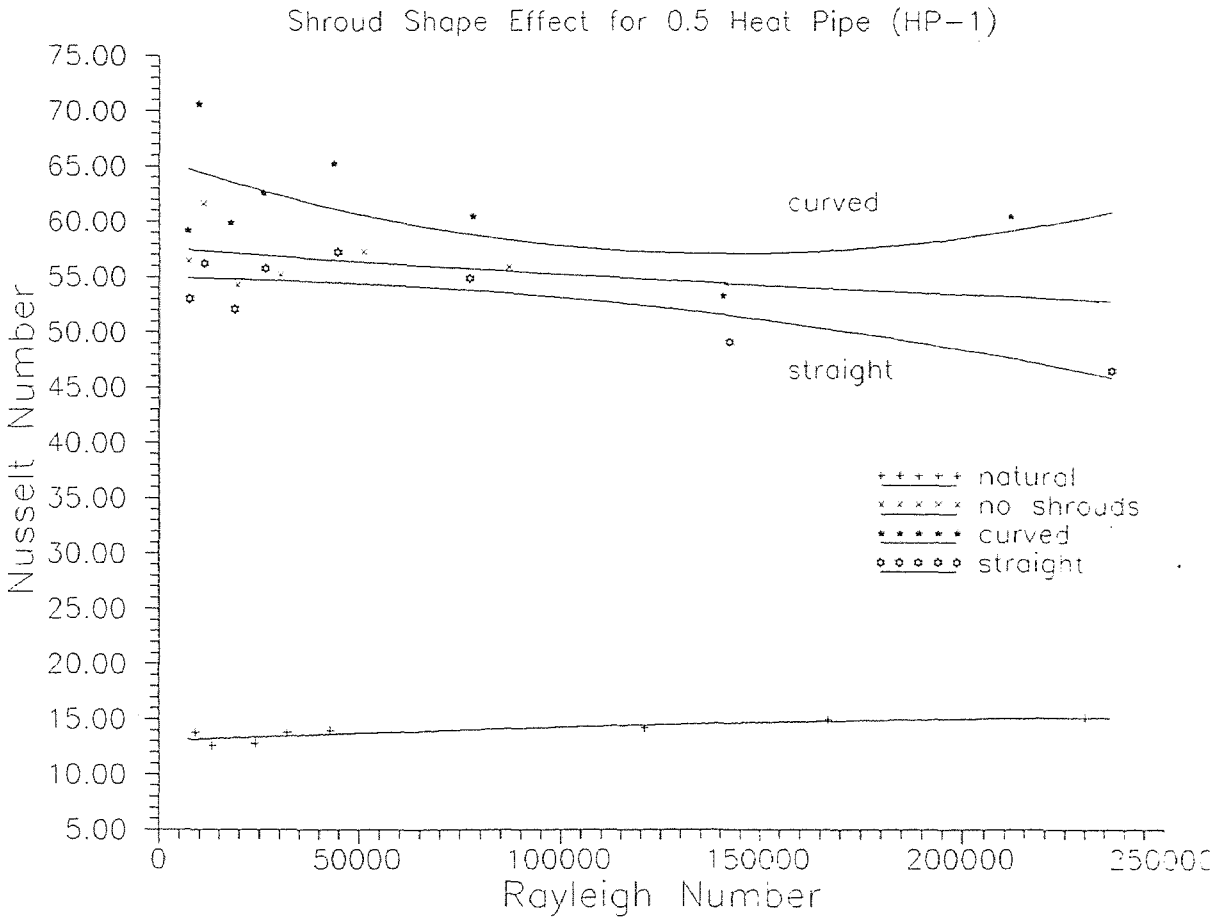

Figure 4-14: Shroud shape effect for 0.5" heat pipe.

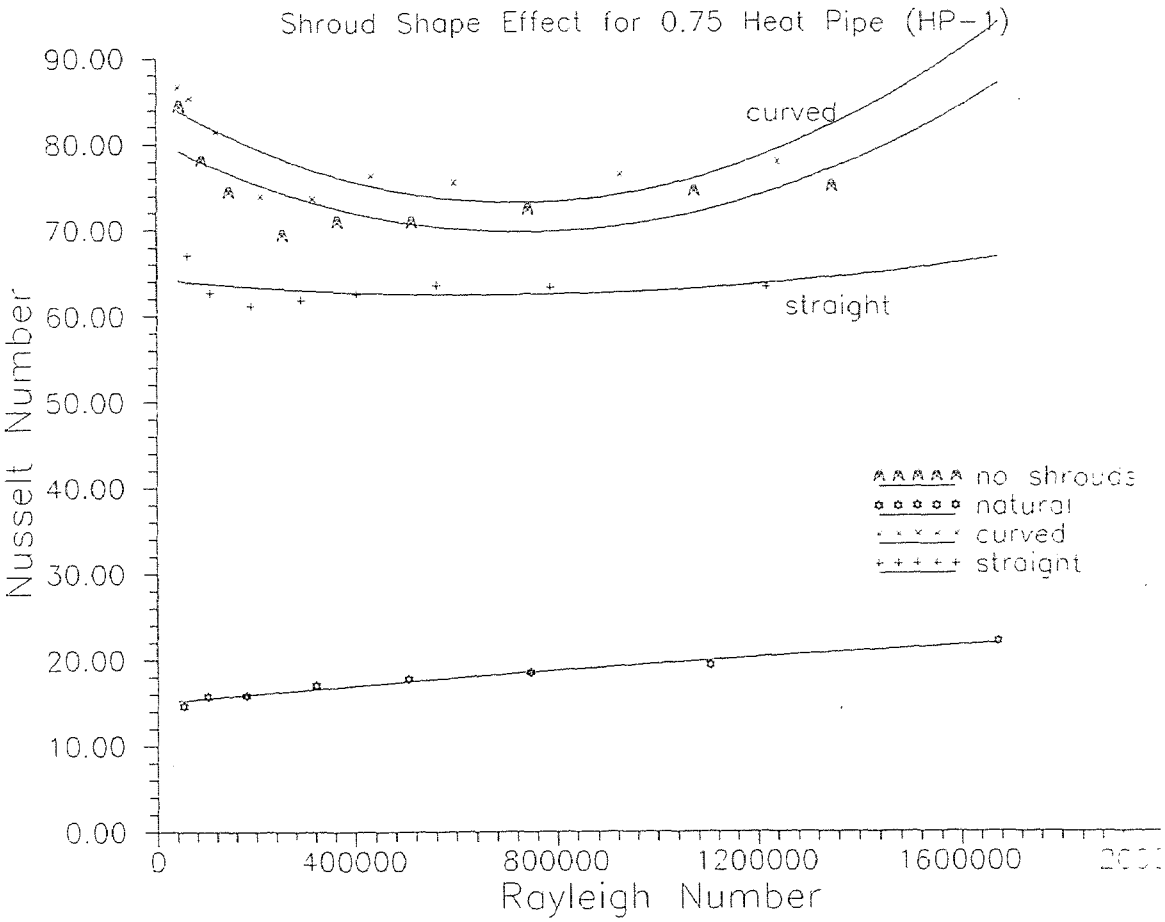

Figure 4-15: Shroud shape effect for 0.75" heat pipe.

4.6 Water Circulation Only Effect

The heat transfer due to water circulation was the last parameter originally set out to be investigated by this thesis. The heat transfer enhancement for the ammonia heat pipe was about 100% (see figure 4-16). The air injection pipe was placed on the bottom and to the extreme left side of the water tank. The heat transfer enhancement was a collective action of both the water circulation and the turbulence waves of the air bubbles as they rise through the tank. The increase in heat transfer due to water circulation only was correctly investigated on the next two graphs (figure 4-17 and 4-18) when the air injection pipe was placed on the same height and to the side of the heat pipe. The air injection rate was 10 SCFH for both heat pipes. The heat transfer enhancement in these two cases starts at a high number and then it decreases as the power inputs of the heat pipe become larger. This is done because at lower heat inputs the thermal boundary layer is large but becomes smaller as the power increases. The larger boundary layer is affected more by the turbulence created from the circulating fluid and as the layer becomes smaller that effect decreases. The heat transfer enhancement is 100% at low power input rates and it decreases to 20% at the higher input rates for the 0.5 inch heat pipe. The heat transfer enhancement was also 100% at low input rates for the 0.75 heat pipe and it becomes 50% at higher input rates. By looking at the two curves of figures 4-17 and 4-18 it is not clear that the two lines (natural convection and water circulation lines) would ever meet even if that this is a very strong possibility since the slope of the natural convection line is positive whereas the slope is negatives for the water circulation line.

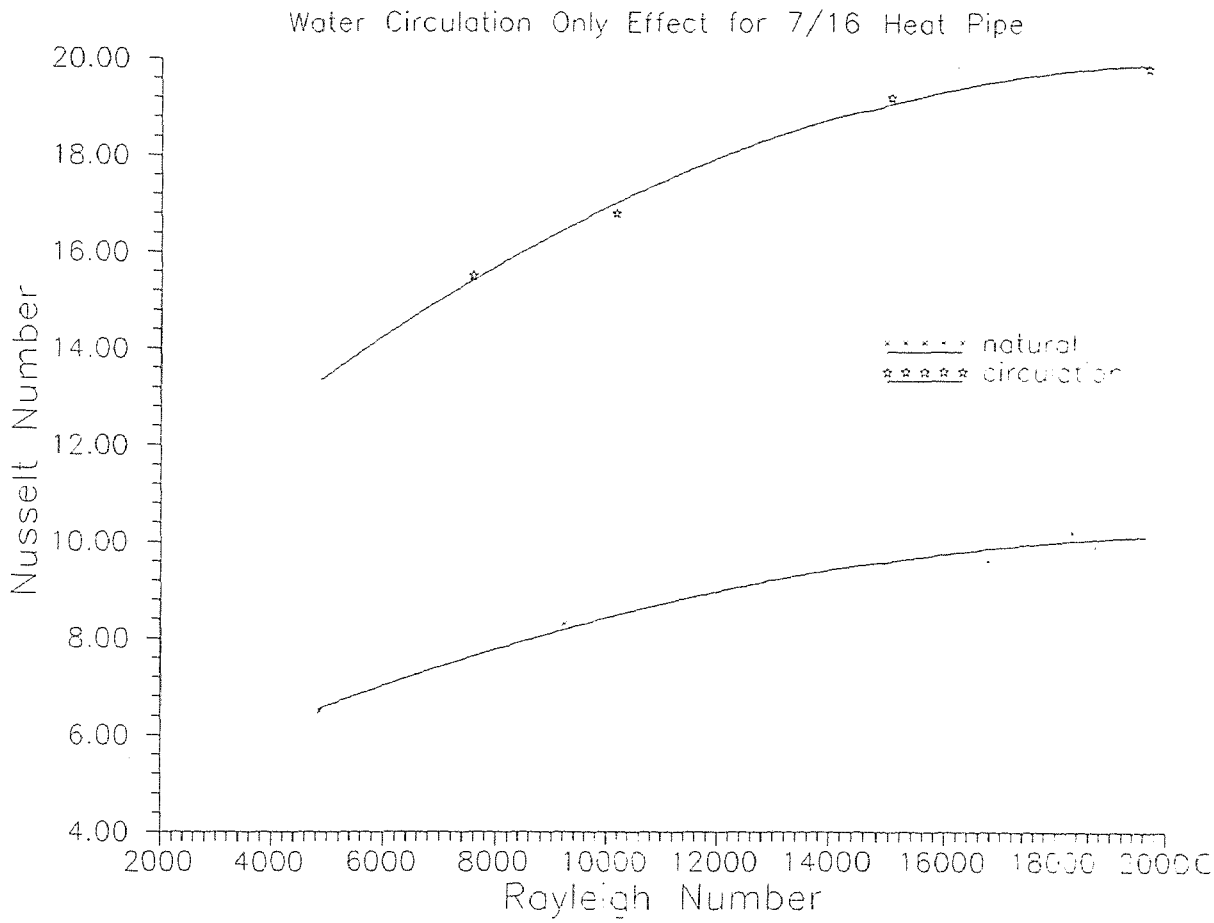

Figure 4-16: Water circulation effect for 7/16" heat pipe.

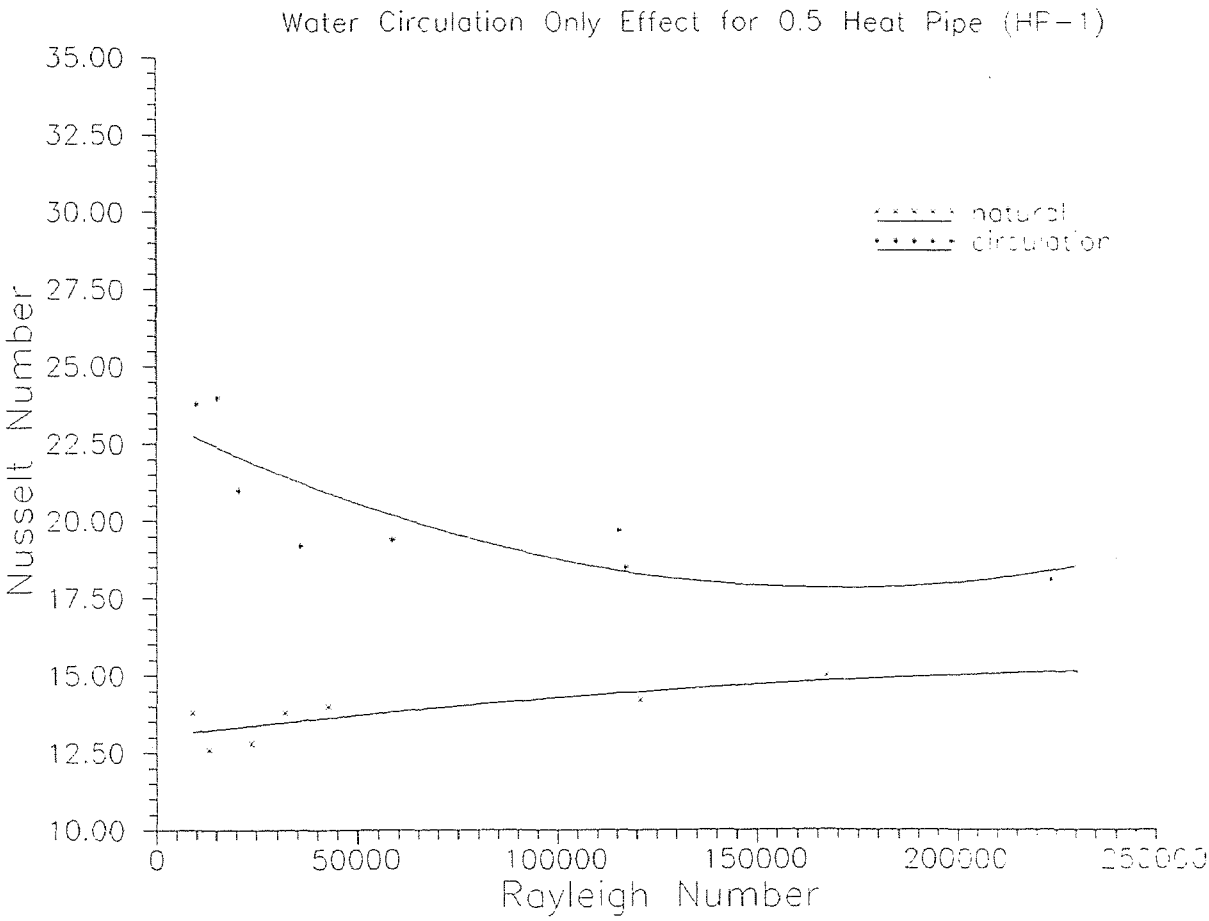

Figure 4-17: Water circulation effect for 0.5" heat pipe.

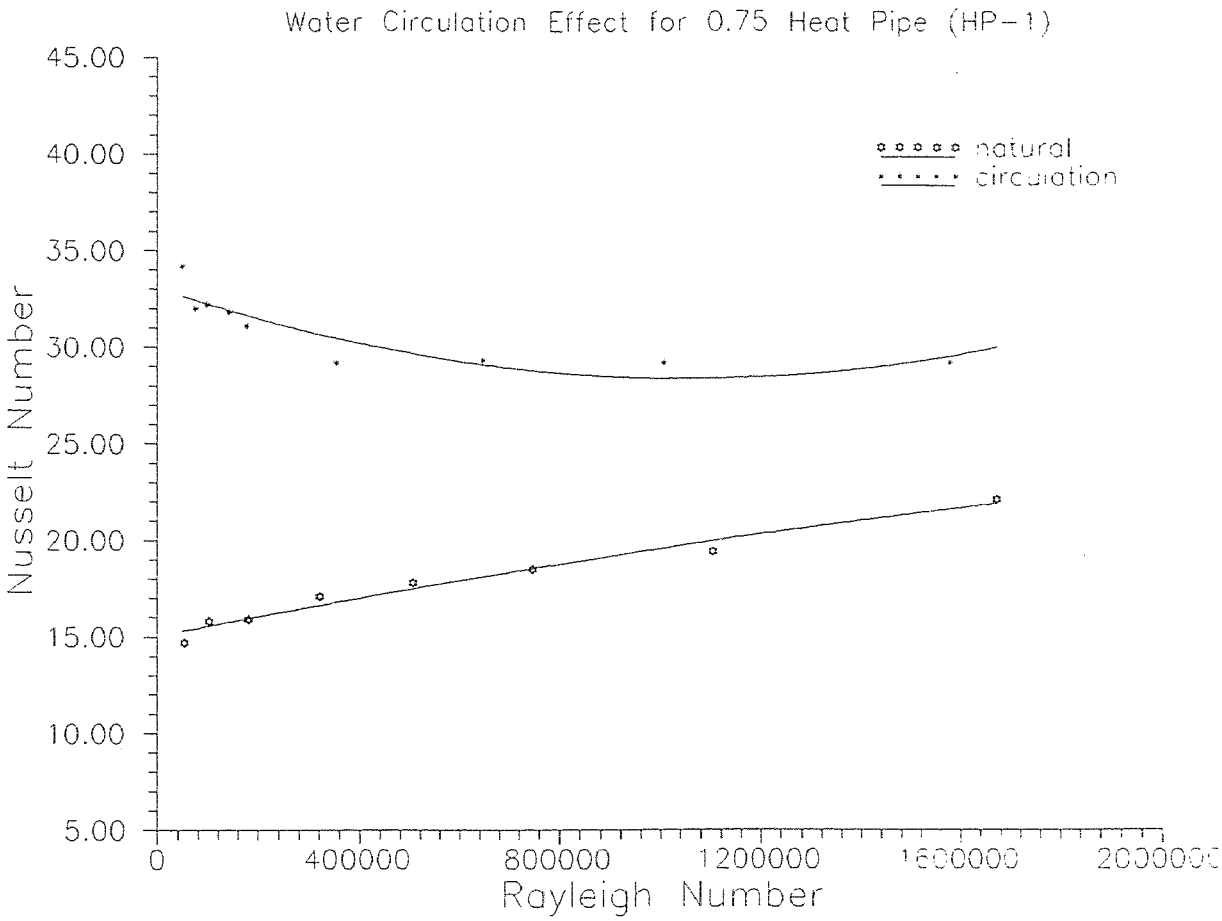

Figure 4-18: Water circulation effect for 0.75" heat pipe.

4.7 Additional Experiments for 0.75 Inch Heat Pipe

4.7.1 Sectional Cooling Effect

Another way of finding the effect on the heat transfer due to a different air injection configuration is by injecting air at the same rates but cooling different sections of the heat pipe at a given time. I used an air injection rate of 5 SCFH and air injection distance of Z/D=5. For the first experiment I had all the ports open on the air pipe. The heat transfer enhancement was 400%. Then the first four ports were left open while the last eleven were taped closed. The heat transfer enhancement was 300% and the temperature difference between the heat pipe and water increased. By looking at the experiment while the data was taken it was evident that the turbulence created by the sectional cooling of the heat pipe was not as great as when all of the ports were open. There were plumes rising from the rest of the heat pipe which were not observed when all of the ports were open. Also the part of the heat pipe which was further away from air injection bubbles small vapor bubbles were created on the surface. The temperature drop along the length of the heat pipe was similar to when all of the ports were open. The heat transfer enhancement was 250% when the middle three ports were open and the plumes rising from either side of the cooled section was observed again. The heat transfer enhancement due to last four ports being open was also 250% but a higher temperature drop along the length of the heat pipe was observed. The temperature inside the water tank increased as much as 6.0 ^{o}C when the last four ports were open as opposed to when all of the ports were open.

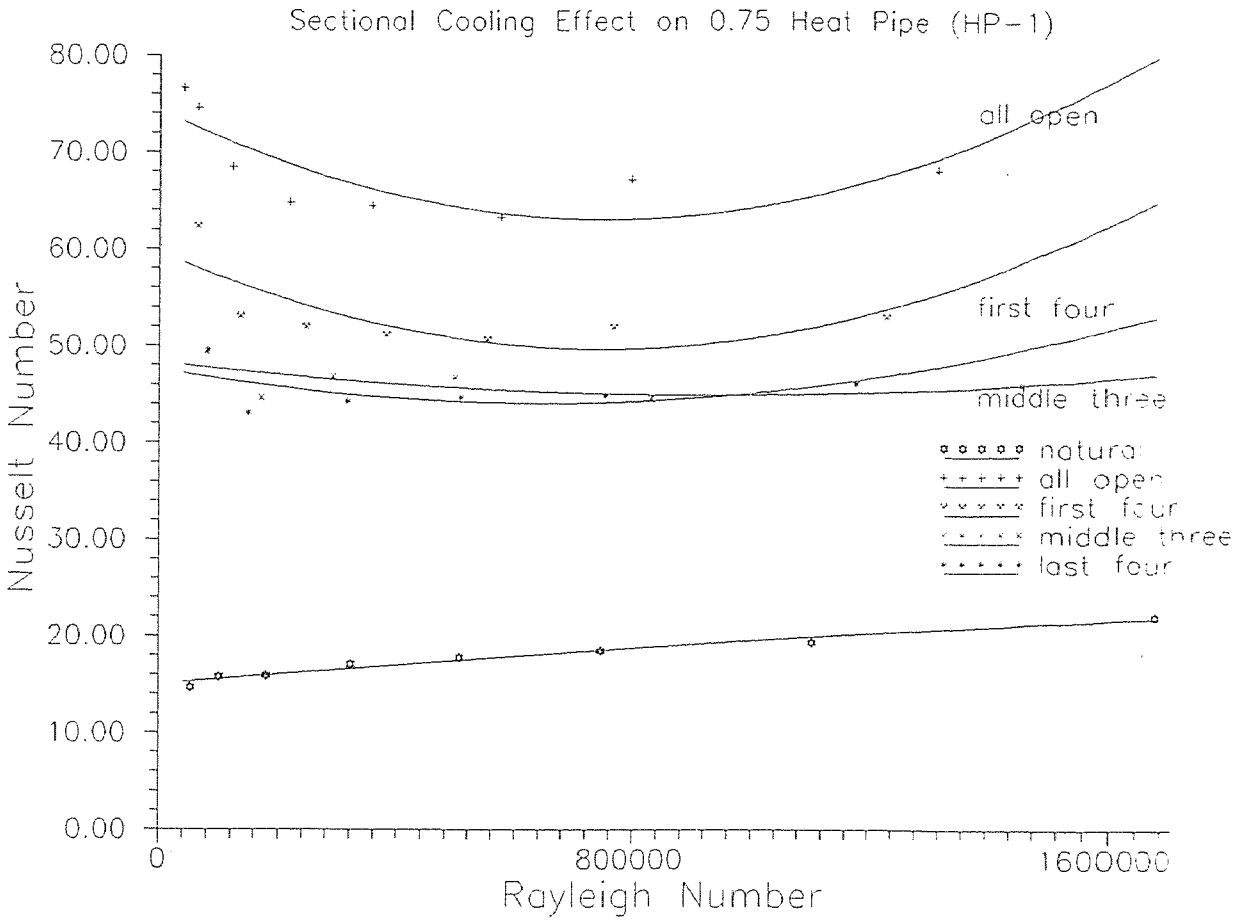

Figure 4-19: Sectional cooling effect for 0.75" heat pipe.

4.7.2 Lower Air Flow Rate Experiments

It was necessary to investigate the heat transfer enhancement due to lower air flow rates. As mentioned in chapter one the industrial applications of this thesis are mainly directed around the nuclear industries and in more detail the steam generator of the power plant. This generator runs at very high temperatures and if a failure in the cooling system occurs that could be fatal. The reason for choosing a heat pipe to represent this generator is the more uniform temperature along the length of the cylinder. To achieve the air flow rates mentioned in sections 4-1 through 4-6 a small air compressor has to be used. If there is a power failure the air compressor will not be able to inject any air and the generator will soon rise to dangerous temperature levels. Lower air injection rates are easy to achieve by pre-compressing the air to a storage tank and having a release mechanism open a safety valve when a power failure occurs. The air flow rates investigated were 2, 1 and 0.5 SCFH at an injection distance of Z/D=5. Due to these smaller flow rates it was not possible to keep all of the holes open since the air will escape from were it will have the least resistance and that would be the first four or five holes. I decided to have three openings (holes 1, 9, and 15) which represents an opening for each of the three sections of the pipe as mentioned in the previous section. The heat transfer coefficient improvement was 350% for the 2 SCFH flow rate, 300% for the 0.5 SCFH flow rate, and 250% for the 1 SCFH flow rate. The reason for having the smaller increase at the 1 SCFH flow rate rather than at the 0.5 SCFH flow rate was that during the 1 SCFH flow rate experiment the air was escaping through port # 15 only which decrease both influence of the bubble by both conduction and turbulence since there was only one opening

and it was located underneath the coolest section of the heat pipe. At the 0.5 SCFH flow rate the ball inside the flow meter was oscillating very vividly. It was not clear in the beginning if this oscillation was caused by impulses in the supply line or by the back pressure of the departing air bubbles. The cause for this oscillation was found by cutting the feed line from the flow meter to the air injection pipe, releasing the supply air to the atmosphere. Once this was done the ball stopped oscillating immediately. The feed line was then immersed in the water tank and the oscillation started again. This lead to the conclusion that the oscillation was not caused due to impulses in the main supply line but due to back pressure of the departing bubbles. The air flow rate was hard to adjust because during the experiments there were times were the air supply line will not carry as much air as it was originally set to, and that caused the air flow to decrease. To avoid this problem a pressure regulator should be installed between the air flow meters and the air injection line or an storage tank could be used with pre-pressurized air. The pressure regulator will dampen pressure fluctuation and reduce flow oscillation. The following table shows the water temperature at the high input power rates for the three air flow rates.

Table 4-2: Water temperatures at selected power inputs

Power Input	2 SCFH	1 SCFH	0.5 SCFH
202 watts	31.4	33.967	36.5
260 watts	36.3	38.567	42.37
315 watts	41.9	43.9	49.4
383 watts	47.8	49.53	56.7

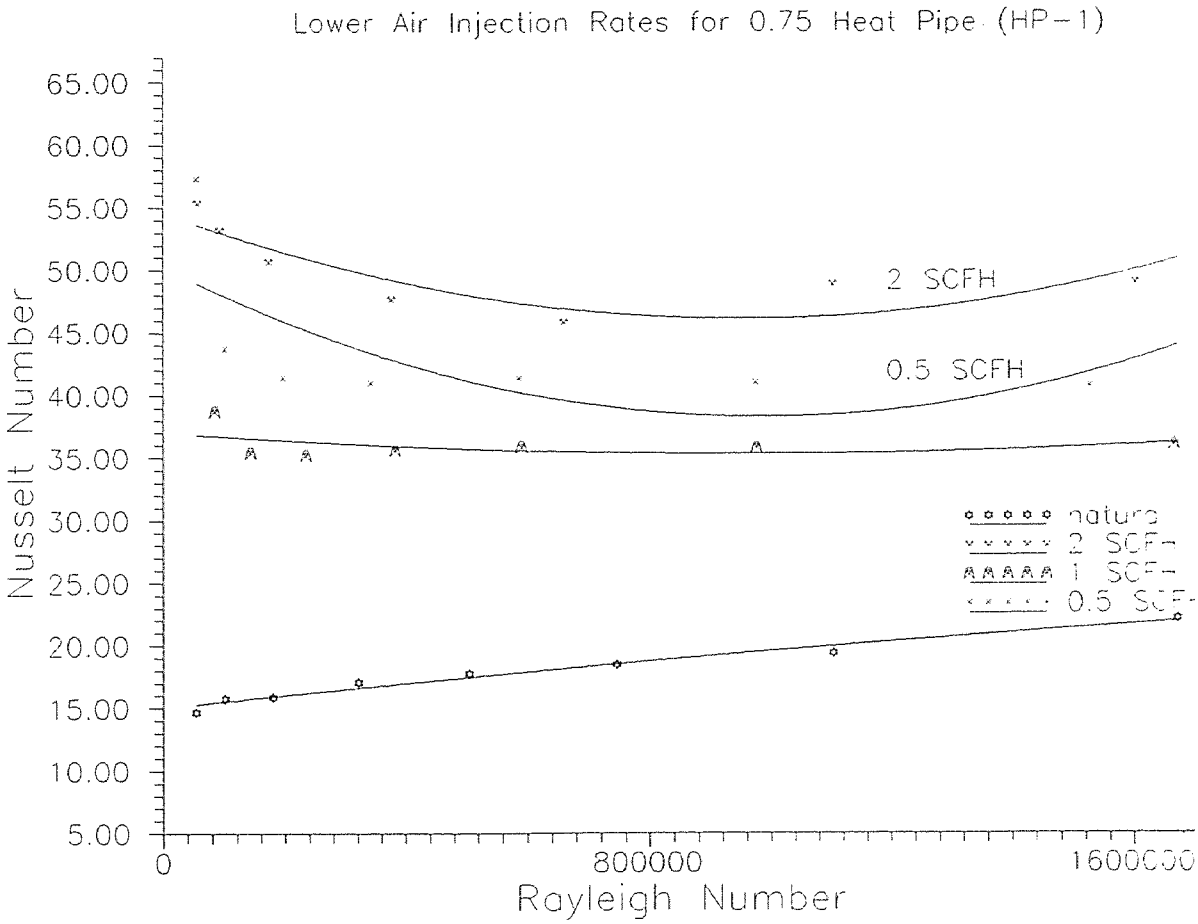

Figure 4-20: Lower air injection rates effect for 0.75" heat pipe.

4.7.3 Air Injection Distance Effect for 2 SCFH and 5 SCFH

The effect of air injection distances at 2 SCFH and 5 SCFH is shown if figures 4-21 and 4-22 respectively. Comparing these two figures with figure 4-6 it can be concluded that the air injection distance has more of an effect at lower air injection rates than it does for higher. The reason for this is that at the lower air injection rate almost the path of an individual bubble is diverted mostly by the hydrodynamic pressure of the water tank the improved circulation within the tank and, the wakes of the previous bubbles. If the injection pipe and heat pipe are aligned, almost all of the bubbles should make contact with the heat pipe and this was not the case for the 5 and 10 SCFH flow rate. The enhancement due to injection distances for the 2 SCFH flow rate was 200% at Z/D=1, 300% at Z/D=5 and, 400% when the injection distance is Z/D=10. For the 5 SCFH curves the augmentation was 300% when Z/D=1 and 400% for both injection distances of Z/D=5 and Z/D=10. For the 10 SCFH curve the increase in heat transfer was 350% when Z/D=1 and 400% for both Z/D=5 and 10 injection distance. The surface temperature of the heat pipe was higher for the 5 SCFH flow rate than for the 2 SCFH flow rate at the higher injection distance (Z/D=10), but since the total amount of wattage for the 2 SCFH (1785 watts) flow rate was less than on the 5 SCFH (1920 watts) flow rate we can not conclude that the reason for this observation is that more air bubbles make contact with the heat pipe's surface. It can be concluded form this experiment that the optimum air injection distance will increase as the air injection rates decrease.

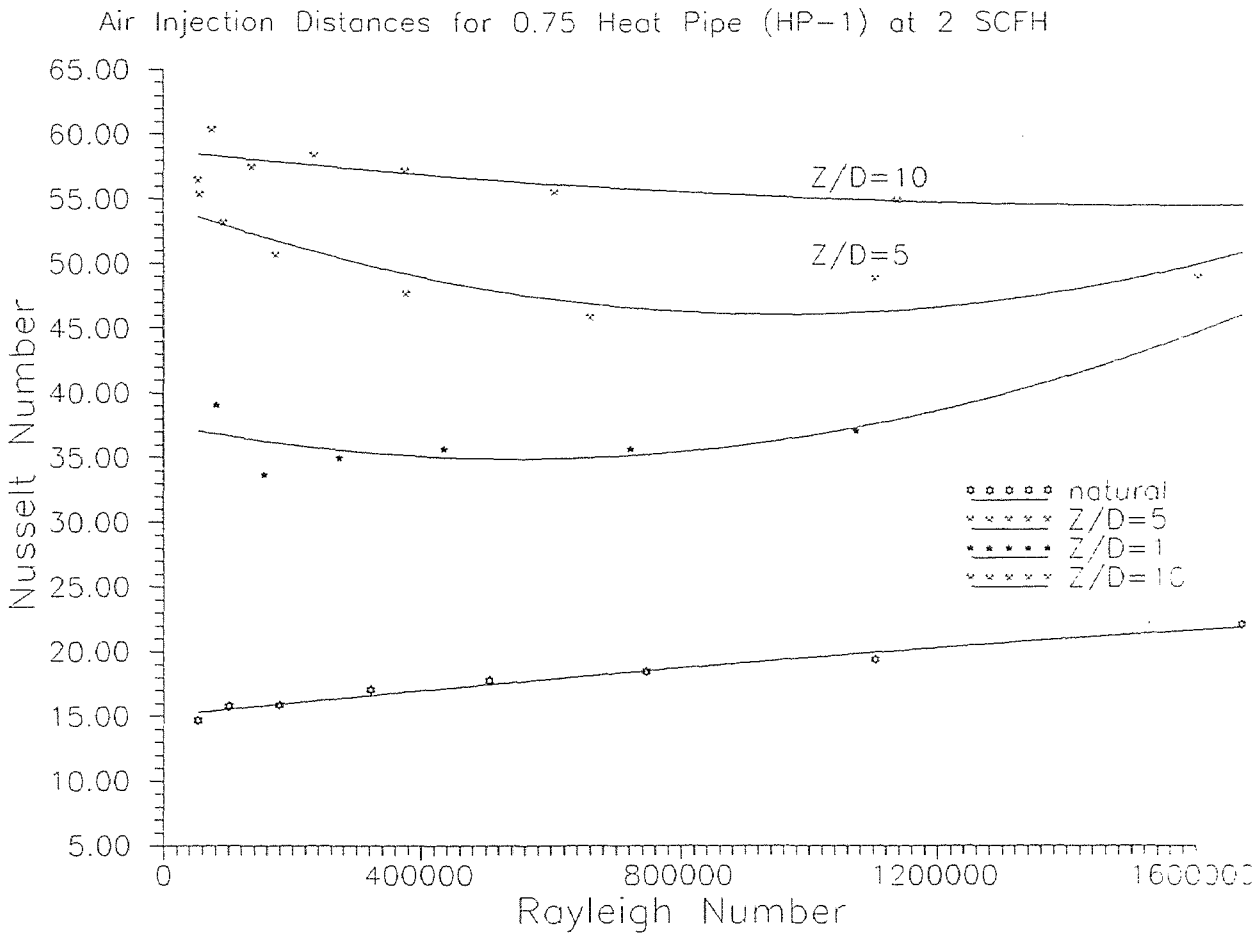

Figure 4-21: Air injection distance effect for 0.75" heat pipe at 2 SCFH.

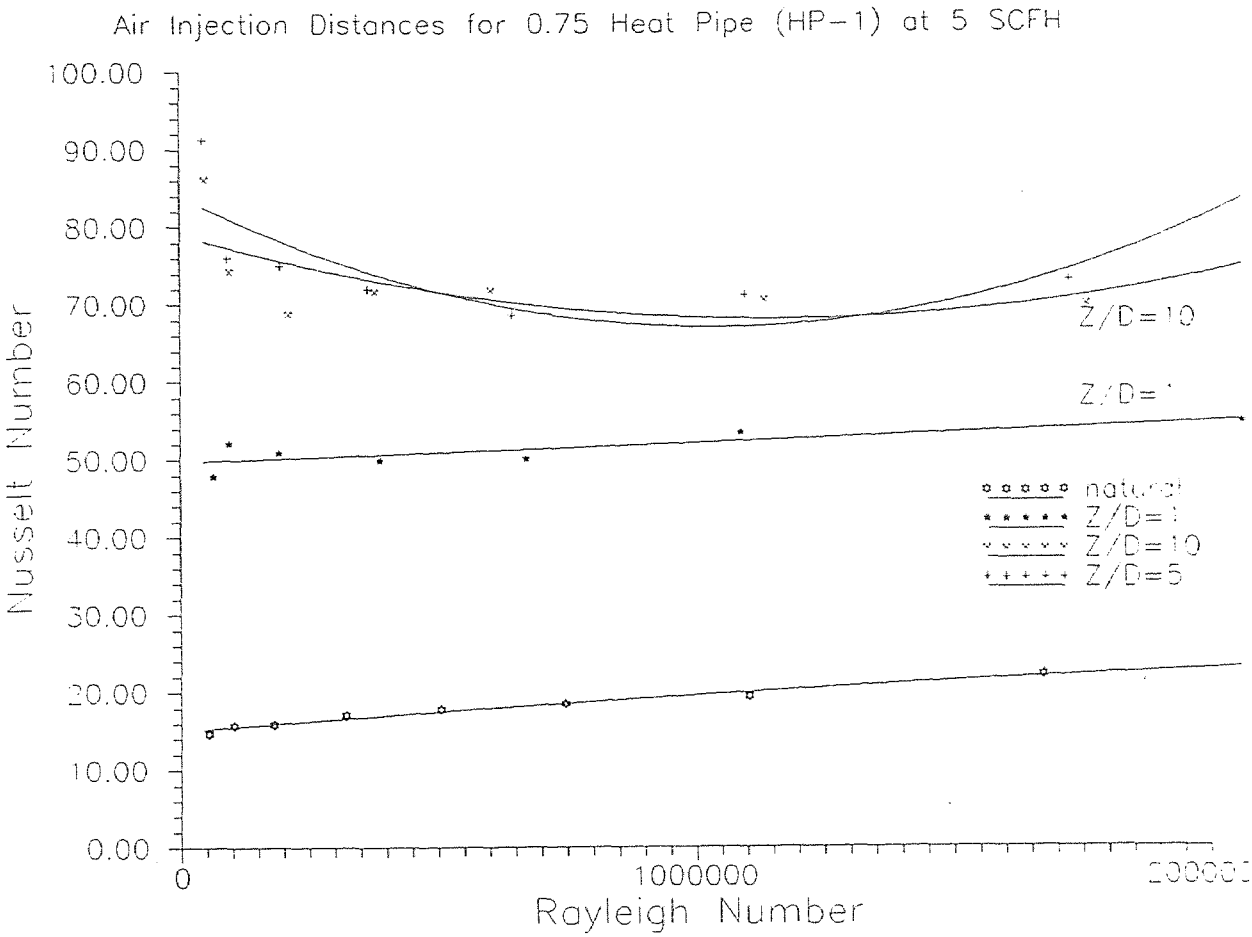

Figure 4-22: Air injection distance effect for 0.75" heat pipe at 5 SCFH.

4.7.4 Initial Water Temperature Effect

Two more experiments were performed to investigate the effect of initial water temperature on the heat transfer enhancement. It is well know that at higher Prantal numbers the boundary layer is thicker and the heat transfer by natural convection decreases. It was assumed that agitating the boundary layer will cause more heat to be transferred to the surrounding fluid since the air bubbles will penetrate the thicker boundary layer. Instead, the heat transfer coefficient is larger when the initial water temperature is higher. The boundary layer thickness also strongly depends on the heat pipe's heat input, and to achieve the high Rayleigh number needed to compare the different curves a lot more power had to be supplied to the heat pipe when the initial water temperature was lower than when it was higher. The heat transfer enhancement was 400% when the initial water temperature was 20.9 °C and 380% when the water temperature was lowered to 15.2 and 18.0 °C. Figure 4-23 shows these three curves. An observation made during these experiments was that the heat capacity of the heat pipe decreased as the water temperature decreased. The heat capacity was about 450 watts when the initial temperature of the water was 21 °C. The wattage decreased to 430 watts at 18.0 °C and 415 watts when the initial temperature was 15.2 °C. An experiment with the initial temperature of 4 °C was attempted on February 24, 1997 but the heat pipe's capacity was exceeded at an input rate of 275 watts and I was forced to exclude that experiment from the presented data.

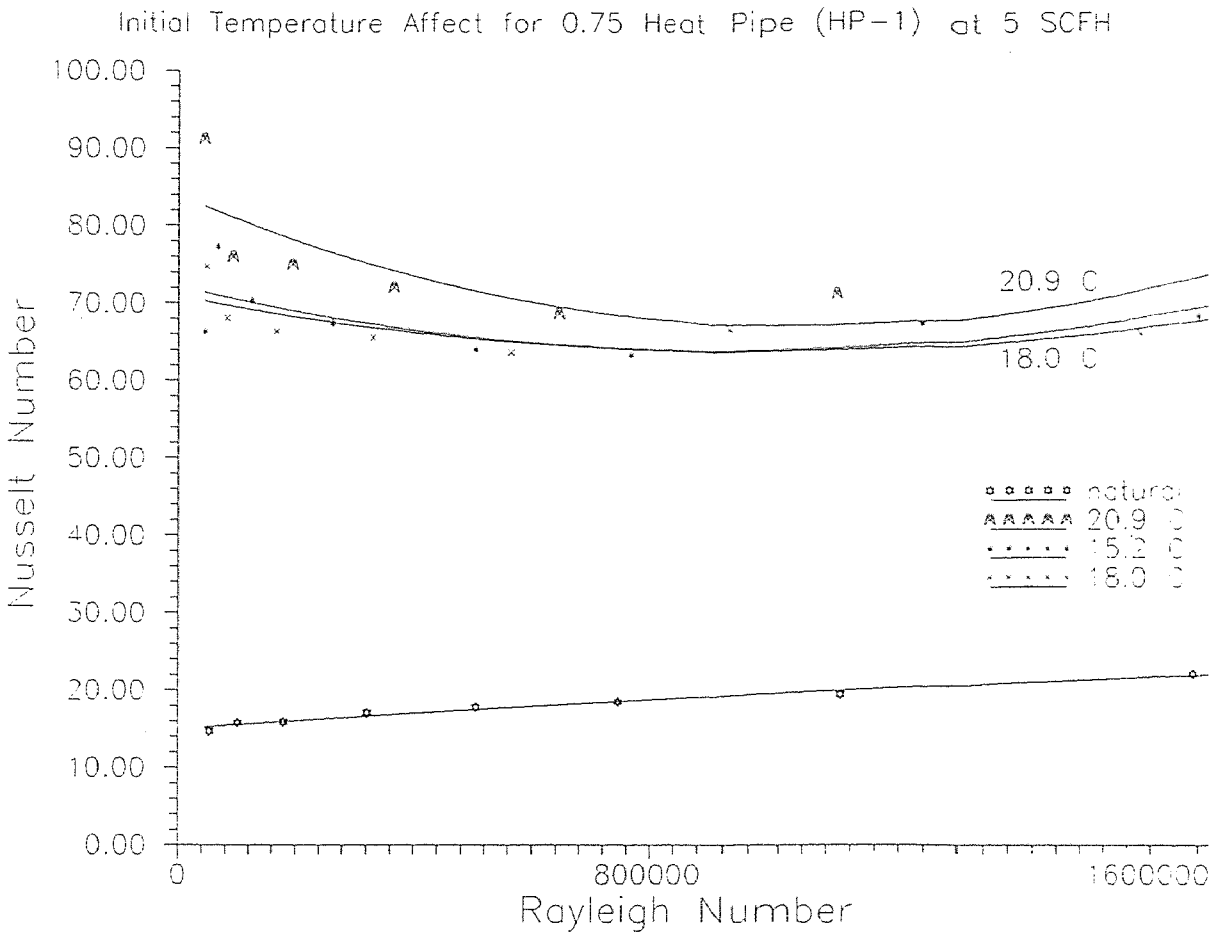

Figure 4-23: Initial water temperature effect for 0.75" heat pipe.

CHAPTER 5

CONCLUSION

This thesis investigates the enhancement of heat transfer from a heat pipe with the aid of gas injection. The heat transfer under natural convection conditions was calculated first, then a valve was activated and air was injected on the lower surface of the heat pipes such that it will enhance the heat transfer by the bubbles' turbulence and conduction with the heat pipe. It was found that the heat transfer will increase if the injection rates increase but there will be a optimum point where the high air injection rate will act as an insulator rather than an enhancement heat transfer agent. The air injection distance plays a major role in the heat transfer enhancement but is more effective at lower air flow rates. Here again there is an optimum distance the air injection can be lowered to because the conduction term of the heat transfer enhancement decreases as the injection distance between the heat pipe and air pipe increases. The air injection configuration has a very small or insignificant effect on the heat augmentation. The heat transfer enhancement strongly depends on the distance and shape of the shrouds placed around the heat pipe. The curved shrouds are more efficient in the larger diameter heat pipe since its physical dimensions restricts them from affecting the heat transfer on the smaller heat pipes. The straight shrouds impede the water circulation and have a negative effect on the heat transfer enhancement. The heat transfer was increased by 30% due to water circulation only. That number was higher in lower power inputs since the boundary layer was thicker at those inputs. The air injection configuration effect

plays a major role when the heat pipe is cooled at different sections at a given time. By injecting air at the hotter part of the heat pipe the heat transfer enhancement is 300% where it is 250% when air is injected at the middle or far portions of the heat pipe. The initial temperature of the surrounding water strongly influences the heat capacity of the heat pipe, the lower the initial temperature the lower the heat capacity of the heat pipe. The thickness of the thermal boundary layer strongly depends on the power input on the heat pipe and not as much in the initial temperature of the water. The curves of the individual heat pipes had a similar trend, but when one tries to compare the trends among the different size heat pipes no similarities are observed. This leads to the conclusion that the trend of the heat pipes strongly depends on the manufacturing techniques and intrinsic properties of the particular heat pipe. The natural convection equations for the ammonia heat pipe is given below.

$$\overline{Nu_D} = 5.5336 + 0.0002536 \cdot Ra_D \qquad \text{Equation (5.1)}$$

for the 0.5" HP-1 heat pipe is

$$\overline{Nu_D} = 13.24 + 0.000105 \cdot Ra_D \qquad \text{Equation (5.2)}$$

and for the 0.75" HP-1 heat pipe is

$$\overline{Nu_D} = 15.01 + 0.000005113 \cdot Ra_D \qquad \text{Equation (5.3)}$$

These equations are found using the least square line method. The natural convection equation for horizontal cylinders is given by Churchill (p. 2.5.7-21) to be:

$$\overline{Nu} = \frac{0.518 \cdot Ra^{1/4}}{\left[1 + (0.559/\mathrm{Pr})^{9/16}\right]^{4/9}} \qquad \text{Equation (5.4)}$$

this correlation does not agree well with the experimental results and the equations given on the previous page because it gives an error of over 100% at low Rayleigh numbers. This error diminishes to 30% at the higher Rayleigh numbers. A more accurate equation given by White (p. 405) is:

$$\overline{Nu_D}^{1/2} = 0.60 + \frac{0.387 \cdot Ra_D^{1/2}}{\left[1 + (0.559/\mathrm{Pr})^{9/16}\right]^{8/27}} \qquad \text{Equation (5.5)}$$

which gives an error of less than 1.0% for the 0.75" heat pipe at the highest Rayleigh number. Table 5-1 gives a tabular summary of the results obtained from the experiments. Figure 5-1 shows the natural convection curves from equations (5.4) and (5.5) and how they compare to the experimental results for the 0.75" HP-1 heat pipe only.

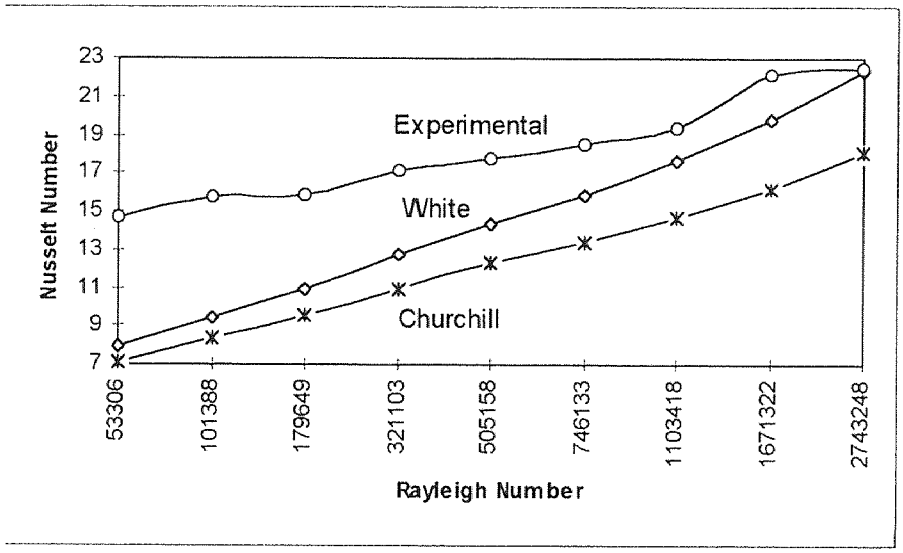

Figure 5-1: Natural convection curve comparison of Churchill's equation, White's equation with the experimental data.

Table 5-1: Tabular form of results

Parameter changed	How h changes	Agreement with existing experiments
Air injection rate	h increases as the injection rate increases up to a maximum point. Then injection rate acts as insulator.	In agreement with [22]
Air injection distance	h increases as the injection distance increases up to an optimum point. The lower the injection rate the farther the optimum point is located.	In agreement with [22] and [17]
Air injection configuration	h does not change much when different injection configurations are used as long as the amount of injected air is constant and the ports are distributed randomly along the length of the injection pipe.	In agreement with [22]
Curved shroud distance	h increases when the distance between the heat pipe and shroud is small but the shroud has a negative effect when the distance between the two increases.	In agreement with [33]
Shroud shape	h increased for curved shroud but straight shroud has a negative effect.	In agreement with [33]
Water circulation	h increases by 100-30% depending on circulation technique.	In agreement with [22]
Sectional cooling	h is higher when all ports are open but the first four ports account for most of the enhancement.	No existing experiments
Initial water temperature	h increases as the initial temperature increases.	In agreement with [38] and [1]

CHAPTER 6

RECOMENDATIONS

This thesis investigated the effect of heat transfer enhancement in relation to the following parameters: injection rates, injection distances, injection configuration, shroud shape, shroud distance, water circulation, initial temperature and sectional cooling. More experiments should be done to validate these results and explore different parameters such as the effect of heat transfer on the: viscosity of the liqui size of air injection hole or air bubbles, hydrodynamic pressure of liquid, size of water tank, extended surfaces from heat pipe and many other shroud shapes. These are just some parameters that one can experiment with, separately or simultaneously with the ones already investigated.

APPENTIX A

7/16" Heat Pipe Data

Air Injection Distance: Z/D=10
Air Injection Rate: 50 SCFH
Initial Water Temperature: 18 °C
Date: 10-29-1996

Table A-1: Air injection rate effect 50 SCFH

Volts	Amps	T_1	T_2	T_3	T_4	T_5	T_6	T_7
22	1.3	21.5	20.3	19.1	25.4	21.1	21.4	19
26	1.6	22.4	21.7	19.6	27.2	21.9	22.3	19.4
30	1.8	24.1	22.9	20.5	30.3	22.9	23.7	20.1
32	2.0	25.6	24.2	21.6	33.8	24.1	25.1	21.3
36.5	2.2	27.5	25.9	22.9	39.5	25.6	27.3	22.3

Table A-1 Continued

Volts	Amps	T_8	T_9	T_{10}	T_{11}	T_{12}	Ra. #	Nu. #
22	1.3	19	18.7	18.4	18.4	18.7	5114	35.6
26	1.6	19.6	19.2	18.8	18.9	19.2	6950	36.3
30	1.8	20.1	20.0	19.6	19.7	20.0	9215	38.0
32	2.0	21.1	20.9	20.6	20.6	20.9	11845	39.4
36.5	2.2	22.0	21.8	21.4	21.7	21.9	14981	40.8

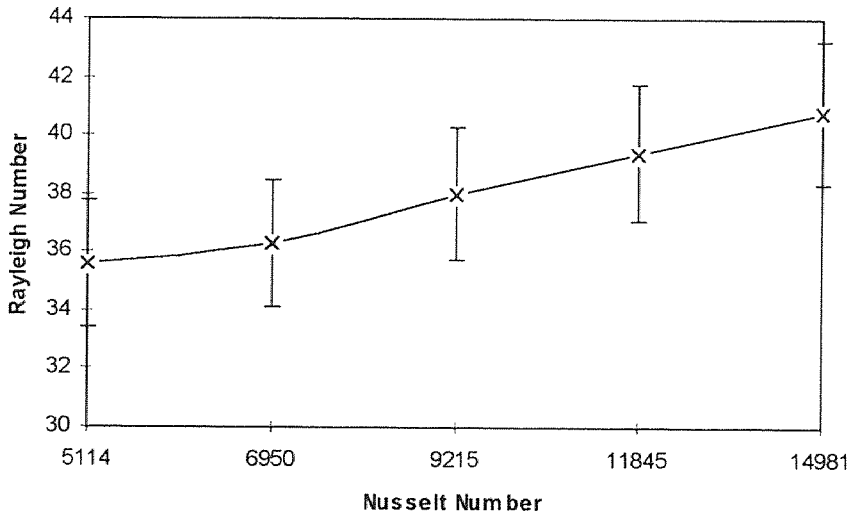

Figure A-1: Rayleigh number versus Nusselt number for 7/16" heat pipe. Air injection 50 SCFH

7/16" Heat Pipe Data

Air Injection Distance: Z/D=10
Air Injection Rate: 30 SCFH
Initial Water Temperature: 17.8 °C
Date: 10-30-1996

Table A-2: Air injection rate effect 30 SCFH

Volts	Amps	T_1	T_2	T_3	T_4	T_5	T_6	T_7
22	1.3	21.4	19.9	19.0	25.3	21.8	22.0	18.8
26	1.6	22.6	21.6	19.5	28.3	22.9	23.4	19.4
30	1.8	24.2	23.2	20.5	31.4	23.8	24.7	20.2
32	2.0	25.8	24.3	21.9	34.0	24.1	25.2	21.3
36.5	2.2	28.2	26.5	23.2	39.0	25.5	27.4	22.5

Table A-2 Continued

Volts	Amps	T_8	T_9	T_{10}	T_{11}	T_{12}	Ra. #	Nu. #
22	1.3	18.4	18.4	18.1	18.2	18.5	5338	30.7
26	1.6	19.0	19.0	18.7	18.8	19.1	7471	33.6
30	1.8	19.9	19.9	19.5	19.5	20.0	10061	35.0
32	2.0	20.8	20.9	20.6	20.6	20.9	12345	36.2
36.5	2.2	22.2	22.2	21.9	22.0	22.3	16128	37.4

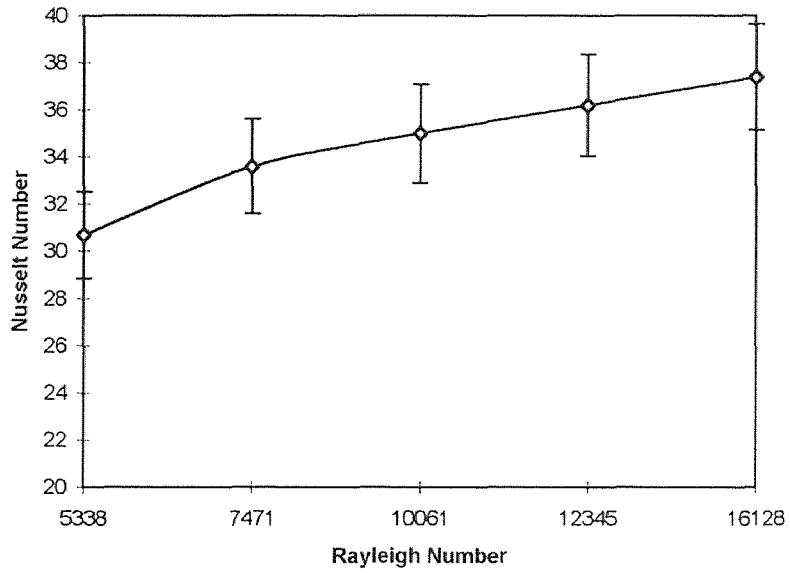

Figure A-2: Nusselt number versus Rayleigh number. Air injection 30 SCFH

7/16" Heat Pipe Data

Air Injection Distance: Z/D=10
Air Injection Rate: 10 SCFH
Initial Water Temperature: 17.8 °C
Date: 10-30-1996

Table A-3: Air injection rate effect 10 SCFH

Volts	Amps	T_1	T_2	T_3	T_4	T_5	T_6	T_7
22	1.3	21.5	20.3	19.0	25.0	21.6	21.8	19.0
26	1.6	22.9	22.2	19.8	28.2	22.9	23.3	19.7
30	1.8	24.9	23.7	21.0	31.0	23.5	24.3	20.8
32	2.0	26.7	25.6	22.5	34.6	24.7	25.8	22.1
36.5	2.2	29.1	27.7	24.5	39.1	26.1	27.4	23.4

Table A-3 Continued

Volts	Amps	T_8	T_9	T_{10}	T_{11}	T_{12}	Ra. #	Nu. #
22	1.3	18.4	18.6	18.2	18.3	18.6	5616	29.5
26	1.6	19.2	19.4	19.0	19.1	19.4	7990	32.3
30	1.8	20.2	20.4	20.0	20.2	20.4	10732	33.97
32	2.0	21.6	21.7	21.3	21.5	21.7	13524	34.7
36.5	2.2	22.9	23.1	22.8	22.9	23.1	18405	34.7

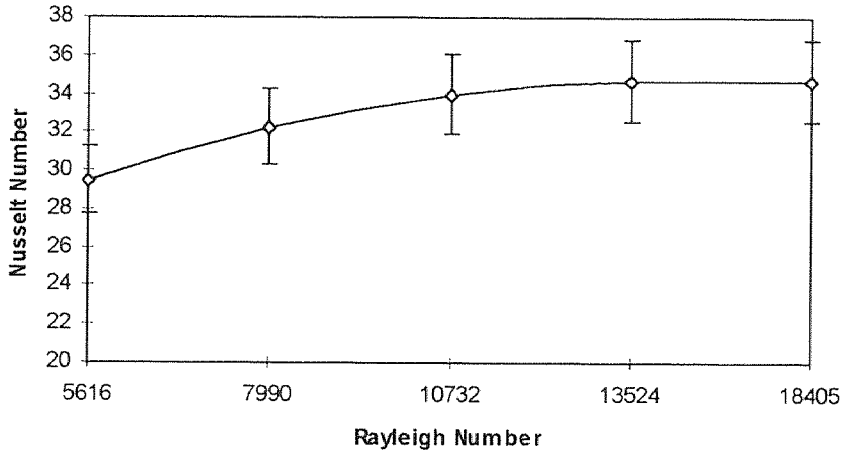

Figure A-3: Nusselt number versus Rayleigh number. Air injection 10 SCFH.

7/16" Heat Pipe Data

Air Injection Distance: Z/D=2
Air Injection Rate: 50 SCFH
Initial Water Temperature: 17.7 °C
Date: 10-31-1996

Table A-4: Air injection distance effect Z/D=2

Volts	Amps	T_1	T_2	T_3	T_4	T_5	T_6	T_7
22	1.3	21.7	20.0	18.5	25.0	21.0	21.3	18.4
26	1.6	22.9	21.2	18.9	27.6	21.8	22.3	18.9
30	1.8	24.3	22.1	19.5	30.2	22.7	23.4	19.5
32	2.0	25.5	23.1	20.4	33.3	23.6	24.6	20.2
36.5	2.2	27.6	24.8	21.9	39.7	25.5	27.0	21.4

Table A-4 Continued

Volts	Amps	T_8	T_9	T_{10}	T_{11}	T_{12}	Ra. #	Nu. #
22	1.3	18.2	18.1	17.7	17.8	18.1	6594	24.4
26	1.6	18.6	18.5	18.1	18.2	18.5	8428	29.6
30	1.8	19.1	19.0	18.7	18.8	19.1	10124	33.2
32	2.0	19.8	19.7	19.4	19.5	19.8	11931	35.0
36.5	2.2	20.9	20.8	20.3	20.6	20.6	15719	35.6

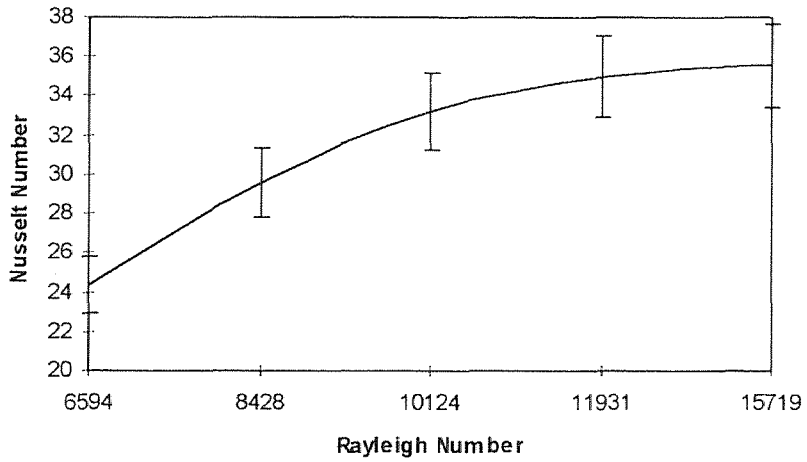

Figure A-4: Nusselt number versus Rayleigh number. Air injection distance Z/D=2

7/16" Heat Pipe Data

Air Injection Distance: Z/D=7
Air Injection Rate: 50 SCFH
Initial Water Temperature: 18 °C
Date: 10-25-1996

Table A-5: Air injection distance effect Z/D=7

Volts	Amps	T_1	T_2	T_3	T_4	T_5	T_6	T_7
22	1.3	21.6	20.0	19.0	24.9	21.9	20.9	18.8
26	1.6	22.9	21.7	19.6	28.0	22.9	22.5	19.3
30	1.8	24.6	23.0	20.5	30.8	23.9	23.9	20.1
32	2.0	26.0	24.1	21.4	34.2	24.9	25.4	20.8
36.5	2.2	27.8	25.7	22.8	39.0	26.3	27.1	21.7

Table A-5 Continued

Volts	Amps	T_8	T_9	T_{10}	T_{11}	T_{12}	Ra. #	Nu. #
22	1.3	18.5	18.4	18.3	18.4	18.9	5228	31.6
26	1.6	19.1	19.0	18.8	18.9	19.4	7623	33.5
30	1.8	19.9	19.7	19.5	19.7	20.2	10339	34.2
32	2.0	20.5	20.5	20.3	20.4	21.0	12498	35.4
36.5	2.2	21.5	21.4	21.2	21.4	21.9	16255	37.6

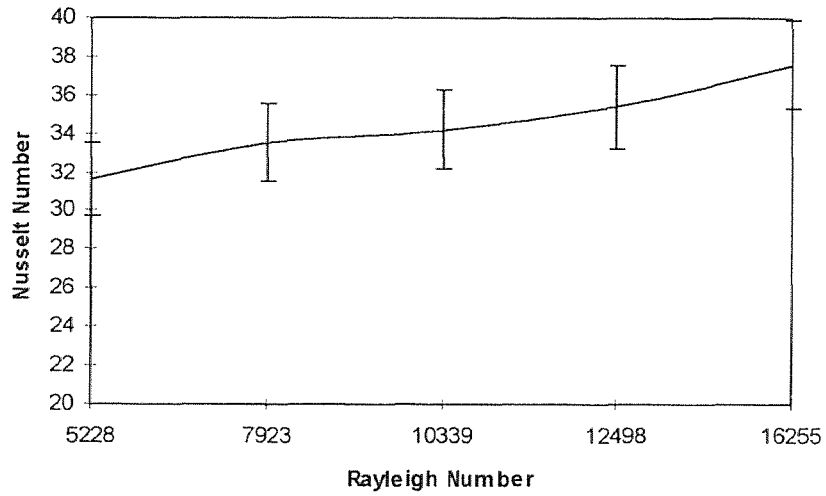

Figure A-5: Nusselt number versus Rayleigh number. Air injection distance Z/D=7

7/16" Heat Pipe Data

Air Injection Distance: Z/D=5
Air Injection Rate: 10 SCFH
Initial Water Temperature: 17.3 °C
Date: 11-6-1996

Table A-6: Air injection configuration effect 10 openings

Volts	Amps	T_1	T_2	T_3	T_4	T_5	T_6	T_7
22	1.3	21.6	19.8	18.5	22.7	25.5	25.8	17.9
26	1.6	23.1	22.0	19.2	23.7	28.3	29.2	18.6
31.5	1.9	25.6	24.0	20.8	25.4	33.1	34.4	19.8
36.5	2.2	28.5	26.5	23.4	28.2	39.9	42.8	21.5

Table A-6 Continued

Volts	Amps	T_8	T_9	T_{10}	T_{11}	T_{12}	Ra. #	Nu. #
22	1.3	17.8	17.5	17.4	17.6	18.2	6941	23.5
26	1.6	18.5	18.2	18.1	18.3	18.9	10061	25.2
31.5	1.9	19.7	19.4	19.3	19.5	20.1	14347	28
36.5	2.2	21.4	21.1	21.0	21.2	21.8	20403	29.3

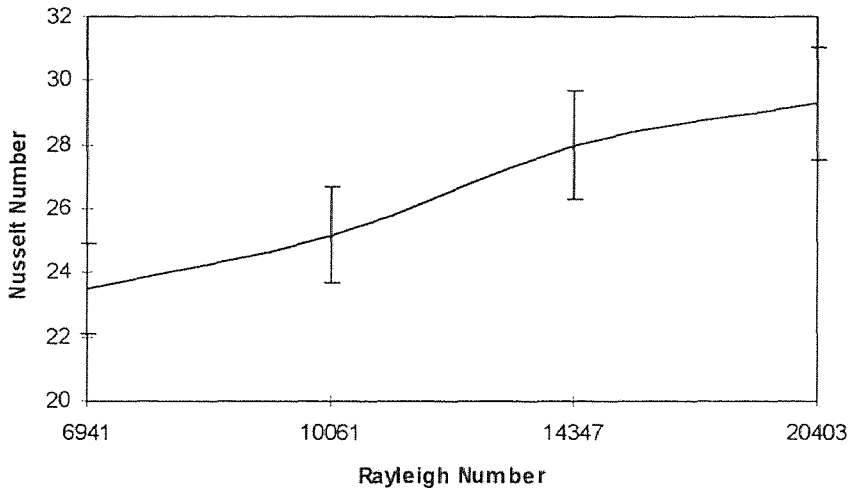

Figure A-6: Nusselt number versus Rayleigh number. Screws # 3, 4, 5, 7, 8, 10, 11, 12, 13, 14 were removed.

7/16" Heat Pipe Data

Air Injection Distance: Z/D=5
Air Injection Rate: 10 SCFH
Initial Water Temperature: 17.2 °C
Date: 11-7-1996

Table A-7: Air injection configuration effect 15 openings

Volts	Amps	T_1	T_2	T_3	T_4	T_5	T_6	T_7
22	1.3	21.5	19.8	18.4	22.1	25.3	26.0	17.8
26	1.6	23.1	22.0	19.2	23.6	28.4	29.3	18.6
31.5	1.9	25.4	24.1	20.7	25.7	32.9	34.2	19.6
36.5	2.2	28.2	26.4	23.7	29.7	41.2	43.7	21.5

Table A-7 Continued

Volts	Amps	T_8	T_9	T_{10}	T_{11}	T_{12}	Ra. #	Nu. #
22	1.3	17.7	17.4	17.3	17.5	18.1	6989	22.9
26	1.6	18.5	18.2	18.1	18.3	18.9	10061	24.3
32	2.0	19.5	19.2	19.1	19.3	19.9	13876	28
36.5	2.2	21.0	20.7	20.6	21.1	21.7	24100	28.4

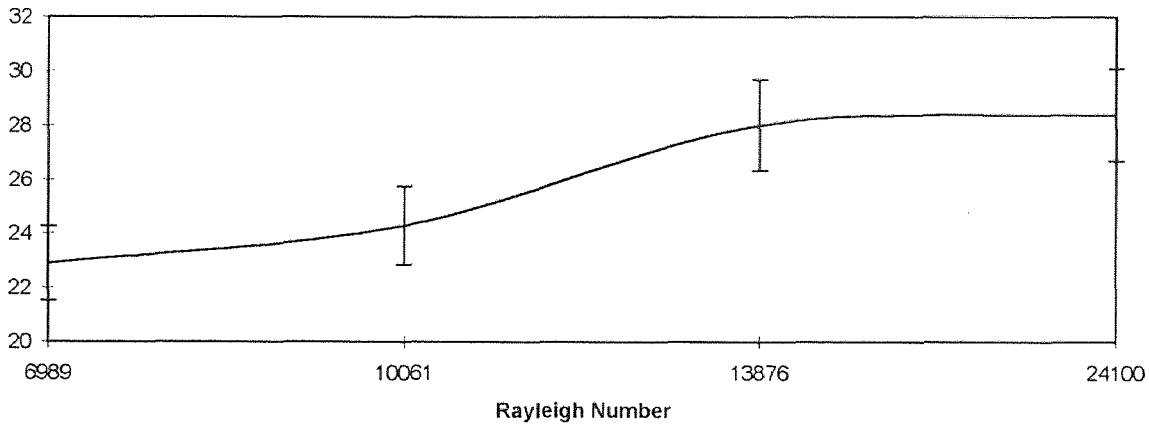

Figure A-7: Nusselt number versus Rayleigh number. All screws were removed.

Air Injection Configuration Effect

Air Injection Distance: Z/D=5
Air Injection Rate: 10 SCFH
Initial Water Temperature: 17.4 °C
Date: 11-6-1996

Table A-8: Air injection configuration effect 6 openings

Volts	Amps	T_1	T_2	T_3	T_4	T_5	T_6	T_7
22	1.3	21.7	19.9	18.5	22.0	25.4	26.1	17.9
26	1.6	23.4	22.1	19.4	23.4	28.4	29.4	18.8
31.5	1.9	25.7	23.9	20.9	25.1	32.8	34.1	19.7
36.5	2.2	28.5	26.4	23.7	29.7	41.2	43.7	21.5

Table A-8 Continued

Volts	Amps	T_8	T_9	T_{10}	T_{11}	T_{12}	Ra. #	Nu. #
22	1.3	17.8	17.5	17.4	17.6	18.2	7144	22.5
26	1.6	18.7	18.4	18.3	18.5	19.0	10242	24.7
31.5	1.9	19.6	19.4	19.3	19.5	20.0	14627	28.0
36.5	2.2	21.4	21.1	21.0	21.2	21.8	20741	28.6

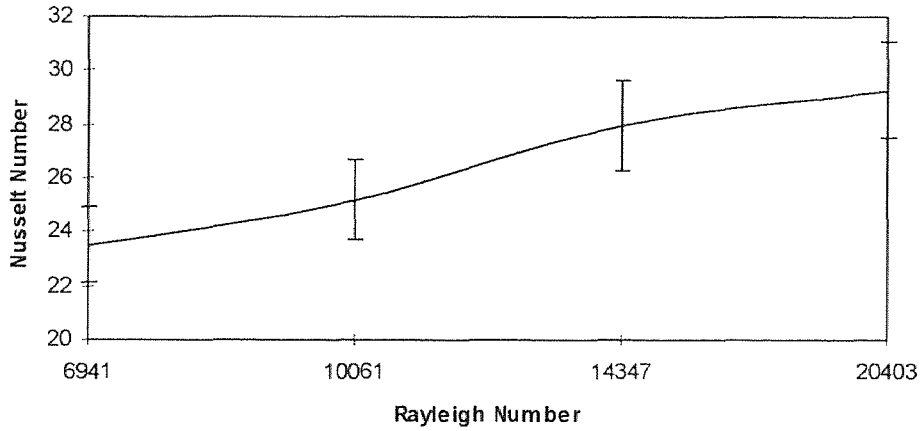

Figure A-8: Nusselt number versus Rayleigh number. Screws # 3, 4, 7, 8, 11, 12 were removed.

7/16" Heat Pipe Data

Air Injection Distance: Z/D=13
Air Injection Rate: 50 SCFH
Initial Water Temperature: 16.8 °C
Date: 11-2-1996

Table A-9: Curved shroud distance effect d/D=2

Volts	Amps	T_1	T_2	T_3	T_4	T_5	T_6	T_7
22	1.3	20.5	18.8	17.9	19.1	22.8	23.6	17.4
26	1.6	21.6	20.9	18.4	20.5	26.0	27.2	17.9
30	1.8	22.9	21.8	18.9	21.7	29.0	30.4	18.2
32	2.0	24.1	22.8	19.7	22.7	32.2	33.8	18.7
36.5	2.2	25.8	24.1	21.1	24.4	37.5	39.5	19.4

Table A-9 Continued

Volts	Amps	T_8	T_9	T_{10}	T_{11}	T_{12}	Ra. #	Nu. #
22	1.3	17.3	17.0	16.9	17.1	17.7	5543	28.0
26	1.6	17.8	17.5	17.4	17.6	18.2	8064	28.7
30	1.8	18.1	17.8	17.7	17.9	18.5	10396	30.5
32	2.0	18.6	18.3	18.2	18.4	19.0	12685	31.5
36.5	2.2	19.0	19.0	18.9	19.1	19.7	16482	32.9

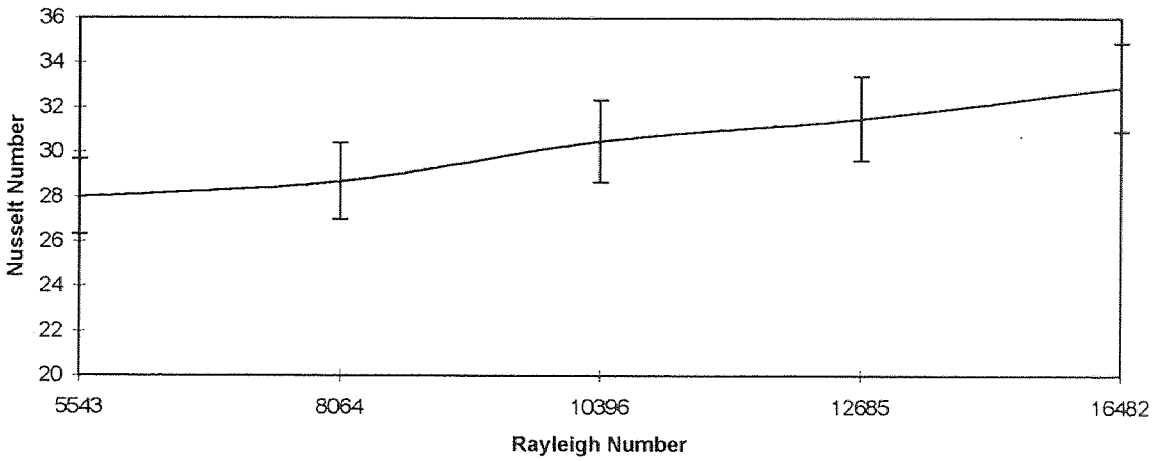

Figure A-9: Nusslet versus Raynolds numbers. Horizontal curved shroud distance d/D=2.

7/16" Heat Pipe Data

Air Injection Distance: Z/D=13
Air Injection Rate: 50 SCFH
Initial Water Temperature: 16.8 °C
Date: 11-2-1996

Table A-10: Curved shroud distance effect d/D=4

Volts	Amps	T_1	T_2	T_3	T_4	T_5	T_6	T_7
22	1.3	20.7	19.0	17.9	18.5	23.1	24.1	17.2
26	1.6	21.6	20.7	18.2	19.6	25.4	26.7	17.5
30	1.8	22.8	21.6	18.8	20.7	28.3	29.8	18.2
32	2.0	23.9	22.6	19.5	21.8	31.2	32.9	19.3
36.5	2.2	25.6	23.9	20.8	23.4	36.1	38.1	19.9

Table A-10 Continued

Volts	Amps	T_8	T_9	T_{10}	T_{11}	T_{12}	Ra. #	Nu. #
22	1.3	17.1	16.8	16.7	16.9	17.5	6348	24.4
26	1.6	17.4	17.1	17.0	17.2	17.8	8734	27.2
30	1.8	18.1	17.8	17.7	17.9	18.5	10031	30.1
32	2.0	19.2	18.9	18.8	19.0	19.6	10055	30.7
36.5	2.2	19.8	19.5	19.4	19.6	20.2	13850	32.2

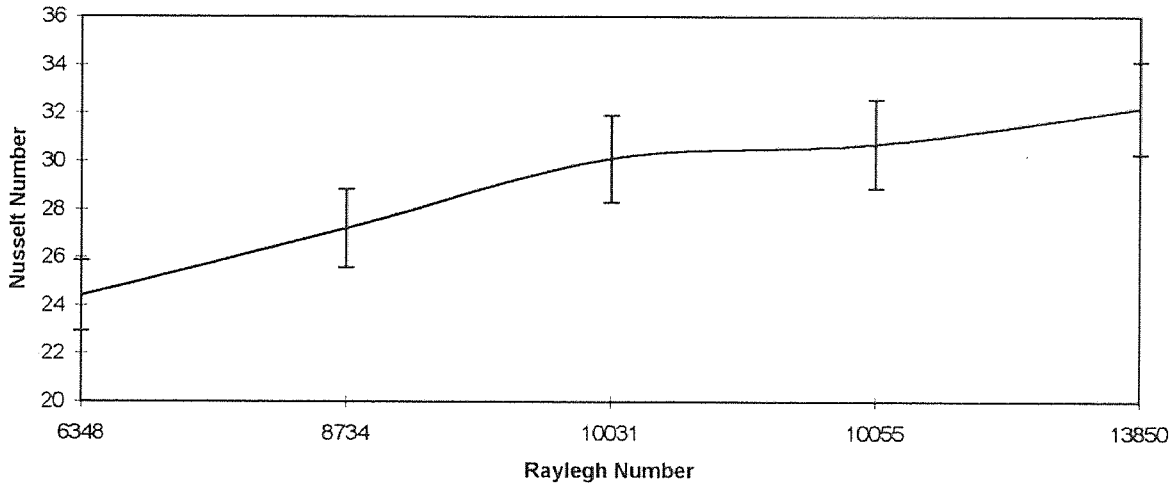

Figure A-10: Nusselt versus Rayleigh number. The horizontal curved shroud distance d/D=4.

7/16" Heat Pipe Data

Air Injection Distance: Z/D=8
Air Injection Rate: 50 SCFH
Initial Water Temperature: 16.8 °C
Date: 11-4-1996

Table A-11: Curved shroud distance effect d/D=1

Volts	Amps	T_1	T_2	T_3	T_4	T_5	T_6	T_7
22	1.3	20.8	19.2	18.0	20.3	24.2	25.1	17.4
26	1.6	21.8	20.9	18.3	21.3	26.3	27.4	17.7
31.5	1.9	23.7	22.4	19.4	23.2	30.7	32.2	18.5
36.5	2.2	25.9	24.3	21.1	25.4	36.2	38.0	19.6

Table A-11 Continued

Volts	Amps	T_8	T_9	T_{10}	T_{11}	T_{12}	Ra. #	Nu. #
22	1.3	17.3	17.0	16.9	17.1	17.7	6225	24.4
26	1.6	17.6	17.3	17.2	17.4	18.0	7706	26.7
31.5	1.9	18.4	18.1	18.0	18.2	18.8	11862	29.7
36.5	2.2	19.5	19.2	19.1	19.3	19.9	16253	32.6

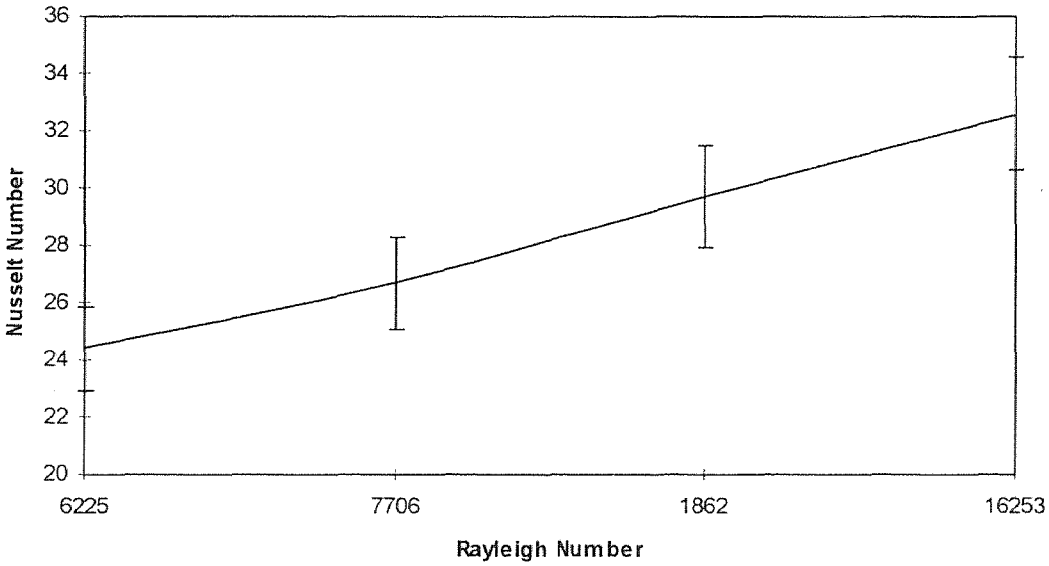

Figure A-11: Nusselt number versus Rayleigh number. The curved shroud distance was d/D=1.

7/16" Heat Pipe Data

Air Injection Distance: Z/D=8
Air Injection Rate: 50 SCFH
Initial Water Temperature: 16.8 °C
Date: 11-2-1996

Table A-12: Straight shroud distance effect d/D=1

Volts	Amps	T_1	T_2	T_3	T_4	T_5	T_6	T_7
22	1.3	20.9	19.2	18.0	20.3	23.9	24.7	17.4
26	1.6	21.9	20.9	18.3	21.4	26.4	27.5	17.7
31.5	1.9	23.7	22.4	19.3	22.9	30.7	32.1	18.4
36.5	2.2	26.0	24.3	21.2	25.4	36.7	38.6	19.4

Table A-12 Continued

Volts	Amps	T_8	T_9	T_{10}	T_{11}	T_{12}	Ra. #	Nu. #
22	1.3	17.3	17.0	16.9	17.1	17.7	6354	23.9
26	1.6	17.6	17.3	17.2	17.4	18.0	7807	26.4
31.5	1.9	18.3	18.0	17.9	18.1	18.7	12044	29.0
36.5	2.2	19.3	19.0	18.9	19.1	19.7	17164	30.7

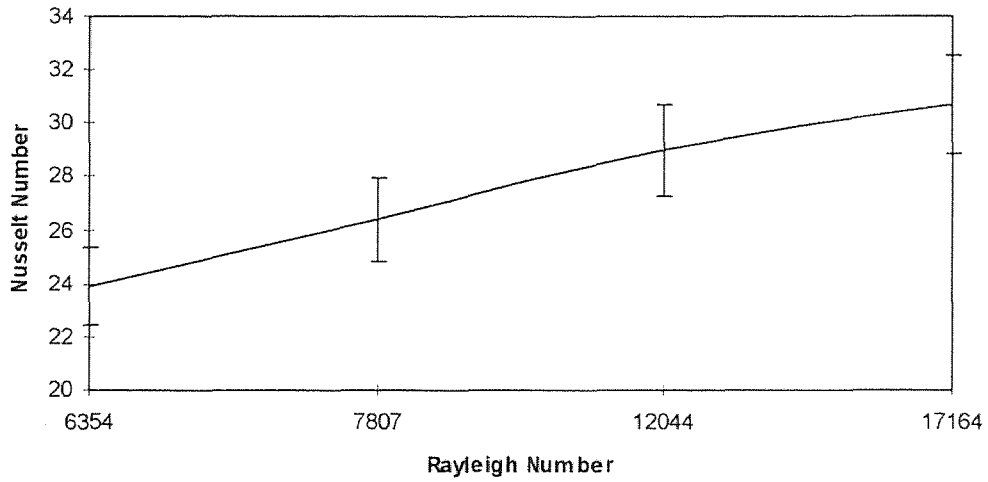

Figure A-12: Nusselt versus Rayleigh number. The straight shrouds distance was d/D=1.

7/16" Heat Pipe Data

Air Injection Distance: Z/D=8
Air Injection Rate: 50 SCFH
Initial Water Temperature: 17.0 °C
Date: 11-6-1996

Table A-13: Air injection distance effect Z/D=8

Volts	Amps	T_1	T_2	T_3	T_4	T_5	T_6	T_7
22	1.3	21.1	19.2	18.3	21.0	24.4	25.0	17.7
26	1.6	22.6	21.4	18.9	22.0	26.9	27.9	18.3
31.5	1.9	24.5	23.0	20.0	23.9	31.2	32.6	19.2
36.5	2.2	27.0	24.9	21.9	26.5	37.1	38.8	20.4

Table A-13 Continued

Volts	Amps	T_8	T_9	T_{10}	T_{11}	T_{12}	Ra. #	Nu. #
22	1.3	17.6	17.3	17.2	17.4	18.0	6047	25.9
26	1.6	18.2	17.9	17.8	18.0	18.6	9270	26.5
31.5	1.9	19.1	18.8	18.7	18.9	19.5	12321	31.1
36.5	2.2	20.3	20.0	19.9	20.1	20.7	17219	32.5

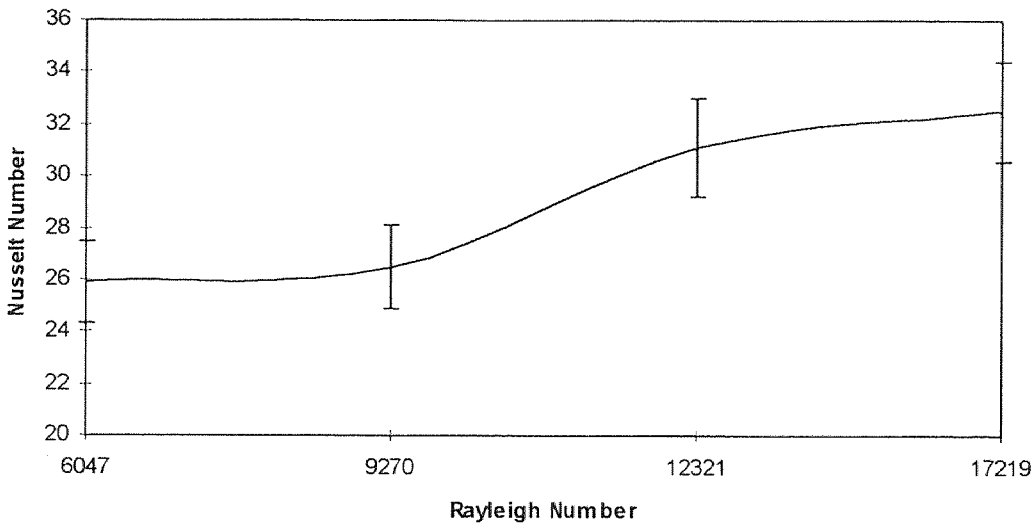

Figure A-13: Nusselt number versus Rayleigh number. There were no shrouds in the water tank.

7/16" Heat Pipe Data

Air Injection Distance: Z/D=20
Air Injection Rate: 10 SCFH
Initial Water Temperature: 17.0 °C
Date: 11-6-1996

Table A-14: Water circulation only effect

Volts	Amps	T_1	T_2	T_3	T_4	T_5	T_6	T_7
19	1.0	23.7	21.9	20.0	21.6	27.2	22.0	20.4
22	1.3	24.4	23.0	20.6	22.7	29.9	23.2	20.5
26	1.6	25.9	25.4	21.7	23.7	33.1	24.4	20.9
30	1.8	27.5	26.9	23.2	24.6	37.5	25.4	21.2

Table A-14 Continued

Volts	Amps	T_8	T_9	T_{10}	T_{11}	T_{12}	Ra. #	Nu. #
19	1.0	20.2	20.4	20.4	20.4	20.4	7574	15.5
22	1.3	20.5	20.5	20.5	20.6	20.6	10174	16.8
26	1.6	20.9	20.9	20.9	20.9	20.9	15005	19.2
30	1.8	21.2	21.2	21.2	21.2	21.2	19635	19.8

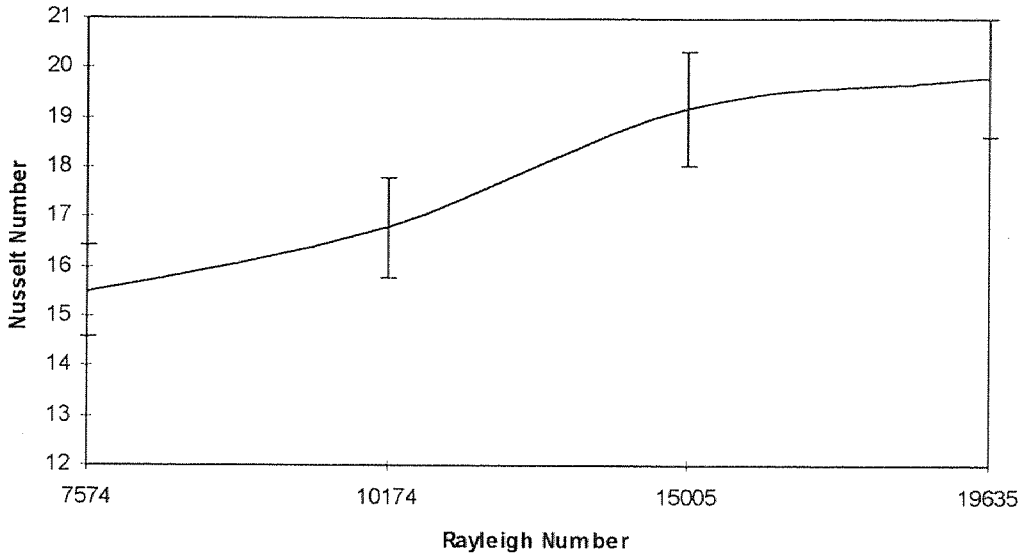

Figure A-14: Nusselt versus Rayleigh numbers. The air injection pipe was placed at the bottom of the water tank.

7/16" Heat Pipe Data

Air Injection Distance: Z/D=0
Air Injection Rate: 00 SCFH
Initial Water Temperature: 18 °C
Date: 11-11-1996
Natural Convection

Table A-15: Natural convection

Volts	Amps	T_1	T_2	T_3	T_4	T_5	T_6	T_7
12	0.5	23.5	21.5	21.5	21.2	24.4	20.8	20.5
16	0.7	24.5	22.7	22.7	22.2	25.9	22.1	20.8
20	1.1	28.0	24.9	26.0	24.0	31.6	24.5	22.5
21	1.2	28.8	25.2	27.6	24.0	32.4	24.6	22.7

Table A-15 Continued

Volts	Amps	T_8	T_9	T_{10}	T_{11}	T_{12}	Ra. #	Nu. #
12	0.5	20.5	20.5	20.5	20.5	20.5	4860	6.5
16	0.7	20.8	20.8	20.8	20.8	20.8	9232	8.3
20	1.1	22.5	22.5	22.5	22.5	22.5	16766	9.6
21	1.2	22.7	22.7	22.7	22.7	22.7	18300	10.2

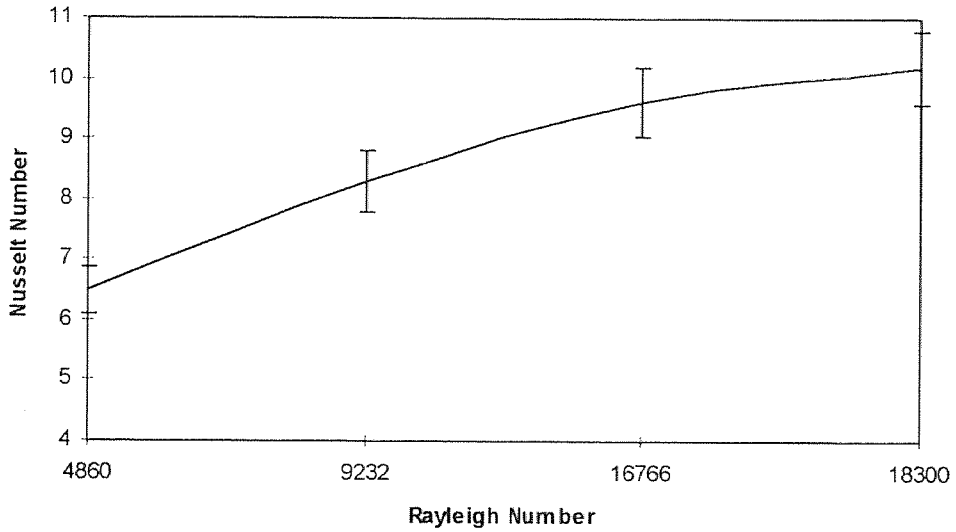

Figure A-15: Nusselt number versus Rayleigh number. Natural convection conditions.

APPENDIX B

0.5" Heat Pipe Data

Air Injection Distance: Z/D=10
Air Injection Rate: 10 SCFH Date: 11-20-1996
Initial Water Temperature: 21 °C

Table B-1: Air injection rate effect 10 SCFH

Volts	Amps	T_1	T_2	T_3	T_4	T_7	T_8
19	2.0	24.2	23.4	21.6	21.7	21.7	21.7
23	2.5	26.2	25.1	24.0	23.0	23.1	23.1
27	3.0	28.9	27.5	27.4	24.9	25.0	25.0
30.5	3.5	31.8	30.6	30.7	27.6	27.4	27.4
34.5	4.0	36.7	34.5	34.6	31.7	30.8	30.8
39.5	4.5	42.1	39.7	40.0	37.5	35.0	35.0
44	5.0	48.9	45.7	46.0	45.3	39.9	39.9
48	5.5	54.8	51.3	52.2	48.4	44.4	44.4

Table B-1 Continued

Volts	Amps	T_9	T_{10}	T_{11}	T_{12}	Ra. #	Nu. #
19	2.0	21.7	27.1	27.1	22.7	5956	70.3
23	2.5	23.1	30.5	30.5	24.7	9415	74.1
27	3.0	25.0	35.1	35.2	26.6	15607	70.3
30.5	3.5	27.4	40.2	40.5	28.5	25295	72.1
34.5	4.0	30.8	46.0	46.0	31.0	45953	70.2
39.5	4.5	35.0	54.0	53.9	34.5	78694	70.6
44	5.0	39.9	62.0	62.0	37.9	145656	60.6
48	5.5	44.4	68.9	68.7	51.5	199650	65.0

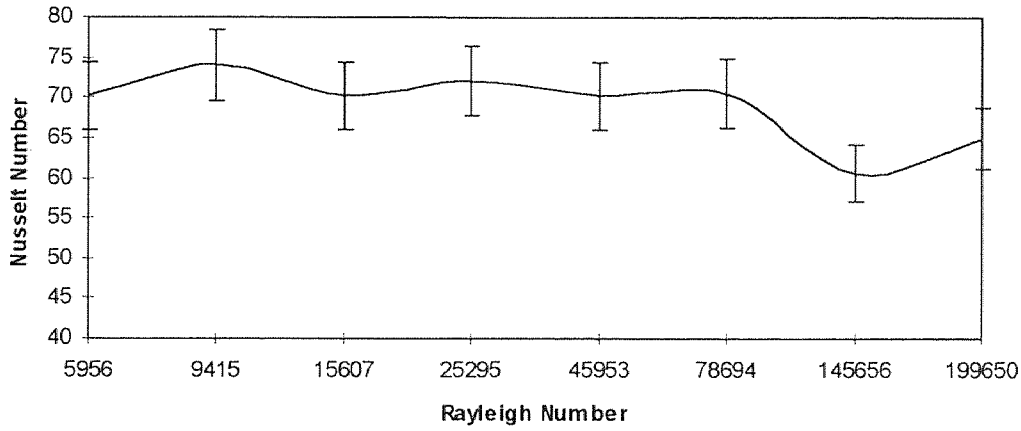

Figure B-1: Nuselt number versus Rayleigh number. Air injection rate 10 SCFH

0.5" Heat Pipe Data

Air Injection Distance: Z/D=10
Air Injection Rate: 30 SCFH Date: 11-21-1996
Initial Water Temperature: 21 °C

Table B-2: Air injection rate effect 30 SCFH

Volts	Amps	T_1	T_2	T_3	T_4	T_7	T_8
19	2.0	23.8	23.3	21.3	21.3	21.3	21.3
23	2.5	25.6	25.0	22.7	22.4	22.4	22.4
27	3.0	28.0	27.2	26.8	24.0	24.1	24.1
30.5	3.5	31.5	30.7	30.4	26.9	27.0	27.0
34.5	4.0	35.5	34.3	34.0	30.0	29.6	29.6
39.5	4.5	40.0	38.7	38.7	35.5	33.5	33.5
44	5.0	47.3	45.2	45.2	42.7	39.1	39.1
48	5.5	53.1	51.4	50.8	47.7	42.9	42.9

Table B-2 Continued

Volts	Amps	T_9	T_{10}	T_{11}	T_{12}	Ra. #	Nu. #
19	2.0	21.3	26.7	26.7	23.0	6398	64.6
23	2.5	22.4	30.1	30.2	24.3	9371	71.8
27	3.0	24.1	34.6	34.5	26.1	16556	63.9
30.5	3.5	27.0	39.4	39.5	28.3	25296	68.1
34.5	4.0	29.6	44.3	44.3	30.2	44637	66.9
39.5	4.5	33.5	50.6	50.6	33.2	73337	69.7
44	5.0	39.1	61.0	60.9	37.7	129404	65.6
48	5.5	42.9	67.6	67.5	40.7	199754	69.6

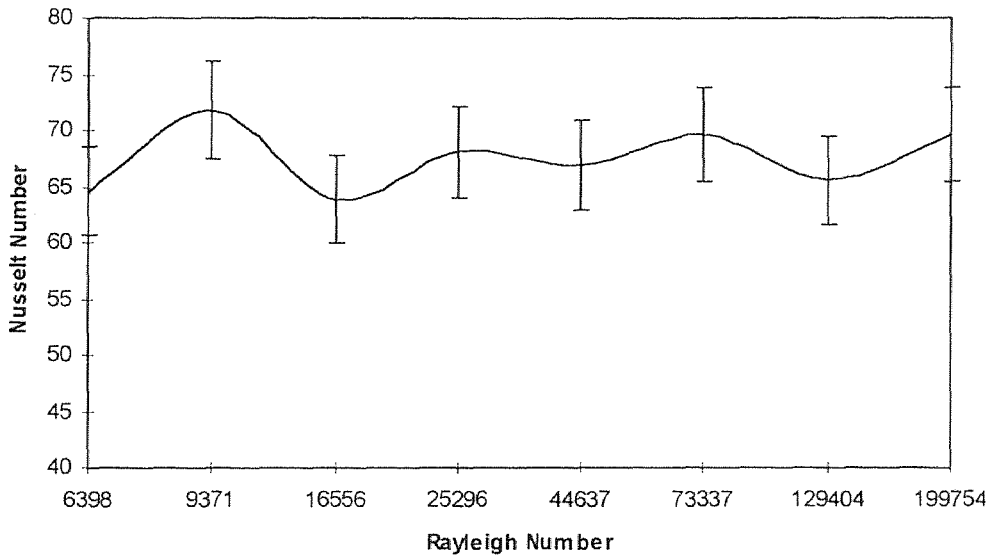

Figure B-2: Nusselt number versus Rayleigh number. Air injection rate 30 SCFH

0.5" Heat Pipe Data

Air Injection Distance: Z/D=10
Air Injection Rate: 50 SCFH Date: 11-25-1996
Initial Water Temperature: 19 °C

Table B-3: Air injection rate effect 50 SCFH

Volts	Amps	T_1	T_2	T_3	T_4	T_7	T_8
19	2.0	23.7	23.4	21.0	21.0	21.1	21.1
23	2.5	25.5	24.9	22.5	22.4	22.4	22.4
27	3.0	27.5	26.9	26.5	23.5	23.6	23.6
30.5	3.5	30.5	29.4	29.1	25.6	25.7	25.7
34.5	4.0	34.6	33.4	33.2	29.0	28.5	28.5
39.5	4.5	38.5	36.9	36.7	3.3	31.8	31.8
44	5.0	45.1	43.7	43.3	40.0	37.0	37.0
48	5.6	52.2	50.4	50.3	46.7	42.1	42.1

Table B-3 Continued

Volts	Amps	T_9	T_{10}	T_{11}	T_{12}	Ra. #	Nu. #
19	2.0	21.1	26.6	26.6	22.3	6610	61.5
23	2.5	22.4	30.1	30.1	24.3	8732	76.7
27	3.0	23.6	34.0	34.1	25.7	16850	61.4
30.5	3.5	25.7	37.9	38.0	27.4	22584	68.4
34.5	4.0	28.5	42.4	42.4	29.4	43289	64.0
39.5	4.5	31.8	48.0	48.2	31.9	65260	70.0
44	5.0	37.0	57.1	57.0	36.1	123515	66.2
48	5.6	42.1	66.7	66.4	40.4	192655	62.4

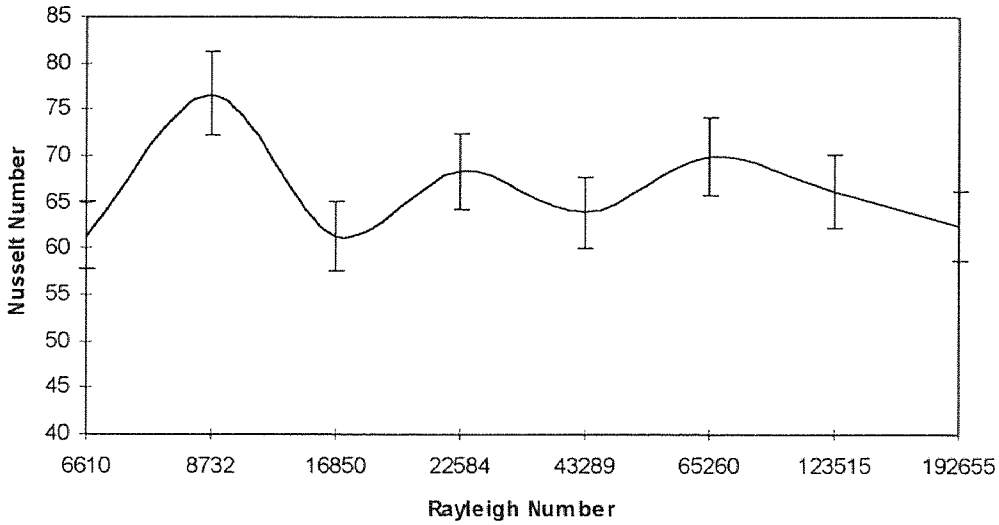

Figure B-3: Nusselt number versus Rayleigh number. Air injection rate 50 SCFH

0.5" Heat Pipe Data

Air Injection Distance: Z/D=2
Air Injection Rate: 10 SCFH Date: 12-16-1996
Initial Water Temperature: 21 °C

Table B-4: Air injection distance effect Z/D=2

Volts	Amps	T_1	T_2	T_3	T_4	T_7	T_8
19	2.0	24.2	23.7	21.2	21.2	21.2	21.2
23	2.5	25.9	25.3	23.1	22.1	22.1	22.1
27	3.0	28.5	27.8	27.5	23.8	23.8	23.8
30.5	3.5	31.1	29.9	29.7	25.3	25.2	25.2
34.5	4.0	34.2	32.8	32.5	28.4	27.1	27.1
39.5	4.5	39.9	38.5	38.2	36.2	31.3	31.3
44	5.0	46.1	43.9	43.7	42.0	35.5	35.5
48	5.5	52.0	49.7	49.6	46.6	39.2	39.2

Table B-4 Continued

Volts	Amps	T_9	T_{10}	T_{11}	T_{12}	Ra. #	Nu. #
19	2.0	21.2	27.4	27.4	22.0	7832	51.9
23	2.5	22.1	30.3	30.7	23.7	12246	54.4
27	3.0	23.8	35.3	35.3	25.8	21439	49,2
30.5	3.5	25.2	39.2	39.2	27.2	28833	51.9
34.5	4.0	27.1	43.2	43.1	28.7	47748	52.3
39.5	4.5	31.3	51.0	50.8	32.1	100145	46.4
44	5.0	35.5	59.7	59.5	35.8	160132	46.6
48	5.5	39.2	67.0	66.7	39.2	238320	47.5

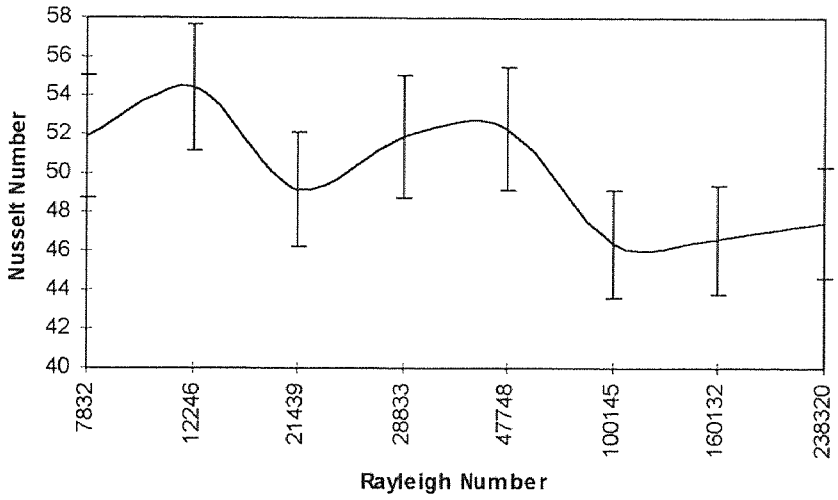

Figure B-4: Nusselt number versus Rayleigh number. Air injection distance Z/D=2

0.5" Heat Pipe Data

Air Injection Distance: Z/D=5
Air Injection Rate: 10 SCFH Date: 11-27-1996
Initial Water Temperature: 21 °C

Table B-5: Air injection distance effect Z/D=5

Volts	Amps	T_1	T_2	T_3	T_4	T_7	T_8
19	2.0	23.9	23.4	21.2	21.1	21.1	21.1
23	2.5	25.6	25.0	22.5	22.0	22.1	22.1
27	3.0	28.0	27.2	26.9	23.6	23.7	23.7
30.5	3.5	31.1	30.1	29.7	25.8	25.8	25.8
34.5	4.0	35.1	34.0	33.9	29.3	28.6	28.6
39.5	4.5	39.7	38.1	37.9	34.6	31.7	31.7
44	5.0	45.6	43.6	43.3	41.1	35.8	35.8
48	5.6	51.7	49.2	48.9	47.5	39.6	39.6

Table B-5 Continued

Volts	Amps	T_9	T_{10}	T_{11}	T_{12}	Ra. #	Nu. #
19	2.0	21.1	26.5	26.5	22.4	7195	59.9
23	2.5	22.1	29.6	29.6	23.9	10160	65.5
27	3.0	23.7	33.9	34.0	25.7	18569	56.4
30.5	3.5	25.8	38.5	38.6	27.6	26792	59.6
34.5	4.0	28.6	43.5	43.4	29.6	49098	57.7
39.5	4.5	31.7	48.9	48.9	32.1	84670	54.8
44	5.0	35.8	57.0	56.7	35.4	143678	53.2
48	5.6	39.6	68.9	68.7	40.2	226664	50.6

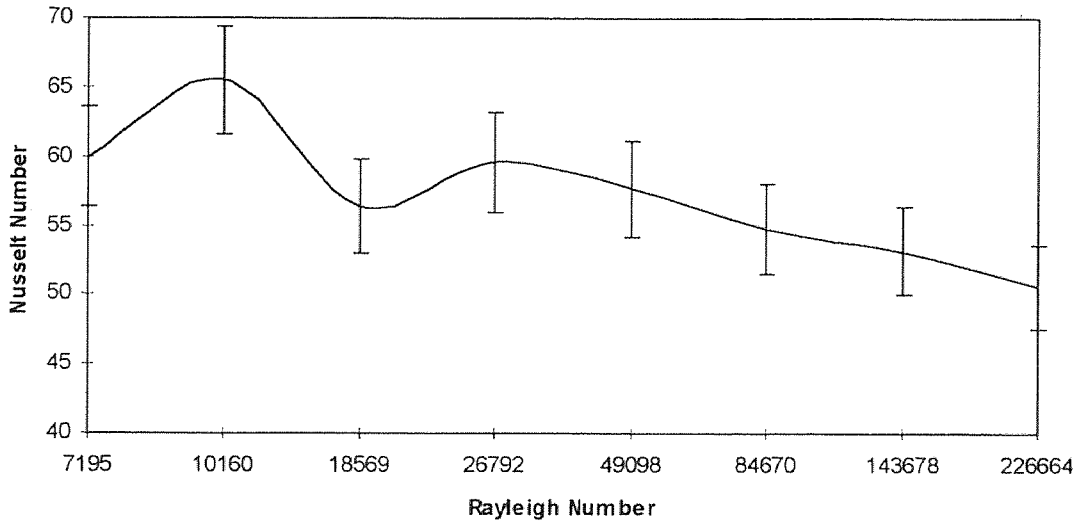

Figure B-5: Nusselt number versus Rayleigh number. Air injection distance Z/D=5

0.5" Heat Pipe Data

Air Injection Distance: Z/D=8
Air Injection Rate: 10 SCFH Date: 12-2-1996
Initial Water Temperature: 20.5 °C

Table B-6: Air injection distance effect Z/D=8

Volts	Amps	T_1	T_2	T_3	T_4	T_7	T_8
19	2.0	24.0	23.6	21.1	21.0	21.0	21.0
23	2.5	26.2	25.5	23.5	22.2	22.3	22.3
27	3.0	28.5	27.7	27.3	23.8	23.9	23.9
30.5	3.5	31.7	30.7	30.4	26.1	26.1	26.1
34.5	4.0	35.7	34.6	34.2	30.1	29.0	29.0
39.5	4.5	40.6	39.2	38.6	36.1	32.7	32.7
44	5.0	46.8	44.8	44.1	42.8	36.6	36.6
48	5.6	54.1	52.0	52.0	48.3	41.8	41.8

Table B-6 Continued

Volts	Amps	T_9	T_{10}	T_{11}	T_{12}	Ra. #	Nu. #
19	2.0	21.0	26.6	26.6	21.8	8030	50.5
23	2.5	22.3	30.2	30.2	23.5	12715	53.1
27	3.0	23.9	34.1	34.1	25.2	20242	52.3
30.5	3.5	26.1	38.8	38.8	27.1	30172	55.4
34.5	4.0	29.0	44.4	44.3	29.4	53070	54.5
39.5	4.5	32.7	51.3	51.2	32.3	90900	53.2
44	5.0	36.6	59.1	58.8	35.6	159069	49.4
48	5.6	41.8	68.6	68.3	40.1	241540	50.5

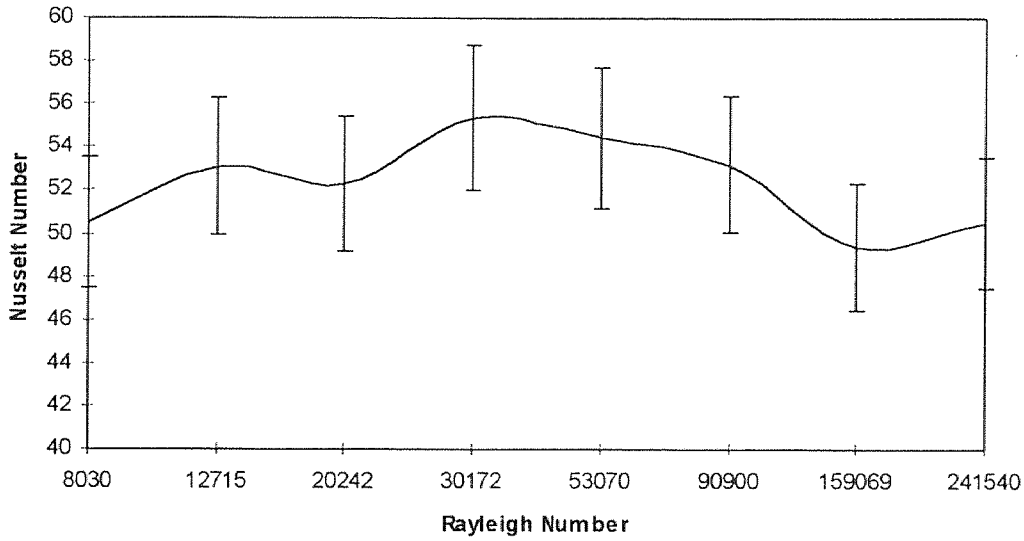

Figure B-6: Nusselt number versus Rayleigh number. Air injection distance Z/D=8

0.5" Heat Pipe Data

Air Injection Distance: Z/D=8
Air Injection Rate: 10 SCFH Date: 12-3-1996
Initial Water Temperature: 20.8 °C

Table B-7: Air injection configuration effect 9 openings

Volts	Amps	T_1	T_2	T_3	T_4	T_7	T_8
19	2.0	24.2	23.7	21.3	21.3	21.3	21.3
23	2.5	26.0	25.4	23.1	22.3	22.3	22.3
27	3.0	28.7	27.8	27.7	23.9	24.0	24.0
30.5	3.5	31.7	30.6	30.4	26.3	26.3	26.3
34.5	4.0	35.8	34.5	34.3	30.2	29.1	29.1
39.5	4.5	40.6	39.1	38.7	36.2	32.6	32.6
44	5.0	46.3	44.9	44.8	42.9	36.5	36.5
48	5.6	53.9	52.0	51.2	48.4	41.8	41.8

Table B-7 Continued

Volts	Amps	T_9	T_{10}	T_{11}	T_{12}	Ra. #	Nu. #
19	2.0	21.3	27.0	27.0	22.3	7582	54.3
23	2.5	22.3	30.1	30.2	23.8	11734	57.4
27	3.0	24.0	34.9	35.0	25.7	21093	50.5
30.5	3.5	26.3	39.4	39.5	27.7	29067	58.1
34.5	4.0	29.1	44.8	44.7	29.9	52812	56.0
39.5	4.5	32.6	51.3	51.2	32.7	92602	52.9
44	5.0	36.5	59.3	59.2	36.0	163033	47.7
48	5.6	41.8	68.2	67.9	40.6	241590	50.6

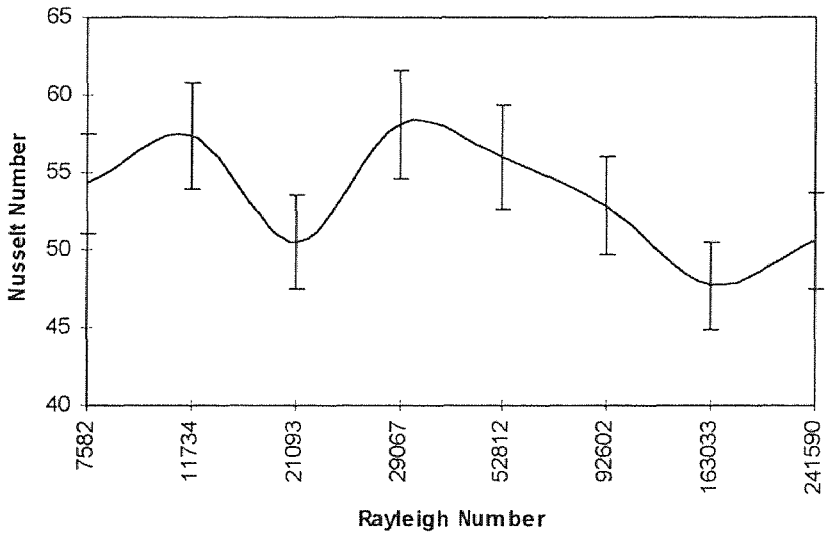

Figure B-7: Nusselt number versus Rayleigh number. Nine screws removed.

0.5" Heat Pipe Data

Air Injection Distance: Z/D=8
Air Injection Rate: 10 SCFH Date: 12-4-1996
Initial Water Temperature: 21 °C

Table B-8: Air injection configuration effect 15 openings

Volts	Amps	T_1	T_2	T_3	T_4	T_7	T_8
19	2.0	24.0	23.5	21.2	21.2	21.2	21.2
23	2.5	25.7	25.1	22.6	22.1	22.1	22.1
27	3.0	28.2	27.5	27.0	23.8	23.8	23.8
30.5	3.5	31.6	30.7	30.4	26.1	26.2	26.2
34.5	4.0	35.8	34.5	34.1	30.1	29.2	29.2
39.5	4.5	40.5	38.8	38.3	35.7	32.6	32.6
44	5.0	45.7	44.4	43.9	41.7	36.7	36.7
48	5.6	54.2	52.1	51.2	48.1	42.2	42.2

Table B-8 Continued

Volts	Amps	T_9	T_{10}	T_{11}	T_{12}	Ra. #	Nu. #
19	2.0	21.2	26.9	26.9	22.6	7240	56.4
23	2.5	22.1	30.1	30.1	24.0	10798	61.6
27	3.0	23.8	34.4	34.5	25.9	19400	54.3
30.5	3.5	26.2	39.6	39.6	28.1	30000	55.2
34.5	4.0	29.2	44.8	44.8	30.3	50853	57.3
39.5	4.5	32.6	51.1	51.0	32.9	86785	55.9
44	5.0	36.7	59.5	59.3	36.4	141250	54.4
48	5.6	42.2	68.8	68.5	40.9	232420	52.9

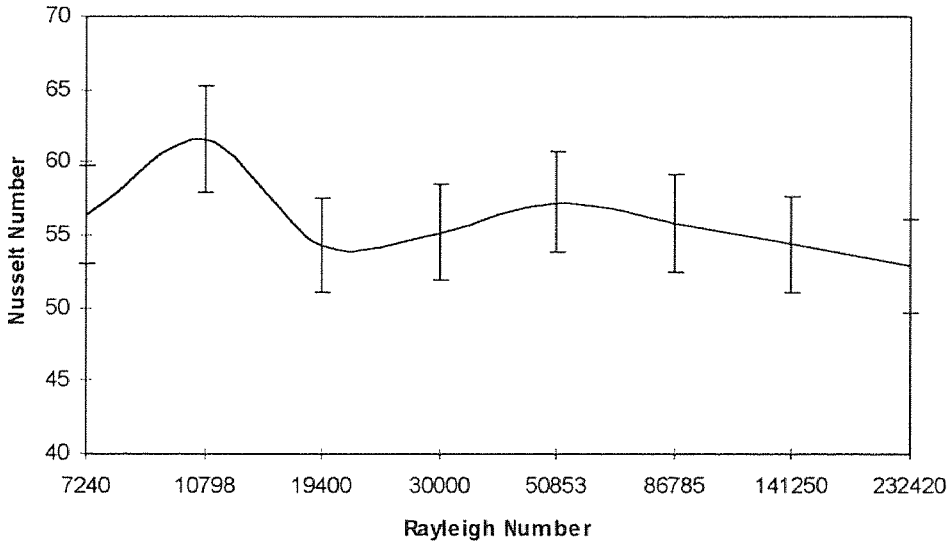

Figure B-8: Nusselt number versus Rayleigh number. No shrouds in water tank

0.5" Heat Pipe Data

Air Injection Distance: Z/D=8
Air Injection Rate: 10 SCFH Date: 12-5-1996
Initial Water Temperature: 21 °C

Table B-9: Curved shroud distance effect d/D=1

Volts	Amps	T_1	T_2	T_3	T_4	T_7	T_8
19	2.0	24.1	23.6	21.4	21.4	21.4	21.4
23	2.5	25.8	25.2	22.7	22.5	22.5	22.5
27	3.0	28.2	27.4	26.9	24.1	24.1	24.1
30.5	3.5	31.1	30.2	29.9	26.2	26.2	26.2
34.5	4.0	34.9	33.7	33.4	29.4	28.9	28.9
39.5	4.5	39.5	38.1	37.7	35.1	32.3	32.3
44	5.0	45.5	43.9	43.4	41.9	36.4	36.4
48	5.6	55.1	52.9	52.6	45.3	43.5	43.5

Table B-9 Continued

Volts	Amps	T_9	T_{10}	T_{11}	T_{12}	Ra. #	Nu. #
19	2.0	21.4	27.2	27.2	23.3	7031	59.2
23	2.5	22.5	30.6	30.7	24.7	9586	70.6
27	3.0	24.1	35.7	35.8	26.6	17658	59.9
30.5	3.5	26.2	39.8	39.9	28.3	25826	62.6
34.5	4.0	28.9	44.6	44.6	30.4	43472	65.3
39.5	4.5	32.3	51.2	51.1	33.0	77883	60.5
44	5.0	36.4	58.8	58.6	36.3	140415	53.3
48	5.6	43.5	73.7	73.5	43.7	211087	60.5

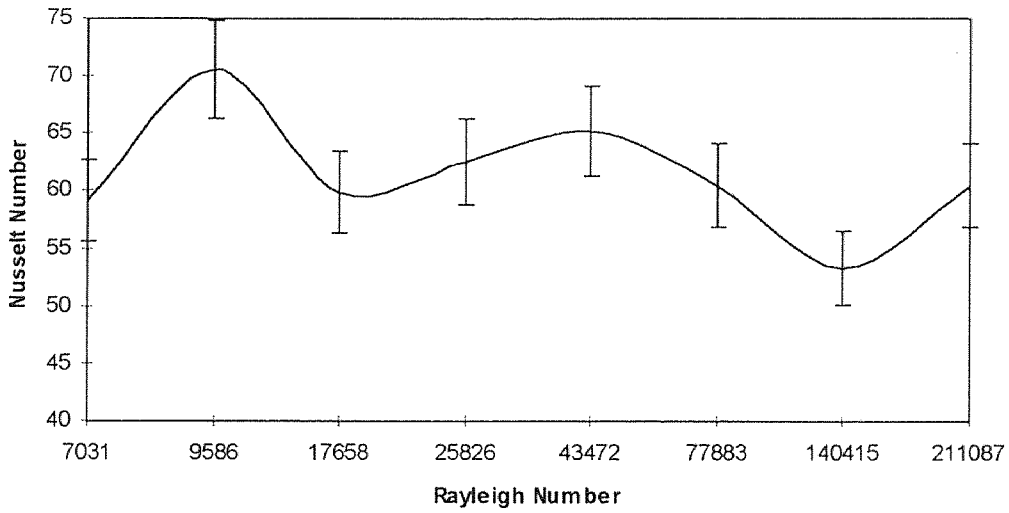

Figure B-9: Nusselt number versus Rayleigh number. Curved shroud distance d/D=1

0.5" Heat Pipe Data

Air Injection Distance: Z/D=8
Air Injection Rate: 10 SCFH Date:12-6-1996
Initial Water Temperature: 21 °C

Table B-10: Curved shroud distance effect d/D=4

Volts	Amps	T_1	T_2	T_3	T_4	T_7	T_8
19	2.0	23.9	23.3	21.1	21.1	21.1	21.1
23	2.5	25.6	24.9	22.4	22.0	22.0	22.0
27	3.0	27.9	27.0	26.6	23.5	23.6	23.6
30.5	3.5	30.7	29.7	29.4	25.2	25.2	25.2
34.5	4.0	34.2	32.9	32.5	28.5	28.0	28.0
39.5	4.5	38.6	37.2	36.7	33.8	31.3	31.3
44	5.0	44.5	42.6	42.0	40.1	35.1	35.1
48	5.6	52.3	49.9	49.1	46.0	40.1	40.1

Table B-10 Continued

Volts	Amps	T_9	T_{10}	T_{11}	T_{12}	Ra. #	Nu. #
19	2.0	21.1	27.0	27.0	21.9	7048	57.3
23	2.5	22.0	30.6	30.6	23.7	10418	60.2
27	3.0	23.6	34.9	35.0	25.6	17930	55.4
30.5	3.5	25.2	38.9	39.0	27.4	24800	61.3
34.5	4.0	28.0	43.3	43.3	29.2	41455	62.9
39.5	4.5	31.3	49.2	49.1	31.8	72680	60.2
44	5.0	35.1	56.3	56.0	35.0	130249	54.9
48	5.6	40.1	72.2	72.0	41.5	217099	54.7

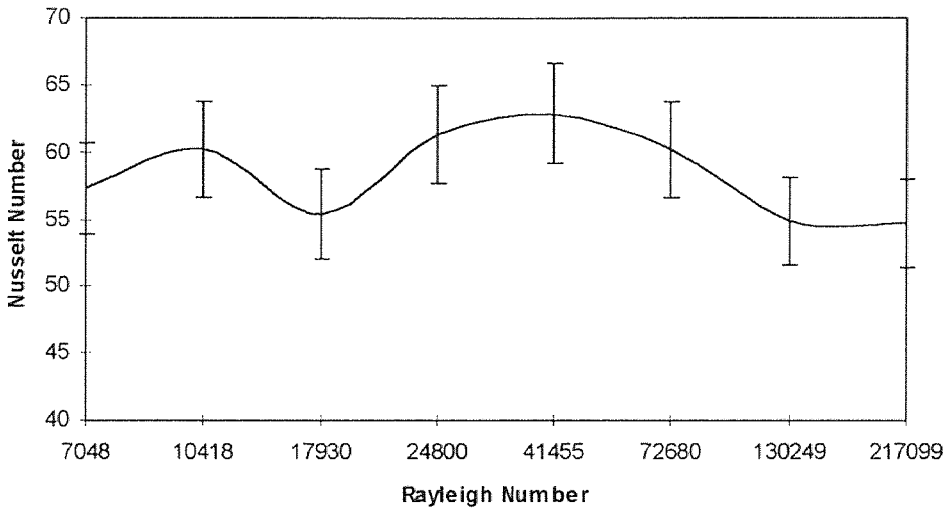

Figure B-10: Nusselt number versus Rayleigh number. Curved shroud distance d/D=4

0.5" Heat Pipe Data

Air Injection Distance: Z/D=8
Air Injection Rate: 10 SCFH Date: 12-10-1996
Initial Water Temperature: 20.5 °C

Table B-11: Straight shroud distance effect d/D=1

Volts	Amps	T_1	T_2	T_3	T_4	T_7	T_8
19	2.0	23.7	23.3	20.8	20.8	20.8	20.8
23	2.5	25.4	24.7	22.4	21.7	21.7	21.7
27	3.0	27.6	26.7	26.4	23.0	23.1	23.1
30.5	3.5	30.4	29.4	29.1	24.9	24.9	24.9
34.5	4.0	34.1	32.8	32.5	28.4	27.5	27.5
39.5	4.5	38.3	36.7	36.6	33.3	30.5	30.5
44	5.0	44.3	42.5	42.1	39.8	34.1	34.1
48	5.6	51.1	48.9	48.3	47.2	38.4	38.4

Table B-11 Continued

Volts	Amps	T_9	T_{10}	T_{11}	T_{12}	Ra. #	Nu. #
19	2.0	20.8	26.9	26.9	21.5	7493	53.0
23	2.5	21.7	30.0	30.1	23.3	11018	56.2
27	3.0	23.1	34.3	34.4	25.2	18703	52.1
30.5	3.5	24.9	38.4	38.4	27.0	26210	55.8
34.5	4.0	27.5	42.9	42.9	28.9	44341	57.3
39.5	4.5	30.5	48.6	48.5	31.3	77091	54.9
44	5.0	34.1	55.8	55.5	34.7	141965	49.1
48	5.6	38.4	66.7	66.4	39.5	236320	46.6

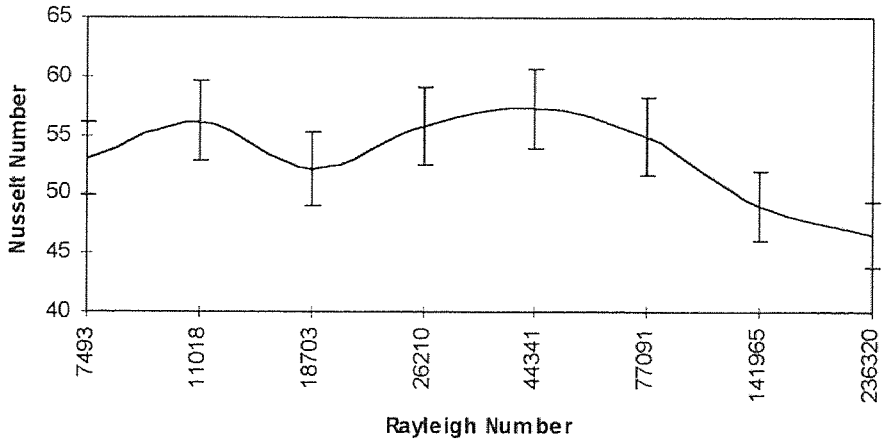

Figure B-11: Nusselt number versus Rayleigh number. Straight shroud distance d/D=1

0.5" Heat Pipe Data

Air Injection Distance: Z/D=0
Air Injection Rate: 10 SCFH Date: 12-11-1996
Initial Water Temperature: 20.8 °C

Table B-12: Water circulation only effect

Volts	Amps	T_1	T_2	T_3	T_4	T_7	T_8
15	1.5	24.4	24.0	21.3	20.9	20.9	20.9
18	1.8	25.7	25.2	23.5	21.4	21.4	21.4
19	2.0	26.2	25.8	25.4	21.3	21.3	21.3
22	2.5	29.6	29.0	28.8	22.6	22.2	22.2
26	3.0	33.6	32.8	32.5	25.6	23.7	23.7
30	3.5	38.9	37.7	37.6	31.3	26.0	26.0
33	3.8	37.9	36.5	36.4	31.1	23.8	23.8
37	4.3	44.2	42.2	42.2	40.6	26.6	26.6

Table B-12 Continued

Volts	Amps	T_9	T_{10}	T_{11}	T_{12}	Ra. #	Nu. #
15	1.5	20.9	26.2	26.2	22.1	9898	23.8
18	1.8	21.4	28.0	28.0	23.8	15232	24.0
19	2.0	21.3	28.8	28.8	22.7	20531	21.0
22	2.5	22.2	33.5	33.5	24.7	35720	19.2
26	3.0	23.7	33.7	33.5	27.3	58439	19.4
30	3.5	26.0	48.2	48.1	30.6	117117	18.5
33	3.8	23.8	49.2	49.1	29.6	115408	19.7
37	4.3	26.6	59.3	59.3	33.7	223603	18.1

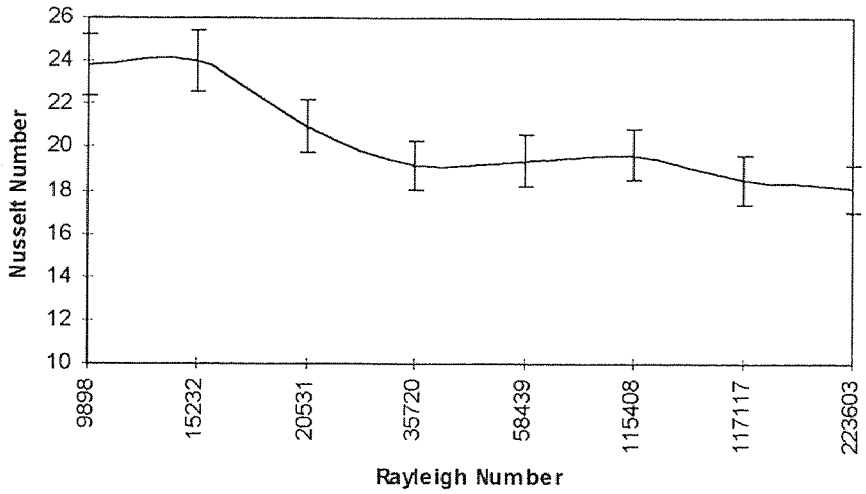

Figure B-12: Nusselt number versus Rayleigh number. Water circulation only.

0.5" Heat Pipe Data

Air Injection Distance: Z/D=0
Air Injection Rate: 0 SCFH Date: 12-12-1996
Initial Water Temperature: 21.1 °C

Table B-13: Natural convection conditions

Volts	Amps	T_1	T_2	T_3	T_4	T_7	T_8
12	1.0	24.2	23.9	21.5	21.1	21.1	21.1
13	1.2	25.3	25.0	22.8	21.5	21.4	21.4
16	1.6	27.6	27.2	27.0	22.6	22.5	22.5
18	1.9	29.9	29.4	29.3	24.1	23.7	23.8
19	2.1	32.4	31.9	31.8	26.1	25.5	25.6
24	2.8	41.2	40.5	40.3	34.0	30.7	30.9
27	3.1	44.8	43.9	43.8	37.8	32.9	33.0
29	3.3	50.0	49.0	48.9	43.7	37.0	37.3

Table B-13 Continued

Volts	Amps	T_9	T_{10}	T_{11}	T_{12}	Ra. #	Nu. #
12	1.0	21.1	25.3	25.3	22.5	8971	13.8
13	1.2	21.4	26.6	26.6	22.6	13139	12.6
16	1.6	22.4	29.5	29.4	23.7	23760	12.8
18	1.9	23.6	32.3	32.3	24.8	31874	13.8
19	2.1	25.3	35.3	35.3	26.0	42750	14.0
24	2.8	30.6	47.0	46.8	30.1	120847	14.2
27	3.1	32.7	52.0	51.8	31.7	167014	15.0
29	3.3	37.4	58.7	58.5	35.0	230037	15.1

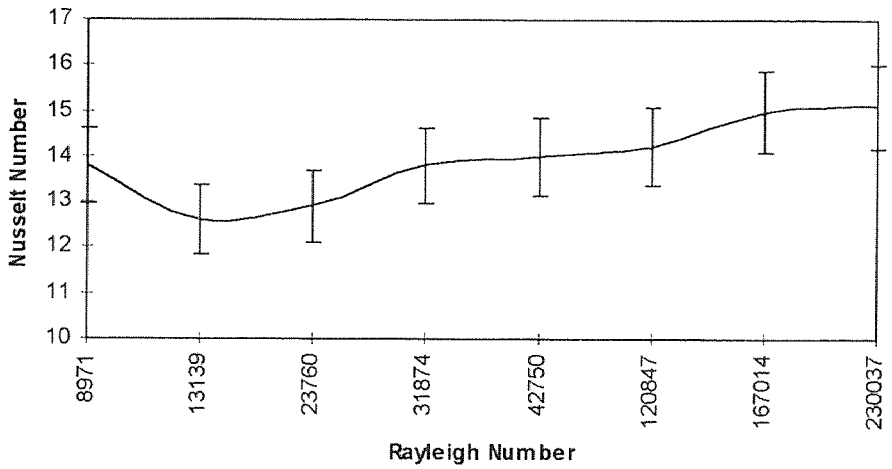

Figure B-13: Nusselt number versus Rayleigh number. Natural convection conditions.

APPENDIX C

0.75" Heat Pipe Data

Date: 2-10-1997 Air Injection Rate: 50 SCFH
Initial Temperature: 20.9 °C
Air Injection Distance: Z/D=5

Table C-1: Air injection rate effect 50 SCFH

Volts	Amps	T_1	T_2	T_3	T_4	T_7	T_8
30	3.3	24.3	23.1	23.6	24.5	37.0	18.6
36	4.0	28.3	25.9	26.4	28.3	44.8	22.9
39	4.4	31.8	29.0	29.6	32.4	50.8	28.9
43	4.8	35.8	32.4	33.1	37.1	60.3	31.6
46	5.2	40.2	36.2	37.0	41.6	68.3	34.8
50	5.6	44.9	40.4	41.1	46.6	82.3	39.1
54	6.0	50.3	44.9	45.7	51.9	94.6	43.4
57	6.4	54.4	48.7	49.4	56.2	120.6	51.2

Table C-1 Continued

Volts	Amps	T_9	T_{10}	T_{11}	T_{12}	Nu. #	Ra. #
30	3.3	23.0	21.1	21.1	21.1	99.7	36443
36	4.0	23.4	24.4	24.4	24.4	89.9	68131
39	4.4	24.5	27.1	27.1	27.1	84.3	111990
43	4.8	25.8	30.2	30.2	30.2	81.9	183935
46	5.2	27.6	33.6	33.6	33.6	80.2	274693
50	5.6	30.0	37.4	37.4	37.4	81.4	386215
54	6.0	32.7	41.4	41.4	41.4	80.0	541918
57	6.4	37.5	45.1	45.1	45.1	84.8	690458

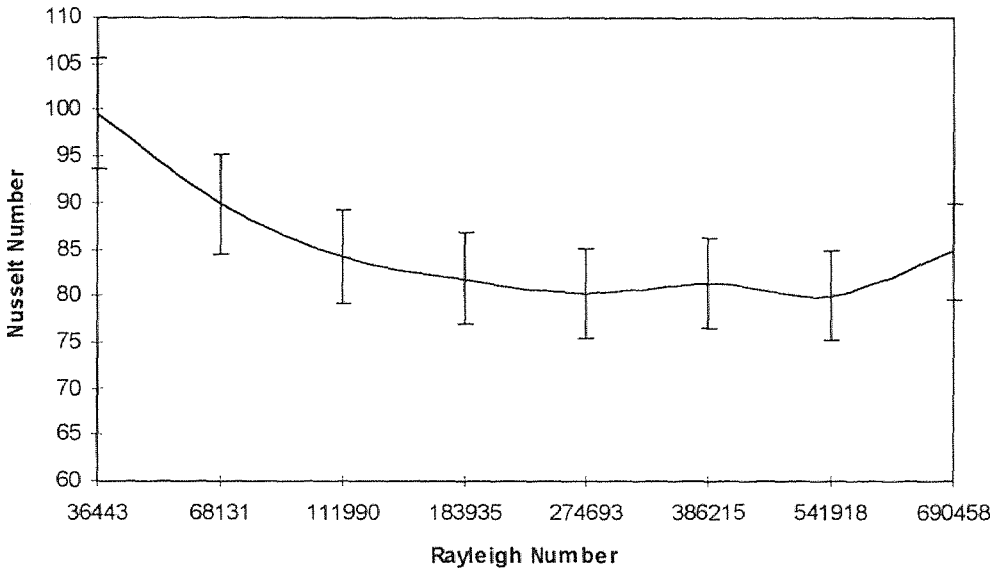

Figure C-1: Nusselt versus Rayleigh number. Air injection rate 50 SCFH.

0.75" Heat Pipe Data

Date: 2-11-1997 Air Injection Rate: 30 SCFH
Initial Temperature: 21.1 °C
Air Injection Distance: Z/D=5

Table C-2: Air injection rate effect 30 SCFH

Volts	Amps	T_1	T_2	T_3	T_4	T_7	T_8
30	3.3	25.0	23.8	24.0	25.0	37.4	23.0
36	4.0	28.8	27.1	27.2	28.9	45.2	25.9
39	4.4	32.2	30.0	30.2	33.1	51.3	28.4
43	4.8	36.9	34.0	34.6	38.3	61.9	32.0
46	5.2	41.7	38.1	38.6	43.2	71.6	35.4
50	5.6	47.8	43.2	43.8	49.3	84.3	39.8
54	6.0	53.1	48.0	48.4	54.7	96.8	43.9
57	6.4	56.9	51.5	5.0	58.6	123.4	49.6

Table C-2 Continued

Volts	Amps	T_9	T_{10}	T_{11}	T_{12}	Nu. #	Ra. #
30	3.3	23.4	22.6	22.6	22.6	95.6	39166
36	4.0	25.7	25.2	25.2	25.2	91.6	69516
39	4.4	28.1	27.8	27.8	27.8	84.3	119691
43	4.8	31.8	31.4	31.4	31.4	79.1	207932
46	5.2	35.4	35.2	35.2	35.2	79.3	303181
50	5.6	40.6	40.1	40.1	40.1	80.2	440728
54	6.0	45.1	44.4	44.4	44.4	81.8	612269
57	6.4	50.8	47.7	47.7	47.7	85.0	797104

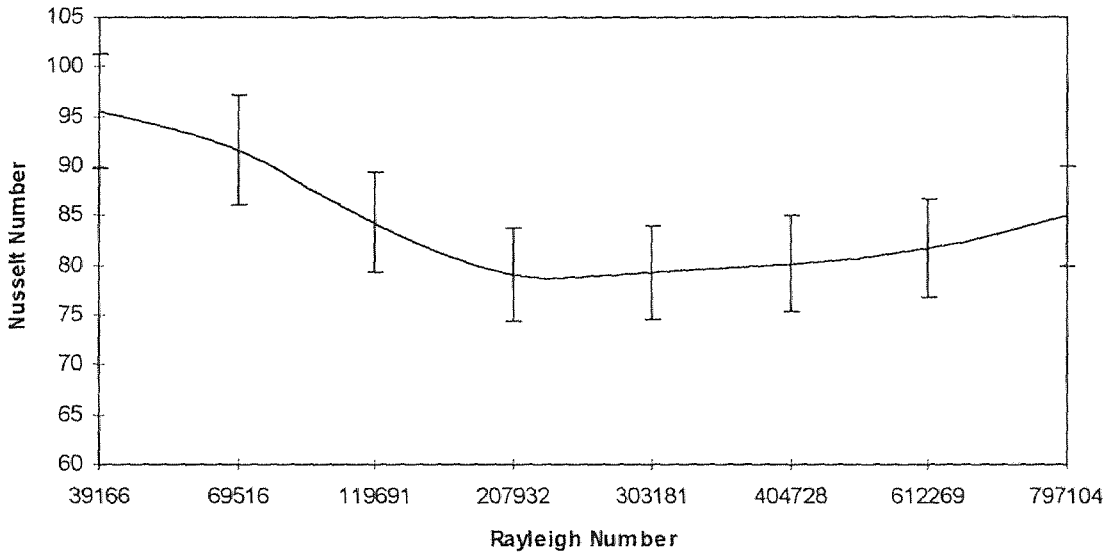

Figure C-2: Nusselt versus Rayleigh number. Air injection rate 30 SCFH.

0.75" Heat Pipe Data

Date: 2-12-1997 Air Injection Rate: 10 SCFH
Initial Temperature: 20.8 °C
Air Injection Distance: Z/D=5

Table C-3: Air injection rate effect 10 SCFH

Volts	Amps	T_1	T_2	T_3	T_4	T_7	T_8
30	3.3	25.1	23.7	24.3	25.3	38.4	24.0
36	4.0	29.2	26.9	27.6	29.5	45.7	26.9
39	4.4	33.5	30.5	31.4	34.1	52.1	29.4
43	4.8	38.5	35.2	36.1	39.7	63.0	32.7
46	5.2	43.6	39.5	40.7	45.0	72.6	36.2
50	5.6	48.9	44.1	45.2	50.5	85.9	40.1
54	6.0	54.8	49.2	50.1	56.3	97.8	44.1
57	6.4	60.9	54.7	55.8	62.3	108.2	48.3

Table C-3 Continued

Volts	Amps	T_9	T_{10}	T_{11}	T_{12}	Nu. #	Ra. #
30	3.3	23.9	22.5	22.5	22.5	84.4	44521
36	4.0	27.3	25.0	25.0	25.0	78.1	89591
39	4.4	30.0	28.3	28.3	28.3	74.4	144667
43	4.8	33.6	32.2	32.2	32.2	69.4	254086
46	5.2	37.3	36.4	36.4	36.4	70.9	364748
50	5.6	41.4	40.5	40.5	40.5	70.9	512324
54	6.0	45.9	45.1	45.1	45.1	72.3	741464
57	6.4	50.4	50.3	50.3	50.3	74.5	1071092

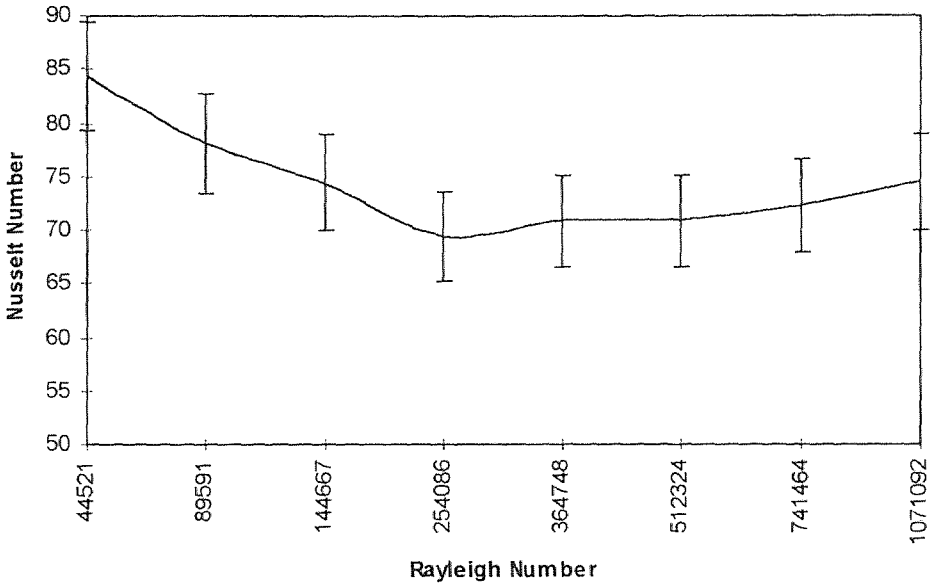

Figure C-3: Nusselt versus Rayleigh number. Air injection rate 10 SCFH.

0.75" Heat Pipe Data

Date: 2-13-1997 Air Injection Rate: 10 SCFH
Initial Temperature: 20.9 °C
Air Injection Distance: Z/D=10

Table C-4: Air injection distance effect Z/D=10

Volts	Amps	T_1	T_2	T_3	T_4	T_7	T_8
30	3.3	25.6	24.3	24.7	25.7	38.9	24.9
36	4.0	29.7	27.8	28.2	29.8	46.2	27.6
39	4.4	33.9	31.3	32.3	35.2	53.8	30.1
43	4.8	39.0	35.7	37.0	40.8	65.0	33.6
4.6	5.2	44.4	40.6	42.1	46.5	75.7	36.8
50	5.6	50.7	46.0	47.1	52.2	86.2	39.5
54	6.0	56.7	51.2	53.0	58.3	98.8	42.8
57	6.4	62.9	57.1	58.5	65.0	109.7	46.7

Table C-4 Continued

Volts	Amps	T_9	T_{10}	T_{11}	T_{12}	Nu. #	Ra. #
30	3.3	25.1	22.8	22.8	22.8	77.8	49279
36	4.0	28.4	25.6	25.6	25.6	76.2	85243
39	4.4	31.2	29.0	29.0	29.0	72.4	157785
43	4.8	35.1	33.1	33.1	33.1	71.2	259389
4.6	5.2	39.0	37.6	37.6	37.6	70.4	386015
50	5.6	42.4	42.5	42.5	42.5	72.6	536878
54	6.0	46.3	47.5	47.5	47.5	73.9	822096
57	6.4	50.6	52.7	52.7	52.7	73.6	1196233

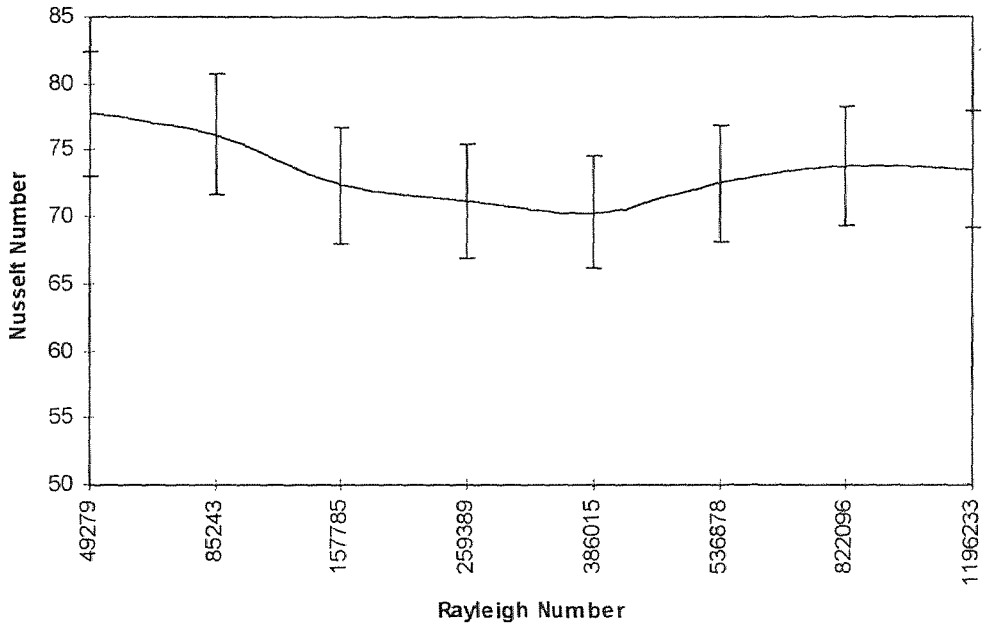

Figure C-4: Nusselt versus Rayleigh number. Air injection distance Z/D=10

0.75" Heat Pipe Data

Date: 2-14-1997 Air Injection Rate: 10 SCFH
Initial Temperature: 21.0 °C
Air Injection Distance: Z/D=2

Table C-5: Air injection distance effect Z/D=2

Volts	Amps	T_1	T_2	T_3	T_4	T_7	T_8
30	3.3	25.6	24.0	24.7	25.7	38.4	25.2
36	4.0	30.3	27.7	28.6	30.6	46.8	28.2
39	4.4	34.5	31.2	32.3	35.4	53.3	30.4
43	4.8	39.8	35.8	37.2	41.1	64.4	34.0
4.6	5.2	45.1	40.5	42.1	46.5	75.8	37.4
50	5.6	51.0	45.4	47.2	52.0	86.5	40.7
54	6.0	56.9	50.8	52.8	58.0	96.8	43.8
57	6.4	63.5	56.2	58.6	64.5	110.9	48.1

Table C-5 Continued

Volts	Amps	T_9	T_{10}	T_{11}	T_{12}	Nu. #	Ra. #
30	3.3	25.3	22.8	22.8	22.8	80.7	47556
36	4.0	28.9	25.7	25.7	25.7	71.3	96590
39	4.4	31.6	28.8	28.8	28.8	67.5	171783
43	4.8	35.4	33.0	33.0	33.0	65.5	284708
4.6	5.2	39.4	37.3	37.3	37.3	65.4	414532
50	5.6	43.3	41.8	41.8	41.8	66.6	577758
54	6.0	47.2	46.7	46.7	46.7	68.4	869378
57	6.4	51.7	51.6	51.6	51.6	66.2	1296895

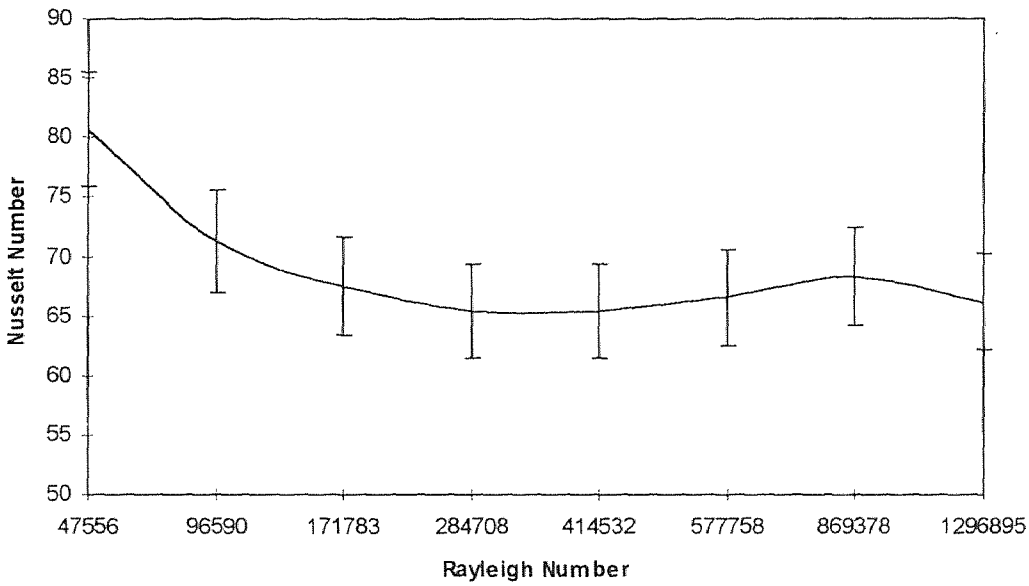

Figure C-5: Nusselt versus Rayleigh number. Air injection distance Z/D=2.

0.75" Heat Pipe Data

Date: 2-15-1997
Initial Temperature: 21.0 °C
Air Injection Distance: Z/D=5

Air Injection Rate: 10 SCFH5
Curved Shroud Distance: d/D=1

Table C-6: Curved shroud distance effect d/D=1

Volts	Amps	T_1	T_2	T_3	T_4	T_7	T_8
30	3.3	24.7	23.5	24.1	25.0	37.9	20.9
36	4.0	28.1	26.1	26.9	28.5	45.3	24.0
39	4.4	31.8	29.2	30.3	32.8	50.9	26.4
43	4.8	36.3	33.0	34.3	38.0	62.6	29.6
4.6	5.2	41.2	37.2	38.6	42.9	73.4	32.9
50	5.6	45.7	41.3	43.0	47.8	82.7	36.1
54	6.0	51.3	45.9	48.0	53.3	107.9	42.6
58	6.6	57.3	51.0	53.3	59.0	125.8	49.3

Table C-6 Continued

Volts	Amps	T_9	T_{10}	T_{11}	T_{12}	Nu. #	Ra. #
30	3.3	21.8	22.3	22.3	22.3	86.6	42359
36	4.0	24.8	24.4	24.4	24.4	85.3	64850
39	4.4	27.6	27.3	27.3	27.3	81.4	118867
43	4.8	31.2	306	306	306	73.9	20945
4.6	5.2	35.1	34.4	34.4	34.4	73.7	314610
50	5.6	38.8	38.2	38.2	38.2	76.3	431720
54	6.0	45.8	42.5	42.5	42.5	75.5	595304
58	6.6	53.3	46.9	46.9	46.9	76.4	922915

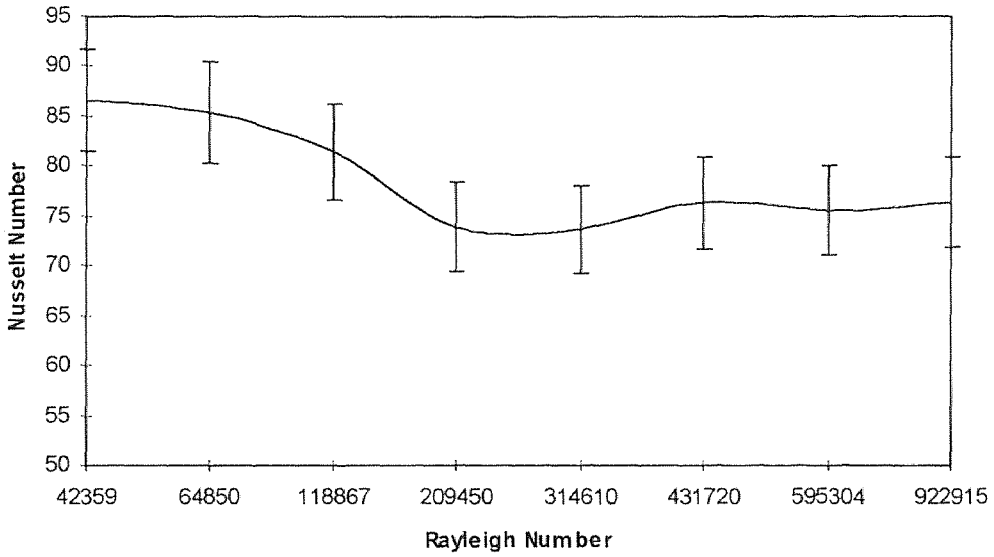

Figure C-6: Nusselt versus Rayleigh number. Curved shroud distance d/D=1

0.75" Heat Pipe Data

Date: 2-17-1997
Initial Temperature: 20.8 °C
Air Injection Distance: Z/D=5

Air Injection Rate: 10 SCFH
Curved Shroud Distance: d/D=3

Table C-7: Curved shroud distance effect d/D=3

Volts	Amps	T_1	T_2	T_3	T_4	T_7	T_8
30	3.3	24.7	23.4	24.0	25.1	38.0	21.2
36	4.0	29.0	26.6	27.7	29.7	45.8	25.4
39	4.4	32.8	29.7	30.9	33.9	52.8	28.1
43	4.8	37.8	33.7	35.2	39.1	63.9	31.7
4.6	5.2	41.9	37.5	39.0	43.9	74.9	35.3
50	5.6	48.0	42.5	44.7	50.3	84.4	40.4
54	6.0	52.8	46.7	49.1	55.2	95.8	42.5
58	6.6	58.9	51.8	53.9	61.3	111.9	47.7

Table C-7 Continued

Volts	Amps	T_9	T_{10}	T_{11}	T_{12}	Nu. #	Ra. #
30	3.3	21.0	22.0	22.0	22.0	76.1	47667
36	4.0	24.6	24.7	24.7	24.7	72.0	87608
39	4.4	27.6	27.3	27.3	27.3	68.6	149926
43	4.8	31.5	30.8	30.8	30.8	63.4	257338
4.6	5.2	35.8	34.2	34.2	34.2	64.4	363653
50	5.6	40.2	38.9	38.9	38.9	63.7	546317
54	6.0	44.4	42.5	42.5	42.5	65.6	723117
57	6.4	49.9	46.9	46.9	46.9	66.5	1109074

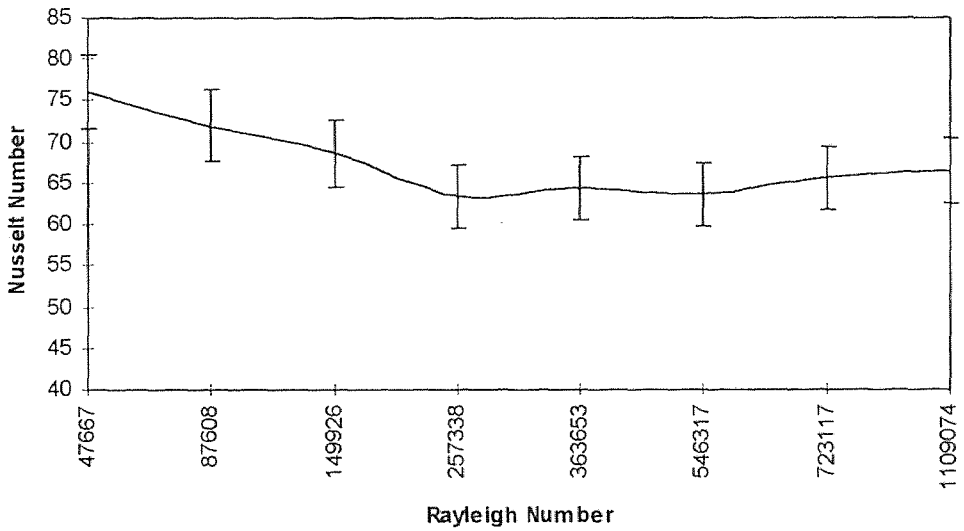

Figure C-7: Nusselt versus Rayleigh number. Curved shroud distance d/D=3.

0.75" Heat Pipe Data

Date: 2-17-1997
Initial Temperature: 21.9 °C
Air Injection Distance: Z/D=5

Air Injection Rate: 10 SCFH
Straight Shroud Distance: d/D=1

Table C-8: Straight shroud distance effect d/D=1

Volts	Amps	T_1	T_2	T_3	T_4	T_7	T_8
30	3.3	26.7	25.0	25.9	27.2	39.4	26.0
36	4.0	31.0	28.1	29.4	31.8	48.2	27.3
39	4.4	34.5	31.3	33.0	36.1	53.8	29.1
43	4.8	38.9	35.2	37.0	41.5	66.5	32.9
4.6	5.2	43.4	39.0	40.8	45.8	74.8	35.7
50	5.6	48.0	42.9	45.2	50.7	85.9	38.9
54	6.0	53.4	47.8	50.1	56.3	96.7	43.2
58	6.6	59.6	52.7	55.1	62.8	113.6	49.4

Table C-8 Continued

Volts	Amps	T_9	T_{10}	T_{11}	T_{12}	Nu. #	Ra. #
30	3.3	27.6	23.6	23.6	23.6	67.0	60514
36	4.0	29.2	26.0	26.0	26.0	62.7	107778
39	4.4	31.0	28.8	28.8	28.8	61.2	188763
43	4.8	34.7	32.4	32.4	32.4	61.9	290883
4.6	5.2	37.9	35.7	35.7	35.7	62.6	402486
50	5.6	41.3	39.1	39.1	39.1	63.6	561549
54	6.0	45.7	43.3	43.3	43.3	63.3	785927
57	6.4	51.8	47.5	47.5	47.5	63.3	1214426

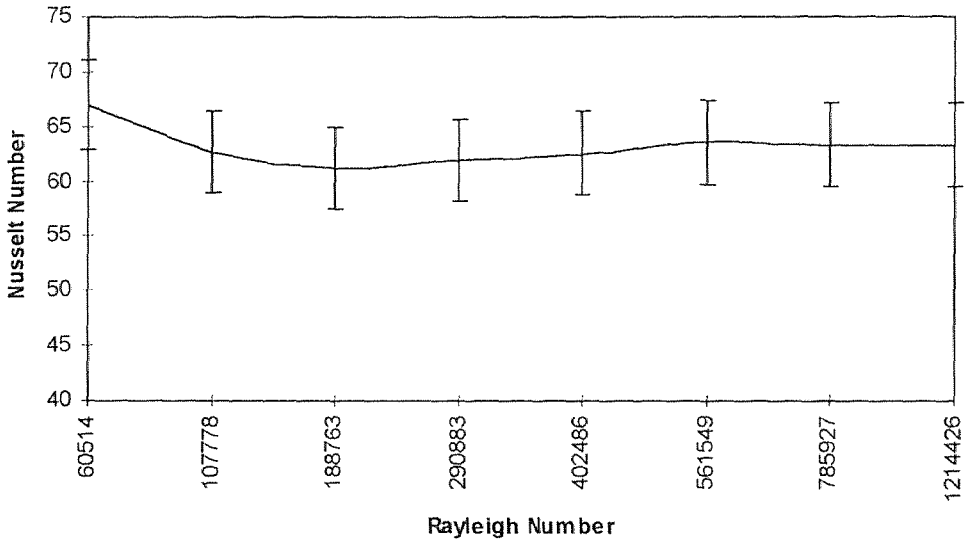

Figure C-8: Nusselt versus Rayleigh number. Straight shroud distance d/D=1.

0.75" Heat Pipe Data

Date: 2-18-1997
Initial Temperature: 21.0 °C
Air Injection Distance: Z/D=0

Air Injection Rate: 10 SCFH
Water Circulation Only

Table C-9: Water circulation only

Volts	Amps	T_1	T_2	T_3	T_4	T_7	T_8
21	2.2	24.1	23.9	24.0	24.2	30.3	20.6
24	2.6	26.0	25.3	25.7	25.8	34.2	22.4
27	2.9	27.9	27.1	27.5	27.7	37.8	22.8
30	3.3	30.4	29.3	29.9	30.1	42.6	23.8
33	3.7	33.2	31.7	32.3	33.1	47.5	25.0
36	4.0	37.1	35.4	35.8	38.0	53.7	27.3
41	4.6	44.4	42.3	42.2	45.3	66.5	32.1
46	5.2	51.4	47.7	47.4	51.6	81.0	36.2

Table C-9 Continued

Volts	Amps	T_9	T_{10}	T_{11}	T_{12}	Nu. #	Ra. #
21	2.2	20.0	21.7	21.7	21.7	34.2	47935
24	2.6	21.3	22.3	22.3	22.3	32.0	73900
27	2.9	21.6	23.3	23.3	23.3	32.2	97050
30	3.3	22.2	24.5	24.5	24.5	31.8	140789
33	3.7	23.5	25.8	25.8	25.8	31.1	175954
36	4.0	25.7	28.1	28.1	28.1	29.2	352665
41	4.6	30.1	32.6	32.6	32.6	29.3	645734
46	5.2	33.8	35.8	35.8	35.8	29.2	1004152

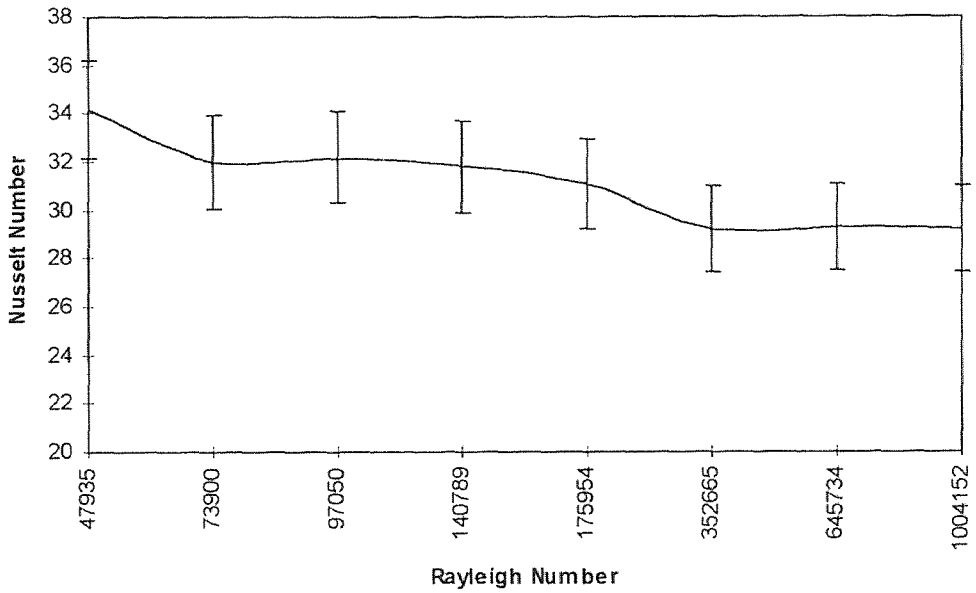

Figure C-9: Nusselt versus Rayleigh number. Water circulation only.

0.75" Heat Pipe Data

Date: 2-19-1997
Initial Temperature: 21.1 °C
Air Injection Distance: Z/D=5

Air Injection Rate: 10 SCFH
#'s: 1,4,7,10,13 screws removed

Table C-10: Air injection configuration effect 5 openings

Volts	Amps	T_1	T_2	T_3	T_4	T_7	T_8
30	3.3	25.3	24.2	24.5	25.3	38.5	22.6
36	4.0	30.2	27.9	28.4	30.2	47.3	26.3
39	4.4	34.4	31.7	32.2	35.3	54.2	29.2
43	4.8	39.0	35.7	36.4	40.5	64.2	32.4
4.6	5.2	44.8	40.9	41.6	46.4	76.5	36.5
50	5.6	49.9	45.8	46.5	51.6	86.8	40.0
54	6.0	56.3	51.3	52.0	58.1	97.9	43.9
59	6.6	63.6	58.0	58.6	65.7	113.3	49.3

Table C-10 Continued

Volts	Amps	T_9	T_{10}	T_{11}	T_{12}	Nu. #	Ra. #
30	3.3	22.3	22.6	22.6	22.6	78.9	47601
36	4.0	25.9	25.6	25.6	25.6	71.3	94690
39	4.4	28.4	28.9	28.9	28.9	66.8	170927
43	4.8	31.0	32.5	32.5	32.5	66.1	271940
4.6	5.2	34.1	37.0	37.0	37.0	66.1	421967
50	5.6	37.1	41.5	41.5	41.5	67.8	557588
54	6.0	40.4	46.7	46.7	46.7	69.7	842818
59	6.6	45.2	52.6	52.6	52.6	69.9	1311931

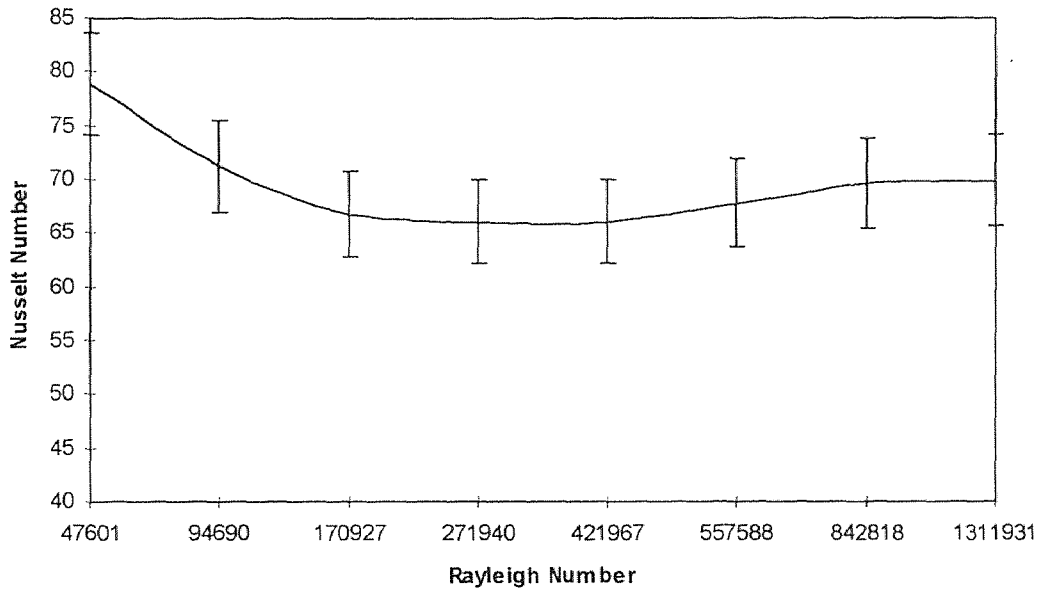

Figure C-10: Nusselt versus Rayleigh number. Five screws removed.

0.75" Heat Pipe Data

Date: 2-20-1997
Initial Temperature: 21.2 °C
Air Injection Distance: Z/D=5

Air Injection Rate: 10 SCFH
#'s: 1,3,5,7,9,11,13,15 screws removed

Table C-11: Air injection configuration effect 8 openings

Volts	Amps	T_1	T_2	T_3	T_4	T_7	T_8
30	3.3	25.6	24.3	24.9	26.5	38.0	22.8
36	4.0	30.3	27.9	28.1	29.9	47.6	26.6
40	4.5	34.8	32.2	32.7	35.9	55.7	29.9
43	4.8	39.2	35.9	36.3	39.7	63.4	32.8
47	5.2	45.5	41.1	41.8	46.2	75.8	36.8
50	5.7	50.0	45.8	46.6	51.6	85.9	40.4
54	6.2	56.7	51.7	52.8	58.6	100.3	45.1
60	6.7	63.4	57.2	58.2	64.9	115.1	50.1

Table C-11 Continued

Volts	Amps	T_9	T_{10}	T_{11}	T_{12}	Nu. #	Ra. #
30	3.3	22.4	23.0	23.0	23.0	84.5	45194
36	4.0	25.3	26.0	26.0	26.0	83.0	82066
40	4.5	28.0	29.9	29.9	29.9	78.1	161102
43	4.8	30.2	32.8	32.8	32.8	70.1	251867
47	5.2	34.8	37.5	37.5	37.5	67.7	410719
50	5.7	39.6	42.0	42.0	42.0	72.6	52697
54	6.2	44.0	47.3	47.3	47.3	72.9	860368
60	6.7	49.9	52.3	52.3	52.3	77.0	1252855

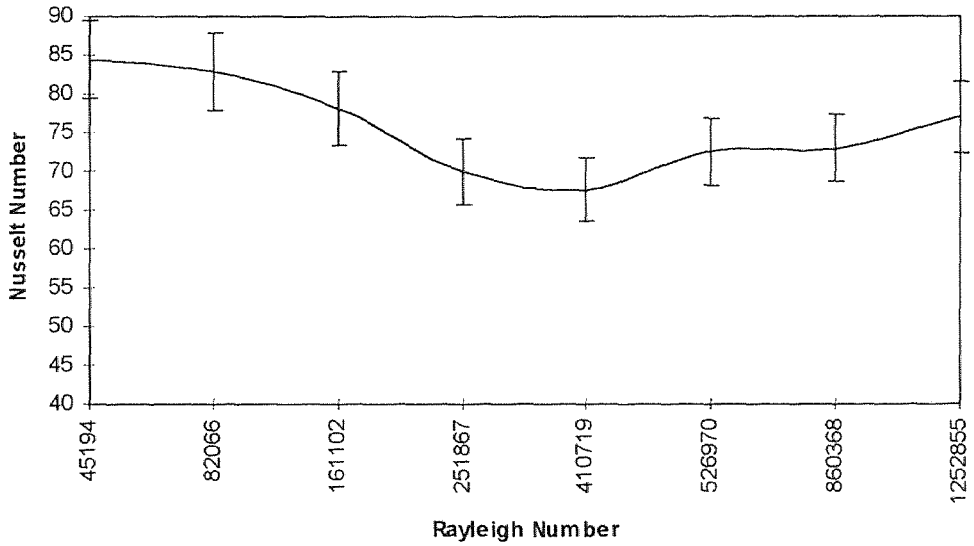

Figure C-11: Nusselt versus Rayleigh number. Eight screws removed.

0.75" Heat Pipe Data

Date: 2-21-1997
Initial Temperature: 20.9 °C
Air Injection Distance: Z/D=0

Air Injection Rate: 00 SCFH
Natural Convection Only

Table C-12: Natural convection

Volts	Amps	T_1	T_2	T_3	T_4	T_7	T_8
15	1.6	24.2	24.6	24.7	24.6	27.9	21.2
20	2.0	27.6	27.6	27.8	27.8	32.9	22.6
23	2.4	31.8	31.6	31.7	31.8	39.2	24.6
26	2.8	37.2	36.8	37.0	37.6	46.5	27.2
29	3.2	42.6	41.9	41.8	43.0	53.4	29.3
32	3.5	48.6	47.5	47.9	49.5	60.4	31.7
35	3.9	54.6	53.2	53.4	55.8	68.9	33.9
38	4.3	61.9	60.2	60.4	62.9	78.3	36.9
42	4.7	73.3	71.5	71.7	74.5	97.8	42.5

Table C-12 Continued

Volts	Amps	T_9	T_{10}	T_{11}	T_{12}	Nu. #	Ra. #
15	1.6	20.8	2.0	22.0	21.9	14.7	53306
20	2.0	22.2	23.5	23.3	23.4	15.8	101388
23	2.4	24.0	26.0	25.8	25.9	15.9	179649
26	2.8	26.5	30.2	30.0	30.1	17.1	321103
29	3.2	28.8	33.8	3.6	33.8	17.8	505158
32	3.5	31.7	38.	38.5	38.6	18.5	746133
35	3.9	34.5	43.0	42.8	42.9	19.4	1103418
38	4.3	38.3	49.3	49.	49.2	22.1	1671322
42	4.7	45.5	59.2	59.0	59.1	22.5	2743248

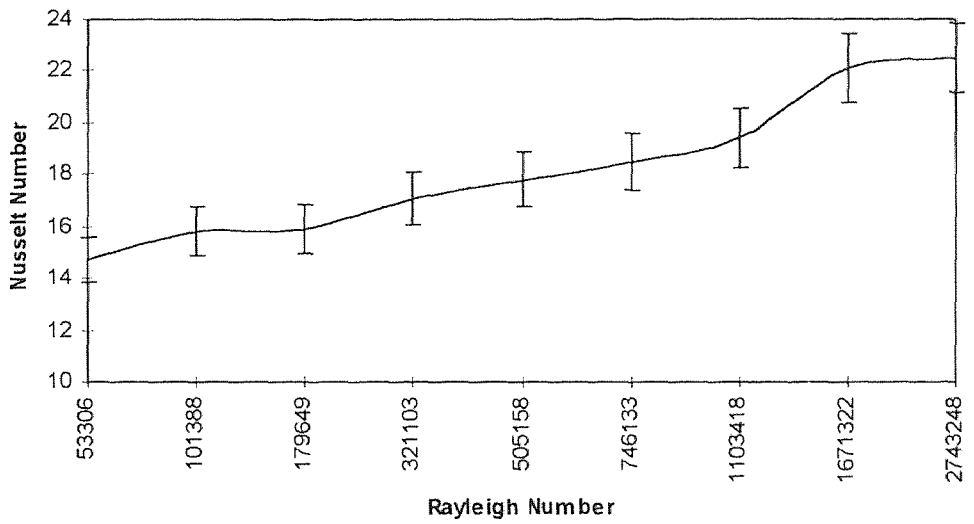

Figure C-12: Nusselt versus Rayleigh number. Natural convection conditions.

APPENDIX D

0.75" Heat Pipe Data

Air Injection Distance: Z/D=5
Initial Temperature: 21.0 °C
Date: 2-24-1997

Air Injection Rate: 5 SCFH
All Screws Open

Table D-1: Sectional cooling effect all 15 ports open

Volts	Amps	T_1	T_2	T_3	T_4	T_7	T_8
27	3.0	24.8	23.9	24.2	25.1	34.8	24.8
33	3.5	28.2	26.4	26.8	28.4	43.3	26.3
36	4.0	32.2	29.9	30.4	32.7	49.2	29.1
40	4.5	36.9	33.8	34.6	38.4	58.8	32.3
45	5.0	42.3	38.5	39.5	44.4	70.5	36.4
49	5.5	48.4	43.9	45.0	50.6	82.2	40.1
53	6.0	54.9	49.4	50.7	57.6	94.6	44.8
58	6.7	62.7	55.9	57.6	65.1	112.4	50.7

Table D-1 Continued

Volts	Amps	T_9	T_{10}	T_{11}	T_{12}	Nu. #	Ra. #
27	3.0	24.2	22.6	22.6	22.6	76.6	40281
33	3.5	25.0	24.8	24.8	24.8	74.6	64295
36	4.0	26.6	27.6	27.6	27.6	68.5	121320
40	4.5	28.7	31.1	31.1	31.1	64.8	218103
45	5.0	31.1	35.2	35.2	35.2	64.5	355441
49	5.5	33.6	39.8	39.8	39.8	63.3	573721
53	6.0	36.7	45.2	45.2	45.2	67.2	795182
58	6.7	48.7	50.8	50.8	50.8	68.3	1315634

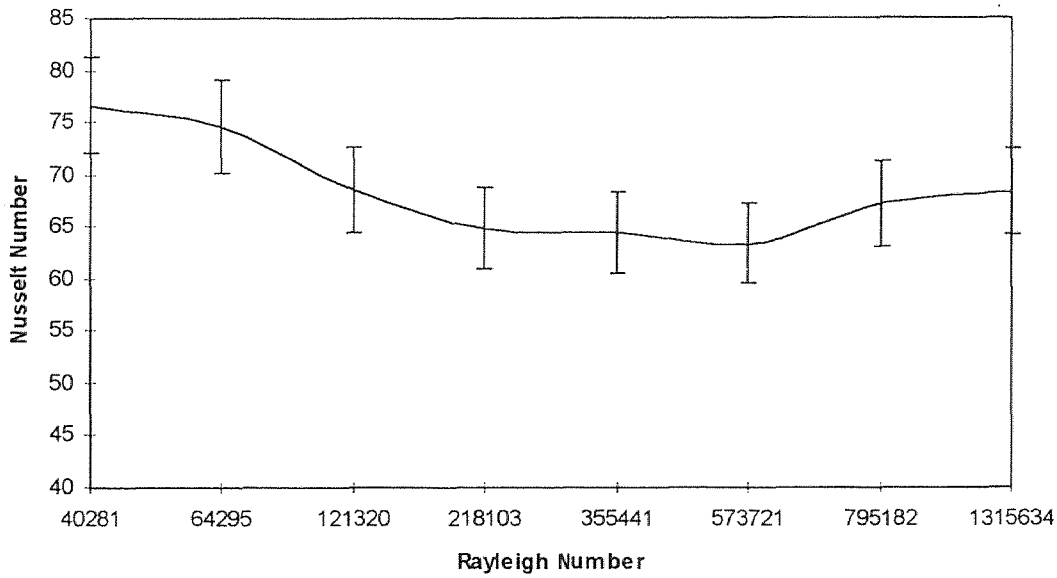

Figure D-1: Nusselt versus Rayleigh number. Air injection rate 5 SCFH.

0.75" Heat Pipe Data

Air Injection Distance: Z/D=5
Initial Temperature: 21.1 °C
Date: 2-26-1997

Air Injection Rate: 5 SCFH
First Four Screws Removed

Table D-2: Sectional cooling effect first 4 ports open

Volts	Amps	T_1	T_2	T_3	T_4	T_7	T_8
30	3.3	26.2	25.5	25.0	25.8	23.2	38.0
36	4.0	31.0	30.1	29.0	31.4	26.6	49.3
40	4.4	36.3	34.4	33.8	36.4	29.2	55.3
43	4.8	40.9	39.1	38.4	41.9	32.3	63.8
46	5.2	46.1	44.1	43.0	47.4	35.6	74.4
50	5.6	52.3	49.6	48.5	53.3	39.4	85.8
54	6.0	58.6	56.4	55.1	60.6	44.3	98.6
58	6.6	66.6	63.0	61.1	67.9	49.6	114.3
65	7.3	74.2	71.1	69.4	77.1	56.4	133.8

Table D-2 Continued

Volts	Amps	T_9	T_{10}	T_{11}	T_{12}	Nu. #	Ra. #
30	3.3	24.3	22.7	22.7	22.7	62.4	64141
36	4.0	27.9	25.6	25.6	25.6	53.1	135229
40	4.4	30.8	29.3	29.3	29.3	52.0	245195
43	4.8	34.0	33.1	33.1	33.1	51.2	380829
46	5.2	37.6	37.1	37.1	37.1	50.7	551136
50	5.6	42.1	41.8	41.7	42.1	52.0	766041
54	6.0	47.4	47.5	47.4	47.7	53.1	1230207
58	6.6	53.0	52.8	52.8	53.1	53.6	1859008
65	7.3	60.8	59.4	59.3	59.5	57.0	2743407

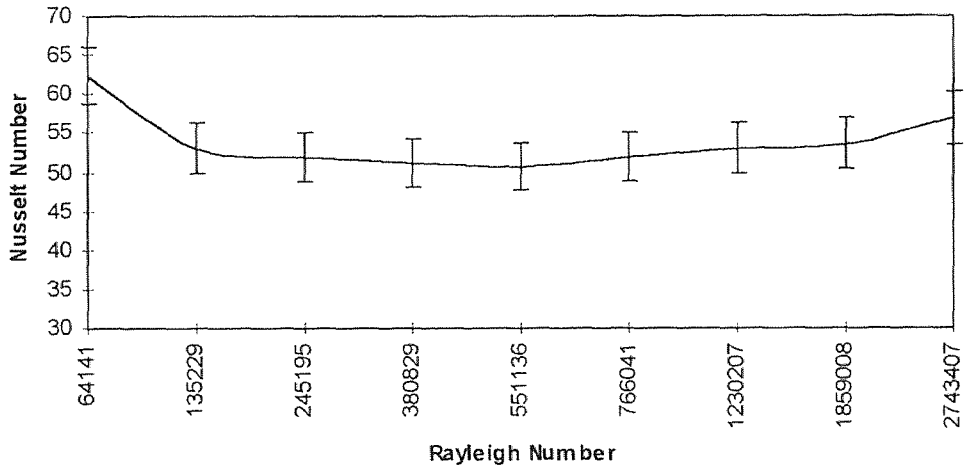

Figure D-2: Nusselt versus Rayleigh number. First four screws removed only.

0.75" Heat Pipe Data

Air Injection Distance: Z/D=5
Initial Temperature: 20.8 °C
Date: 2-24-1997

Air Injection Rate: 5 SCFH
Screws #'s: 7,8,9 Open

Table D-3: Sectional cooling effect middle 3 ports open

Volts	Amps	T_1	T_2	T_3	T_4	T_7	T_8
30	3.3	269.6	24.6	26.3	26.9	24.3	39.2
36	4.0	32.2	28.5	31.3	33.3	27.9	50.4
40	4.5	37.4	32.9	36.2	38.5	31.0	58.6
46	5.0	43.3	37.6	42.3	45.2	34.8	72.3
50	5.6	51.1	44.5	49.5	53.4	40.6	88.3
56	6.3	59.9	51.5	57.6	62.3	46.7	105.2
62	7.1	69.4	59.6	66.4	72.0	54.1	125.8

Table D-3 Continued

Volts	Amps	T_9	T_{10}	T_{11}	T_{12}	Nu. #	Ra. #
30	3.3	25.3	22.6	22.5	22.5	49.4	78873
36	4.0	29.4	25.6	25.6	25.7	44.6	169747
40	4.5	33.0	29.5	29.4	29.7	46.8	290881
46	5.0	37.3	33.6	33.5	33.8	46.7	495381
50	5.6	43.4	39.0	38.9	39.2	44.6	828872
56	6.3	50.0	45.0	45.0	45.2	46.1	1459375
62	7.1	58.0	52.0	52.0	52.2	49.0	2399293

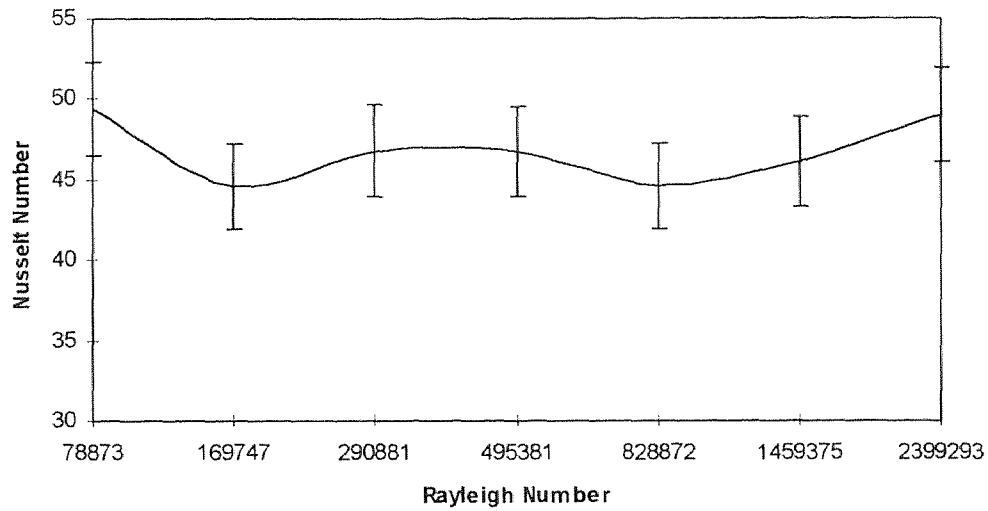

Figure D-3: Nusselt versus Rayleigh number. Middle three screws open.

0.75" Heat Pipe Data

Air Injection Distance: Z/D=5
Initial Temperature: 21.3 °C
Date: 2-28-1997

Air Injection Rate: 5 SCFH
Last Four Screws Open

Table D-4: Sectional cooling effect last 4 ports open

Volts	Amps	T_1	T_2	T_3	T_4	T_7	T_8
30	3.3	26.8	26.0	27.2	27.3	25.2	39.7
36	4.0	31.9	30.4	32.4	33.6	29.0	51.0
40	4.5	36.6	35.0	36.8	38.7	32.1	57.5
44	50	41.8	40.2	42.8	45.1	36.8	70.7
48	5.5	47.9	45.5	48.5	51.5	41.4	82.5
53	6.0	54.9	51.5	55.4	58.8	47.0	9.4
60	6.8	63.2	59.8	64.1	68.1	54.7	118.4
65	7.4	72.9	68.5	72.7	77.5	63.5	137.4

Table D-4 Continued

Volts	Amps	T_9	T_{10}	T_{11}	T_{12}	Nu. #	Ra. #
30	3.3	26.1	23.4	23.2	23.2	49.6	81767
36	4.0	30.1	26.2	26.2	26.2	43.1	148653
40	4.5	33.2	29.5	29.6	29.9	44.3	315016
44	50	37.8	33.8	34.0	34.2	44.7	505456
48	5.5	42.3	38.2	38.4	38.5	44.9	751610
53	6.0	48.0	43.4	43.7	43.7	46.2	1178116
60	6.8	55.5	49.3	49.6	49.6	48.3	2080735
65	7.4	64.1	56.6	56.8	56.9	48.8	3137099

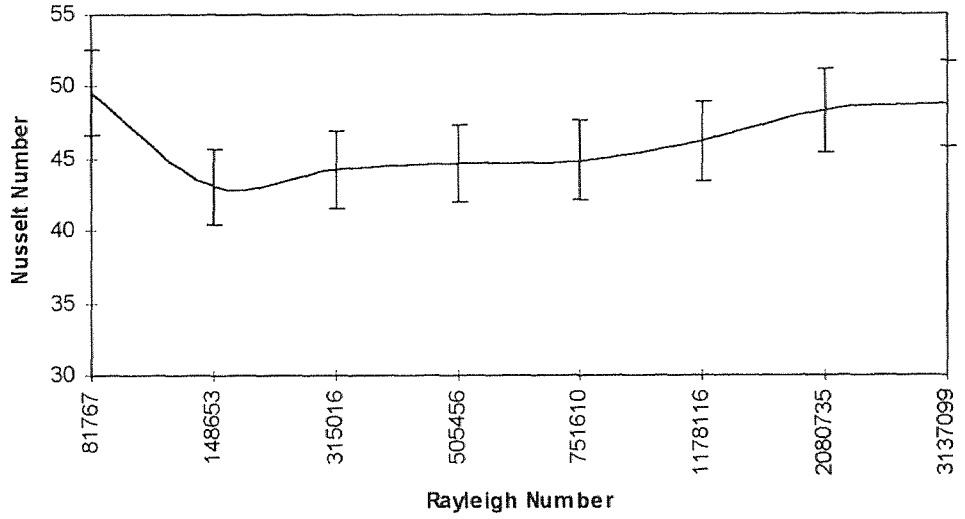

Figure D-4: Nusselt versus Rayleigh number. Last four screws open.

0.75" Heat Pipe Data

Air Injection Distance: Z/D=5
Initial Temperature: 21.1 °C
Date: 3-2-1997

Air Injection Rate: 2 SCFH
Screws #: 1, 9, 15 Open

Table D-5: Air injection rate effect 2 SCFH

Volts	Amps	T_1	T_2	T_3	T_4	T_7	T_8
27	3.0	25.8	24.3	25.2	25.2	22.8	36.1
32	3.5	29.5	27.3	28.3	28.6	25.7	43.0
36	4.1	33.7	30.2	31.9	33.4	28.4	50.2
43	4.8	10.2	36.2	38.5	40.6	33.3	64.8
48	5.4	47.8	42.3	45.5	48.2	38.9	80.4
55	6.3	56.4	48.5	53.1	57.1	46.7	103.2
62	7.0	64.4	58.0	62.7	65.3	51.6	123.8

Table D-5 Continued

Volts	Amps	T_9	T_{10}	T_{11}	T_{12}	Nu. #	Ra. #
27	3.0	23.3	22.6	22.5	22.5	55.4	55811
32	3.5	26.5	24.7	24.7	24.7	53.2	92315
36	4.1	29.4	27.0	27.1	27.4	50.7	172777
43	4.8	34.3	31.2	31.4	31.5	47.7	376412
48	5.4	40.1	36.1	36.5	36.4	45.9	659546
55	6.3	47.7	41.7	42.1	41.9	48.9	1102085
62	7.0	52.1	47.7	47.9	47.8	49.6	2025157

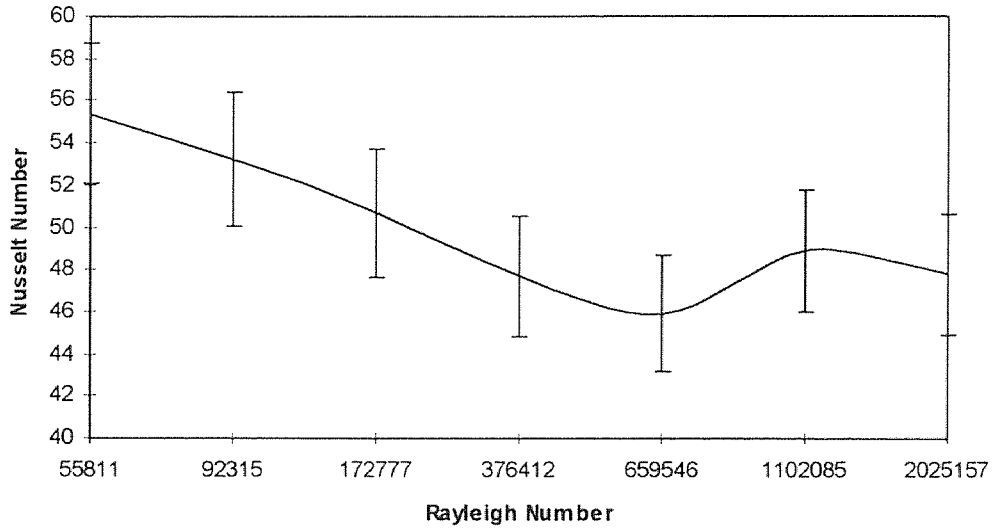

Figure D-5: Nusselt versus Rayleigh number. Air injection rate 2 SCFH.

0.75" Heat Pipe Data

Air Injection Distance: Z/D=5
Initial Temperature: 21.1 °C
Date: 3-3-1997

Air Injection Rate: 1 SCFH
Screws #: 1, 9, 15 Open (Only #15 operational)

Table D-6: Air injection rate effect 1 SCFH

Volts	Amps	T_1	T_2	T_3	T_4	T_7	T_8
27	3.0	27.4	25.6	27.0	27.2	22.5	38.7
31	3.4	30.4	29.9	30.2	30.7	25.0	44.6
34	3.8	34.2	32.8	33.7	35.0	28.5	49.7
38	4.3	39.2	36.7	38.1	39.8	34.1	57.6
42	4.8	44.4	41.8	43.0	45.2	37.2	67.6
48	5.4	52.0	49.0	50.6	53.1	42.8	84.5
53	6.0	59.7	56.0	57.8	60.9	48.7	98.7
58	6.6	68.0	63.2	66.5	69.9	55.8	16.9

Table D-6 Continued

Volts	Amps	T_9	T_{10}	T_{11}	T_{12}	Nu. #	Ra. #
27	3.0	22.3	23.1	23.4	23.2	38.7	83725
31	3.4	24.1	24.8	25.4	25.1	35.4	142697
34	3.8	28.0	27.3	27.8	27.5	35.2	234569
38	4.3	31.9	30.3	30.7	30.5	35.6	382744
42	4.8	35.0	33.7	34.2	34.0	35.9	590592
48	5.4	40.1	38.4	38.8	38.5	35.8	975710
53	6.0	45.3	43.8	44.1	43.8	36.0	1664245
58	6.6	52.0	49.4	49.7	49.5	36.5	2694645

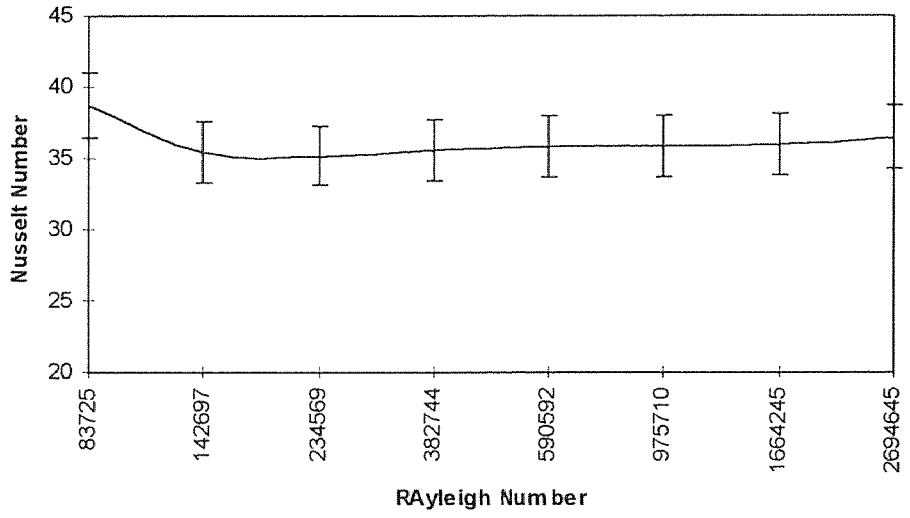

Figure D-6: Nusselt versus Rayleigh number. Air injection rate 1 SCFH.

0.75" Heat Pipe Data

Air Injection Distance: Z/D=5
Initial Temperature: 21.1 °C
Date: 3-4-1997

Air Injection Rate: 0.5 SCFH
Screws #: 1, 9, 15 Open

Table D-7: Air injection rate effect 0.5 SCFH

Volts	Amps	T_1	T_2	T_3	T_4	T_7	T_8
25	2.7	25.1	24.2	25.0	24.7	23.3	35.8
30	3.3	29.7	27.7	28.6	28.2	25.8	40.9
34	3.8	34.3	31.6	33.1	33.8	28.5	48.7
38	4.3	40.0	36.0	37.9	39.5	31.8	57.5
43	4.9	47.0	42.4	44.7	46.6	36.2	71.2
48	5.4	55.0	49.7	52.4	54.8	41.2	85.1
53	6.0	64.8	58.5	61.4	64.8	47.3	101.0
58	6.6	74.0	68.7	72.6	76.6	54.5	119.0

Table D-7 Continued

Volts	Amps	T_9	T_{10}	T_{11}	T_{12}	Nu. #	Ra. #
25	2.7	24.2	22.3	22.2	22.2	57.3	53250
30	3.3	27.2	24.5	24.6	24.8	43.7	100003
34	3.8	30.2	27.6	27.8	27.8	41.4	196322
38	4.3	33.6	31.3	31.5	31.5	41.0	341931
43	4.9	38.2	36.3	36.6	36.6	41.4	586305
48	5.4	43.5	42.3	42.4	42.4	41.0	973936
53	6.0	50.0	49.2	49.6	49.5	400.7	1525596
58	6.6	57.7	56.5	56.9	56.7	38.3	3164954

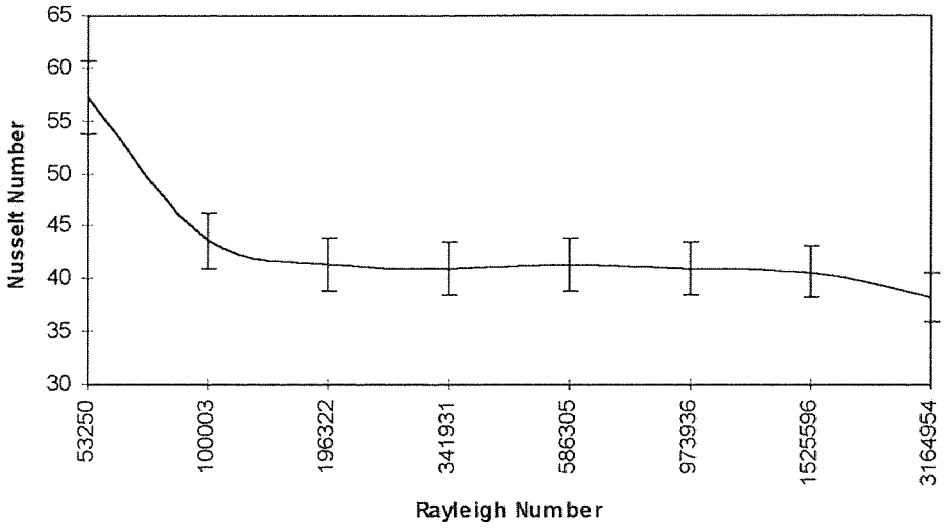

Figure D-7: Nusselt versus Rayleigh number. Air injection rate 0.5 SCFH.

0.75" Heat Pipe Data

Air Injection Distance: Z/D=1
Initial Temperature: 21.1 °C
Date: 3-5-1997

Air Injection Rate: 2 SCFH
Screws #: 1, 9, 15 Open

Table D-8: Air injection distance effect for 2 SCFH at Z/D=1

Volts	Amps	T_1	T_2	T_3	T_4	T_7	T_8
27	3.0	26.2	25.6	26.7	26.6	24.1	37.2
31	3.5	30.6	29.3	30.8	31.3	27.0	44.8
36	4.0	34.8	33.1	35.0	35.9	29.5	52.1
40	4.5	39.6	37.7	39.8	40.4	31.9	60.0
45	5.0	45.9	42.9	46.2	48.2	36.8	74.2
49	5.5	53.9	51.0	54.5	56.8	42.3	86.8
53	6.0	62.9	59.0	63.2	66.3	47.9	101.7
58	6.6	72.6	67.9	72.8	75.8	54.9	119.8

Table D-8 Continued

Volts	Amps	T_9	T_{10}	T_{11}	T_{12}	Nu. #	Ra. #
27	3.0	24.7	22.6	22.6	22.6	39.1	81790
31	3.5	28.1	24.9	24.8	24.8	33.7	155031
36	4.0	31.0	27.7	27.4	27.4	35.0	272383
40	4.5	33.6	30.8	30.6	30.5	35.7	434965
45	5.0	39.2	34.8	34.8	35.0	35.1	721878
49	5.5	44.7	41.8	41.8	42.0	37.1	1073001
53	6.0	50.8	48.4	48.4	48.7	36.7	2004343
58	6.6	58.2	56.0	55.9	56.2	38.4	3092151

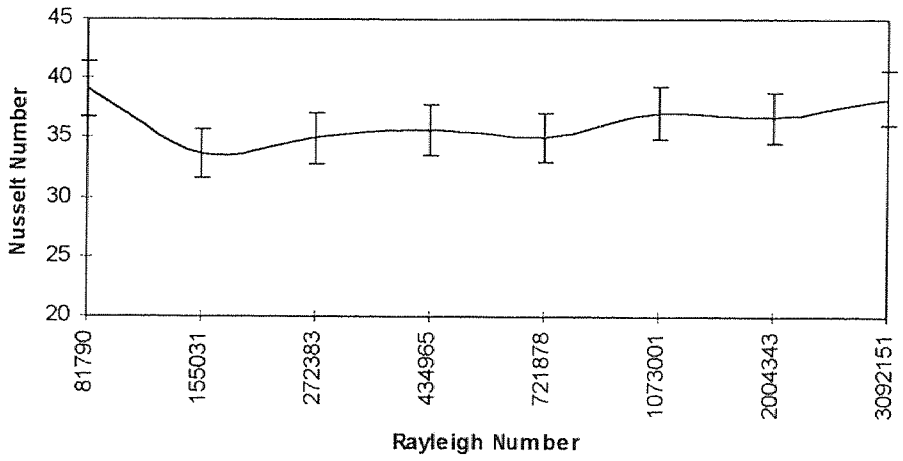

Figure D-8: Nusselt versus Rayleigh number. Air injection distance Z/D=1

0.75" Heat Pipe Data

Air Injection Distance: Z/D=1
Initial Temperature: 20.8 °C
Date: 3-6-1997

Air Injection Rate: 5 SCFH
Screws #: 1, 5, 9, 15 Open

Table D-9: Air injection distance effect for 5 SCFH at Z/D=1

Volts	Amps	T_1	T_2	T_3	T_4	T_7	T_8
27	3.0	25.5	24.2	25.2	25.4	22.5	35.6
32	3.6	28.5	26.4	27.5	28.9	25.3	42.7
38	4.3	33.5	30.4	32.0	34.3	28.6	51.6
45	5.0	40.1	35.8	38.0	41.5	33.3	6.8
50	5.7	47.8	42.4	45.1	49.5	39.0	84.9
56	6.4	56.0	49.8	52.8	57.9	46.1	102.3
64	7.2	66.4	58.3	62.2	68.3	54.6	127.7

Table D-9 Continued

Volts	Amps	T_9	T_{10}	T_{11}	T_{12}	Nu. #	Ra. #
27	3.0	23.2	22.1	22.1	22.0	47.9	63846
32	3.6	26.7	24.0	23.9	23.8	52.1	94004
38	4.3	30.0	27.1	26.8	26.7	50.9	190855
45	5.0	35.2	31.2	31.0	30.8	49.9	388724
50	5.7	41.6	36.6	36.4	36.5	50.1	670771
56	6.4	49.5	42.9	42.7	43.1	53.7	1087070
64	7.2	58.8	49.7	49.5	49.9	54.7	2060066

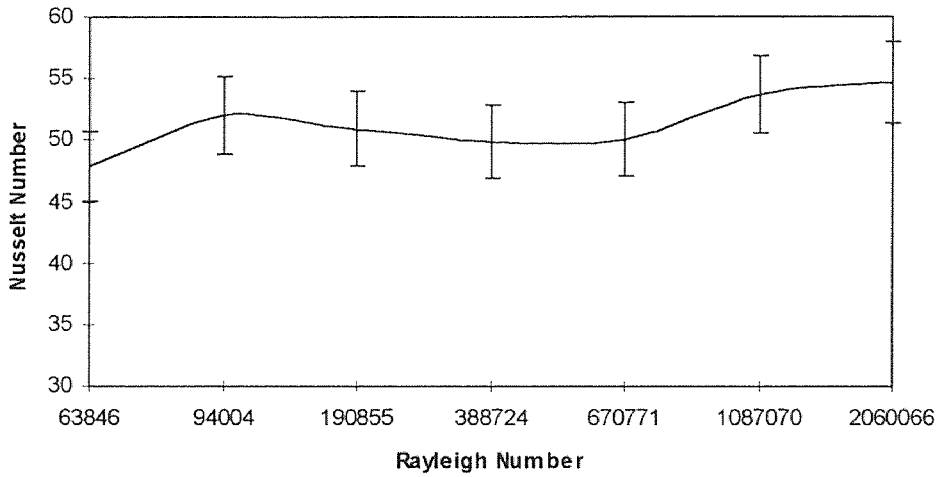

Figure D-9: Nusselt versus Rayleigh number. Air injection rate 5 SCFH.

0.75" Heat Pipe Data

Air Injection Distance: Z/D=10 Air Injection Rate: 5 SCFH
Initial Temperature: 21.1 °C Screws #: 1, 5, 9, 15 Open
Date: 3-6-1997

Table D-10: Air injection distance effect for 5 SCFH at Z/D=10

Volts	Amps	T_1	T_2	T_3	T_4	T_7	T_8
30	3.4	26.2	25.2	25.3	25.9	26.6	39.1
36	4.1	30.2	28.2	28.8	30.2	27.9	47.3
42	4.8	35.6	32.6	33.8	36.7	31.8	61.0
49	5.5	42.2	38.3	39.7	43.7	38.3	77.0
54	6.1	49.4	44.5	46.3	51.1	44.5	91.7
60	6.8	58.4	52.6	54.9	61.0	54.5	113.7
64	7.2	66.3	60.9	64.3	68.1	60.1	138.6

Table D-10 Continued

Volts	Amps	T_9	T_{10}	T_{11}	T_{12}	Nu. #	Ra. #
30	3.4	27.3	23.4	23.3	23.8	86.2	48201
36	4.1	30.9	25.8	25.6	26.0	74.3	96062
42	4.8	34.7	29.4	29.4	29.8	68.8	210401
49	5.5	40.4	34.4	34.3	34.7	71.7	378017
54	6.1	46.5	39.9	39.9	40.2	71.8	602383
60	6.8	55.1	47.0	46.9	47.2	70.6	1133725
64	7.2	63.0	54.1	54.0	54.2	70.0	1755529

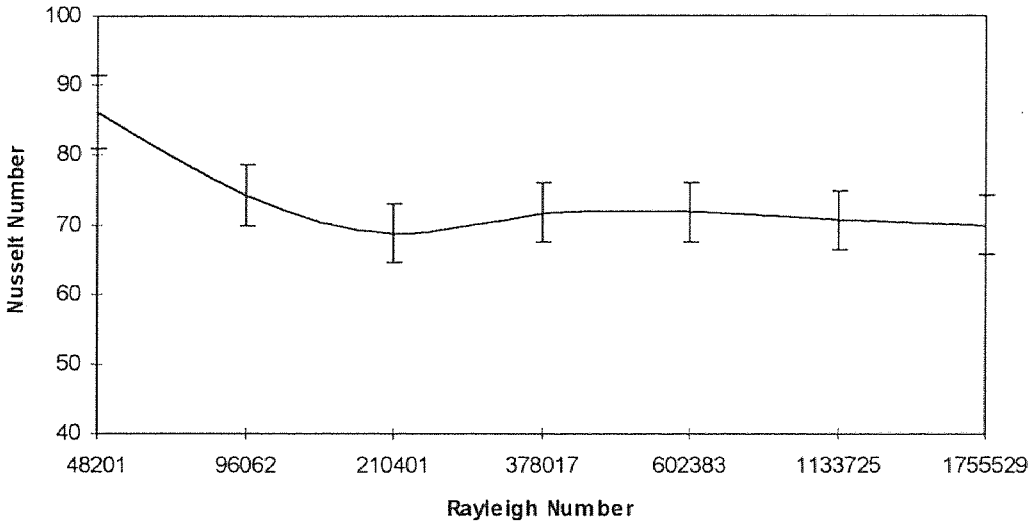

Figure D-10: Nusselt versus Rayleigh number. Air injection distance Z/D=10

0.75" Heat Pipe Data

Air Injection Distance: Z/D=10
Initial Temperature: 21.4 °C
Date: 3-7-1997

Air Injection Rate: 2 SCFH
Screws #: 1, 9, 15 Open

Table D-11: Air injection distance effect for 2 SCHF at Z/D=10

Volts	Amps	T_1	T_2	T_3	T_4	T_7	T_8
27	3.0	25.1	24.1	25.0	25.1	22.1	36.1
31	3.4	27.9	26.5	27.4	27.9	25.6	41.6
35	4.0	31.6	29.1	30.9	32.4	29.3	51.4
40	4.5	35.9	33.7	35.2	37.3	39.6	57.3
44	5.0	40.8	38.2	39.9	42.9	37.0	68.8
49	5.5	47.3	43.8	46.2	49.8	42.4	82.0
56	6.3	57.4	50.4	54.5	59.2	50.2	105.3
62	7.0	63.6	58.6	62.5	68.3	57.6	122.1

Table D-11 Continued

Volts	Amps	T_9	T_{10}	T_{11}	T_{12}	Nu. #	Ra. #
27	3.0	22.0	22.3	22.3	22.3	56.6	53568
31	3.4	25.6	24.2	24.3	24.5	60.4	74300
35	4.0	29.2	26.4	26.6	26.8	57.5	135533
40	4.5	32.7	30.0	30.2	30.2	58.4	232472
44	5.0	37.0	33.6	34.0	33.8	57.2	374005
49	5.5	42.3	38.4	38.5	38.6	55.6	604785
56	6.3	50.0	44.4	44.8	44.7	55.0	1136105
62	7.0	57.3	49.8	50.0	49.9	53.9	1941143

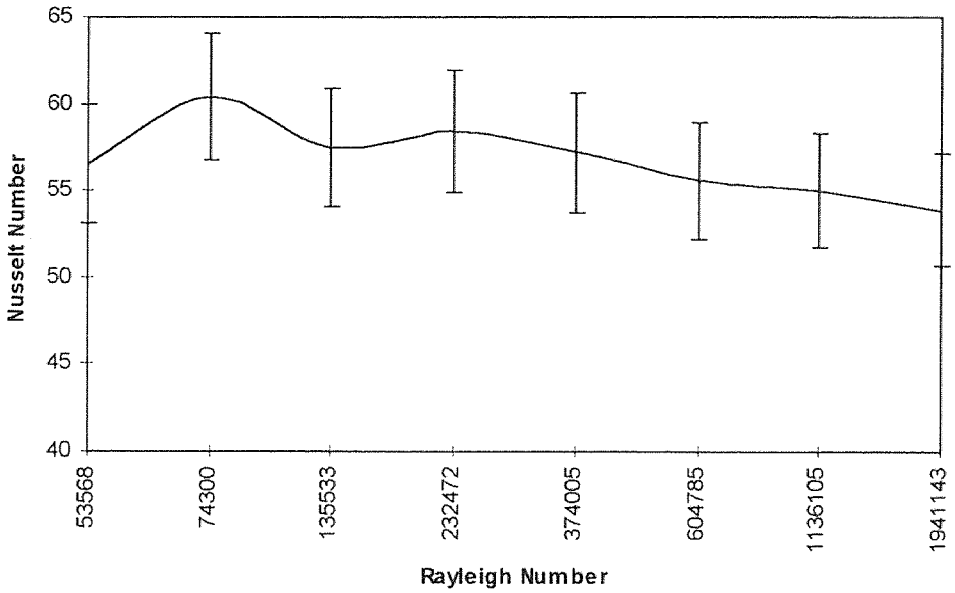

Figure D-11: Nusselt versus Rayleigh number. Air injection rate 2 SCFH.

0.75" Heat Pipe Data

Air Injection Distance: Z/D=5
Initial Temperature: 20.9 °C
Date: 3-7-1997

Air Injection Rate: 5 SCFH
Screws #: 1, 5, 9, 15 Open

Table D-12: Air injection distance effect for 5 SCFH at Z/D=5

Volts	Amps	T_1	T_2	T_3	T_4	T_7	T_8
30	3.4	25.3	24.4	25.0	25.9	22.1	38.4
36	4.0	29.9	27.8	29.0	30.6	31.3	47.7
42	4.7	35.6	32.7	34.3	37.6	31.7	59.4
48	5.4	41.9	38.0	40.2	44.1	38.8	76.0
54	6.2	49.8	44.0	46.7	52.0	55.3	94.5
60	6.8	58.3	51.3	54.4	60.4	65.3	113.5
66	7.3	66.5	58.8	62.1	68.8	68.7	132.5

Table D-12 Continued

Volts	Amps	T_9	T_{10}	T_{11}	T_{12}	Nu. #	Ra. #
30	3.4	22.3	23.8	23.3	23.2	91.2	43475
36	4.0	31.3	25.8	26.0	26.0	76.0	92346
42	4.7	33.8	30.1	30.5	30.4	75.0	193916
48	5.4	38.7	34.6	35.0	34.9	72.0	365136
54	6.2	44.6	39.6	39.9	39.8	68.6	644270
60	6.8	51.3	46.3	46.3	46.5	71.1	1095393
66	7.3	66.3	52.8	52.8	53.2	72.9	1722259

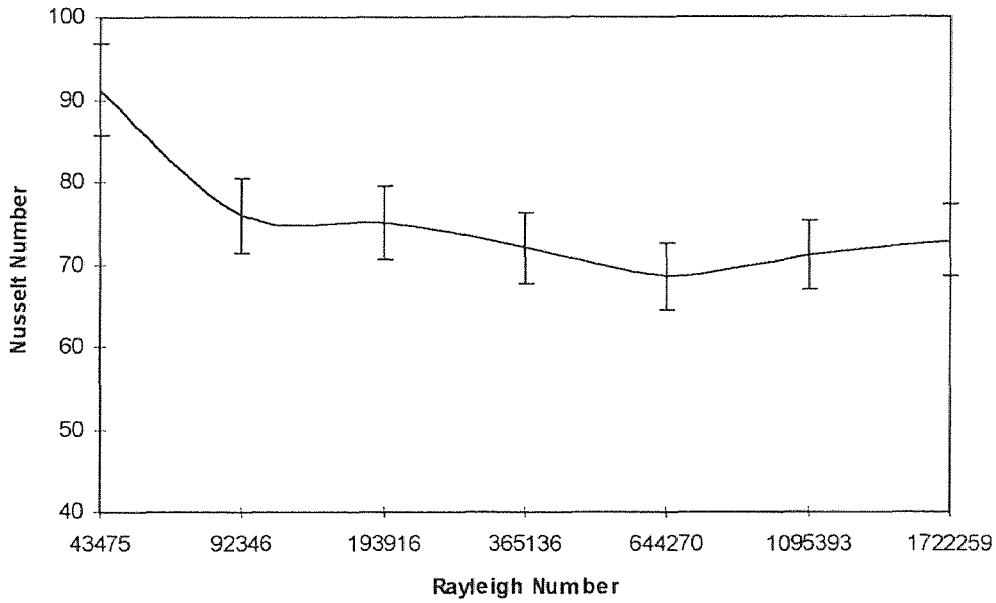

Figure D-12: Nusselt versus Rayleigh number. Injection distance Z/D=5.

0.75" Heat Pipe Data

Air Injection Distance: Z/D=5
Initial Temperature: 15.2 °C
Date: 3-10-1997

Air Injection Rate: 5 SCFH
Screws #: 1, 5, 9, 15 Open

Table D-13: Initial water temperature effect 15.2 °C

Volts	Amps	T_1	T_2	T_3	T_4	T_7	T_8
31	3.4	20.6	19.1	20.1	20.6	23.2	34.9
36	4.0	25.2	22.7	23.7	24.8	28.2	44.1
41	4.6	30.9	27.4	29.0	31.2	33.5	53.8
46	5.2	36.8	32.6	34.8	38.2	42.1	71.1
52	5.8	45.4	39.0	41.6	46.1	50.4	85.8
56	6.4	53.0	46.0	49.5	53.7	59.4	100.8
61	6.8	60.2	52.9	56.0	61.9	81.1	148.4

Table D-13 Continued

Volts	Amps	T_9	T_{10}	T_{11}	T_{12}	Nu. #	Ra. #
31	3.4	21.8	17.2	17.2	17.2	66.3	44584
36	4.0	25.8	20.5	20.7	21.0	77.3	66843
41	4.6	29.9	24.4	25.0	25.1	70.4	124660
46	5.2	35.6	29.1	29.5	29.5	67.4	262053
52	5.8	41.6	34.6	35.0	35.0	64.0	504064
56	6.4	48.2	41.2	41.4	41.4	63.3	766894
61	6.8	62.2	47.4	47.7	47.7	67.3	1235615

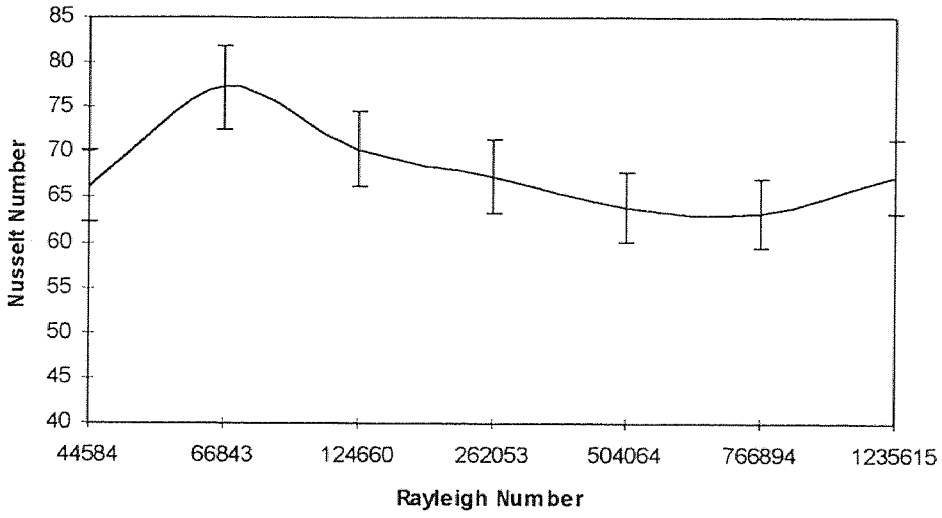

Figure D-13: Nusselt versus Rayley number. Initial tamperature 15.2 °C.

0.75" Heat Pipe Data

Air Injection Distance: Z/D=5
Initial Temperature: 18.0 °C
Date: 3-11-1997

Air Injection Rate: 5 SCFH
Screws #: 1, 5, 9, 15 Open

Table D-14: Initial water temperature effect 18.0 °C

Volts	Amps	T_1	T_2	T_3	T_4	T_7	T_8
30	3.4	23.0	22.2	22.8	24.0	22.3	3.4
34	4.0	27.4	25.6	26.4	28.1	29.9	45.1
41	4.6	32.9	29.8	31.4	34.0	35.0	56.3
46	5.2	39.9	35.9	38.0	41.6	42.1	70.7
51	5.8	47.0	42.0	45.0	49.2	49.8	86.1
56	6.4	55.7	49.4	52.5	58.0	59.2	103.6
62	7.0	64.0	56.6	60.4	66.6	69.8	124.2

Table D-14 Continued

Volts	Amps	T_9	T_{10}	T_{11}	T_{12}	Nu. #	Ra. #
30	3.4	29.2	20.4	20.5	20.6	74.7	47650
34	4.0	29.7	23.1	23.3	23.4	67.9	83062
41	4.6	33.0	26.9	27.0	27.0	66.3	166624
46	5.2	38.1	32.4	32.5	32.5	65.5	330386
51	5.8	43.8	37.7	37.8	37.9	63.6	564214
56	6.4	50.9	44.7	44.8	44.9	66.6	926853
62	7.0	58.5	50.9	51.0	50.9	66.0	1580450

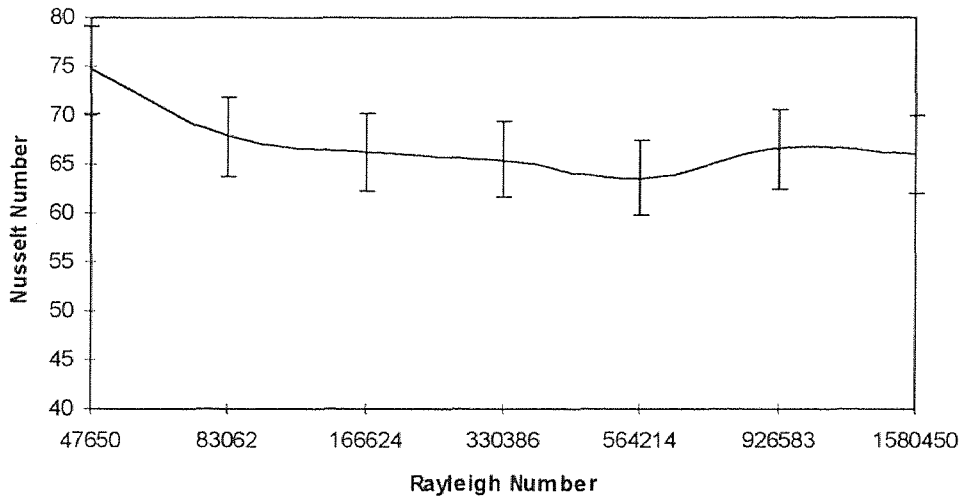

Figure D-14: Nusselt versus Rayleigh number. Initial temperature 18.0 °C.

REFERENCES

1. Akira, T. and Likoudis, P., "Natural Convection heat transfer from a vertical plate-I. Enhancement with gas injection," *International Journal of Heat and Mass Transfer*, Vol. 37 997-1003 (1994).

2. Bejan, Adrian, *Advanced Engineering Thermodynamics*, North Carolina: John Wiley & Sons Co., 1988

3. Berenson, P. J., "Experiments on pool-boiling heat transfer," *International Journal of Heat and Mass Transfer*, Vol. 5 985-999 (1962).

4. Berges, A. E., "Enhancement of heat transfer," *Sixth International Heat Transfer Conference*, Toronto, 6, 1978, 89.

5. Berges, A. E., et al, *Two-Phase Flow and Heat Transfer in the Power and Process Industries*, New York: Hemisphere Publishing Co., 1981.

6. Brighton, J. A., and Hughes, W. F., *Fluid Dynamics: Schaum's Outline Series*, 2nd Ed., New Jersey: McGraw Hill, Inc., 1991.

7. Chen, X., and Viziroglu N. T., *Two Phase Flow and Heat Transfer: China-U.S. Progress*, New York: Hemisphere Publishing Co., 1985.

8. Churchill, S. W. and Humbert, H. S., "Correlating equations for laminar and turbulent free convection from horizontal cylinder," *International Journal of Heat and Mass Transfer*, Vol. 18 1049-1052 (1975).

9. Churchill, S. W., *Single- Phase Convective Heat Transfer*, New York: Hemisphere Publishing Co., 1983.

10. Crowther, D. J. and Padet, J., "Measurement of the local convection coefficient by pulsed photothermal radiometry," *International Journal of Heat and Mass Transfer*, Vol., 34, No.12 3075-3081 (1991).

11. Cole, R. and Sjoerd, Van Stralen, *Boiling Phenomena: Physicochemical and Engineering Fundamentals and Applications*, New York: Hemisphere Publishing Co., 1979.

12. Durst F., et al, *Two-Phase Momentum, Heat and Mass Transfer: In Chemical, Process, and Energy Engineering Systems*, New York: Hemisphere Publishing Co., Vol. 1 &2, 1979.

13. Gaertner, R. F., "Photographic study of nucleate pool boiling on a horizontal surface," *Journal of Heat Transfer*, February 1965 pp. 17-29.

REFERENCES
(Continued)

14. Ginoux, J.J., *Two-Phase Flows and Heat Transfer with Application to Nuclear Reactor Problems*, New York: Hemisphere Publishing Co., 1978.

15. Gusev, S. and Shklover G., "Free convection from horizontal cylinders with air injection," *Heat Transfer-Soviet Research*, Vol. 23 1073-1078 (1991).

16. Gusev, S. and Shklover G., "Effect of variable physical properties on free-convective heat transfer near a horizontal cylinder," *Journal of Engineering Physics*, Vol. 53 229-236 (1987).

17. Hahne, E. and Muler J., "Boiling on a finned tube and tube finned tube bundle," *International Journal of Heat and Mass Transfer*, Vol. 26 849-859 (1983).

18. Hahne, E. and Windisch, R., "Heat transfer for boiling on finned tube bundles," *International Communication for Heat and Mass Transfer*, Vol. 12 355-368 (1985).

19. Hamburger, L. G., "On the growth and rise of individual vapour bubbles in nucleate pool boiling," *International Journal of Heat and Mass Transfer*, Vol. 8 1369-1386 (1965).

20. Hsieh, S. J., *Engineering Thermodynamics*, New Jersey, Simon & Schuster Co., 1993.

21. Hwang, T. H. and Yao, S. C., "Crossflow boiling heat transfer in tube bundles," *International Communication in Heat and Mass Transfer*, Vol. 13 493-502 (1986).

22. Iguchi, M. et al, "Heat transfer between bubbles and liquid during cold gas injection," *ISIL International*, Vol. 32 865-872 (1992).

23. Kakac, S. and Verizoglu T. N., *Two- Phase Flows and Heat Transfer*, New York: Hemisphere Publishing Co., 1976.

24. Kenning, D. B. R. and Kao Y. S., "Convective heat transfer to water containing bubbles: Enhancement not dependent on thermocapillarity," *Journal of Heat Transfer*, Vol. 15 1709-1717 (1972).

25. Konsetov, V.V., "Heat transfer during bubbling of gas through liquid," *International Journal of Heat and Mass Transfer*, vol. 9 1103-1108 (1966).

REFERENCES
(Continued)

26. Lindon, Thomas C., *Heat Transfer*, Simon & Schuster Co., New Jersey, 1992.

27. Leontiev, A. I., "Turbulent boundary layers with injection and suction," *Heat Transfer-Soviet Research*, Vol. 23, No. 3, 371-377 (1991).

28. Lu, S. M. and Lee, D. J., "The effects of heating on pool boiling," *International Journal of Heat and Mass Transfer*, Vol. 34, No.1 127-134 (1991).

29. Marsters, G. F., "Natural convective heat transfer from a horizontal cylinder in the presence of nearby walls," *Canadian Journal of Chemical Engineering*, Vol. 53, 144-149 (1975).

30. Masakazu, T. and Kaneyasu, N., "The stirring effect of bubbles upon the heat transfer to liquids," *Japanese Research-Heat Transfer* 5(2), 31-43 (1976).

31. Monde, M. and Mitsutake, Y., "Enhancement of heat transfer due to bubbles passing through a narrow vertical rectangular channel," *International Journal in Multiphase Flow*, Vol. 15, No.5, 803-814 (1989).

32. Morgan, V. T., *The overall convective heat transfer from smooth circular cylinders, Advances in Heat Transfer*, Vol. 11, New York, Academic Press, 199-264 (1975).

33. Pfeil, D. and Sparrow, E., "Enhancement of natural convection heat transfer from a horizontal cylinder due to vertical shrouding surfaces," *Transactions of the ASME*, Vol. 106 124-130 (1984).

34. Pitts, D. R., and Sissom, L. E., *Theory and Problems of Heat Transfer: Schaum's Outline Series*, New Jersey: McGraw Hill Inc., 1977.

35. Ronald, C. et al, Bubbles, *Drops and Particles*, New York, Academic Press, 1978.

36. Tong, L. S., *Boiling Heat Transfer and Two-Phase Flow*, New York: John Wiley & Sons, Inc., 1965.

37. Westwater, J. M., "Boiling heat transfer," *International Communication in Heat and Mass Transfer*, Vol. 15 381-400 (1988).

38. White, F. M., *Heat and Mass Transfer*, New York: Addison-Wesley Publishing Co., 1991.